

Merging Molecular Recognition and Catalysis with Model Systems

by

Roelof Jan Pieters
Drs., Chemistry
State University Groningen, the Netherlands

submitted to the Department of Chemistry in partial fulfillment of the
requirements for the degree of
Doctor of Philosophy

at the
Massachusetts Institute of Technology
February 1995

© 1995 Massachusetts Institute of Technology
All rights reserved

Signature of Author



Department of Chemistry

January 9, 1995

Certified by



Professor Julius Rebek, Jr.

Thesis Supervisor

Accepted by



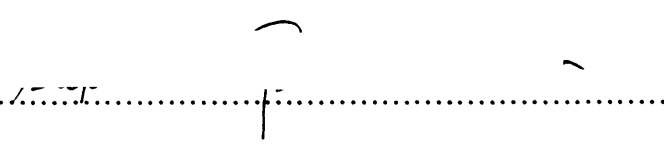
Professor Dietmar Seyferth

Chairman, Departmental Committee on Graduate Students

Science

MAR 01 1995

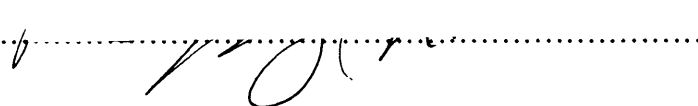
This doctoral thesis has been examined by a Committee of the Department of Chemistry as follows:

Professor S. L. Buchwald


Chairman

Professor J. Rebek, Jr.


Thesis Supervisor

Professor P. T. Lansbury, Jr.


-Aan mijn moeder en ter nagedachtenis aan mijn vader-

Merging Molecular Recognition and Catalysis with Model Systems

by

Roelof Jan Pieters

Submitted to the Department of Chemistry on January 9, 1995 in partial fulfillment of the requirements for the Degree of Doctor of Philosophy in Chemistry

Abstract

Synthetic adenine receptors were used in the development of catalytic agents. These receptors contain a carbazole unit and two Kemp's imide surfaces complementary to adenine. Adenine affinities are by 6-7 kcal mol⁻¹ in chloroform due to hydrogen bonding and π -stacking. In solvents competitive for hydrogen bonds affinities decrease to 2.6 kcal mol⁻¹ (water).

Initial efforts were directed towards the creation of a metal center within the receptor molecule as a center for catalysis. The application of a water-soluble version of the Kemp's imide modules enabled substrate binding in this most bio-relevant medium. A receptor linked to 2,2'-bipyridine combined with Cu(II) was used in the hydrolysis of an activated adenosine 5'-phosphotriester.

To fully exploit the binding potential of the adenine receptors, we returned to organic solvents (chloroform) and catalytic coupling reactions were developed. A coupling of two adenosine derivatives, an active ester and an amine was enhanced 10-fold by a bisubstrate template. In a separate experiment, the coupling product was capable of accelerating the formation of the original template, which is itself formed from an active ester and an amine. Thus a formal replication cycle was created. Template effects were supported by competitive inhibition, control molecules, solvent effects, molecular modeling, and mathematical simulations. Sizable accelerations (10^3) were observed in bimolecular coupling reactions in which the two reaction partners associate in a way that results in a close proximity of the reactive groups.

Template effects were explored in more detail with a series of potential bisubstrate templates. Their efficacy varied dramatically with their structure in the enhancement of the coupling of two adenosine derivatives. The reaction inside the best template is 700-fold faster than the background reaction.

In complementary studies a coupling between n-butylamine and an adenosine active ester was enhanced by receptors outfitted with various functional groups, positioned for polar transition state stabilization. The highest acceleration (250-fold) was due to a carboxylate group.

The adenine receptors were linked to a peptide backbone for potential use with peptide nucleic acids (PNAs).

RNA hydrolysis was effected with a receptor linked to 2,2'-bipyridine.

Thesis Supervisor: Dr. Julius Rebek, Jr.

Title: Camille Dreyfus Professor of Chemistry

Acknowledgements

The work described here was accomplished thanks to a large number of people. I want to thank all the people that have passed through the Rebek group throughout the years, many of them have given me invaluable advice and the necessary criticism to progress. It has been very interesting and rewarding to work with people with such diverse backgrounds. Especially I would like to thank my "baymates" Thomas Jenny, Steve Watton, Qing Feng and Xavier Garcias for putting up with my excitement as well as my despair, caused by the ups and downs of research. I thank the people with whom I was fortunate to collaborate and whose perspectives on science have broadened my horizons: Belinda Tsao for her work on the kinetics on the phosphotriesters and mathematical wizardry; Stefan Wölfl for his work on RNA hydrolysis and for his faith in my molecules; Ivan Huc I thank for a fruitful collaboration on the catalysis in chloroform. His enthusiasm, intelligence and energy have been very inspiring and have raised the work to a higher level. Hopefully we will have more chances to collaborate in the future. The work described here would have taken several years longer if it weren't for the four O'clock coffee club: Ken Shimizu, Anthony England, Alexandre Huboux, Blake Hamman and Linda Szabo as well as many 'guests' on the steps and in the coffeehouse. I thank them for their friendship and the many hours well-spent complaining, joking brainstorming, pigeon feeding, reciting Letterman, etc. This daily break will be dearly missed. I also want to thank my previous supervisors Profs. Ben Feringa and Mike Doyle for their enthusiasm and guidance and for having faith in my abilities as a chemist. I want to thank my parents for providing an encouraging environment which stimulated me to go to university and for supporting my endeavors in far and strange places. Julius Rebek, I thank for his support, encouragement, sense of humor, knowledge of wine, for giving me the freedom to explore my own ideas, and for showing me the importance of aiming high. His seemingly effortless way of managing his research and other academic and industrial commitments never cease to amaze me.

Roelof Jan (Roland) Pieters

Table of Contents

Abstract.....	7
Acknowledgements.....	9
Table of Contents.....	11
List of Figures.....	14
List of Schemes.....	17
List of Tables.....	18
Chapter I. An Introduction to Molecular Recognition and Catalysis.....	19
I.1 Supramolecular Chemistry, Molecular Recognition and Catalysis.....	19
I.2 Synthetic Receptors.....	20
I.3 Template Catalysis.....	25
I.4 Other Enzyme models.....	27
I.5 Catalysis by Functionalized Adenine Receptors.....	30
Chapter II. Synthesis and Binding Studies of New Molecular Clefts for Recognition and Catalysis.....	33
II.1 Introduction.....	33
II.2 Synthesis.....	34
II.3 Binding Studies.....	37
II.4 Metal Ion Binding.....	40
II.5 Conclusions.....	41
II.6 Experimental Section.....	41

Chapter III. Hydrolysis of Phosphate Triesters by a Novel Cleft. Influence of Binding on Rate Acceleration.....	47
III.1 Introduction.....	47
III.2 Catalytic Hydrolysis	48
III.3 Influence of binding.	52
III.4 Conclusions.....	54
III.5 Experimental Section	55
Chapter IV. Reciprocal Template Effects in Bisubstrate Systems: A Replication Cycle	57
IV.1 Introduction.....	57
IV.3 Template Effects.....	61
IV.4 Solvent Effects.	62
IV.5 Molecular Modeling.....	63
IV.6 Simulation vs. Experiment.....	64
IV.7 Reciprocal Template Effects	65
IV.8 Bimolecular Coupling Reactions	68
IV.9 Conclusion.....	69
IV.10 Experimental Section	70
Chapter V. Template Effects and Polar Transition State Stabilization in Catalysis of Organic Reactions	77
V.1 Introduction.....	77
V.2 Template Catalysis in Bisubstrate Systems.	78
V.3 Binding studies.....	83

V.4	Conformational Preferences Templates.....	86
V.5	Discussion Template Catalysis	88
V.6	Catalyzed Hydrolysis in CHCl ₃	89
V.7	Catalysis by Functional Groups.....	91
V.8	Polar Transition State Stabilization.....	95
V.9	Conclusions.....	98
V.10	Experimental Section	98
Chapter VI. Synthesis of Adenine Receptors Linked to a Peptide Backbone.		109
VI.1	Introduction.....	109
VI.2	Synthesis.....	111
VI.3	Conclusions.....	112
VI.4	Experimental Section	113
Chapter VII Synthetic Catalysts for RNA Hydrolysis		115
VII.1	Introduction.....	115
VII.2	RNA hydrolysis with Adenine Receptors.....	117
VII.3	Conclusions.....	119
VII.4	Experimental Section	121
Appendix.....		123

List of Figures

Figure I-1.	Synthetic receptors developed by Hamilton and Still	21
Figure I-2.	Hosts of Wilcox and Zimmerman.....	22
Figure I-3.	Diederich's pyrene binder.....	22
Figure I-4.	Breslow's cyclodextrin dimer and guest.	23
Figure I-5.	Dougherty's receptor for the investigation of cation- π interactions.....	24
Figure I-6.	Host-guest systems of Lehn and Hamilton that use electrostatic interactions.....	24
Figure I-7.	Sanders' host and guest which associate through metal-ligand binding.	25
Figure I-8.	Template catalysis applied in catenane formation and acceleration of an S_N2 reaction.	26
Figure I-9.	Reactions catalyzed by Sanders' cyclic porphyrin trimer.....	27
Figure I-10.	A catalytic cyclophane and a reference compound.	28
Figure I-11.	A quinuclidinone enolization catalyst.	29
Figure I-12.	Reactions catalyzed by model systems through polar transition state stabilization.	29
Figure I-13.	The carbazole based adenine receptor used throughout this thesis for substrate binding.	31
Figure II-1.	The binding of adenine derivatives by diimide receptors.....	34
Figure II-2.	Observed NOE signals for 206	36
Figure II-3.	Binding mode of 213 to 210	39

Figure II-4.	Minimized structures of the complex of 212 with the diimide	40
Figure II-5.	Electronic absorption spectra of the titration of 211 with 0.25 equiv portions of CuCl ₂	41
Figure III-1.	The hydrolysis of the phosphate triesters.	48
Figure III-2.	The mechanism of hydrolysis of phosphotriesters 303 or 304	49
Figure III-3.	Minimized structure of the host-guest complex between 304 (darkened structure) and metal free 301	53
Figure IV-1.	Schematic representation of a template enhanced coupling reaction.....	58
Figure IV-2.	The binding of adenine derivatives by diimide receptors.....	58
Figure IV-3.	Structures of amines and active esters.	59
Figure IV-4.	Structures of coupling products/templates.	62
Figure IV-5.	Absorption increases at 330 nm over time for the reaction between 401 and 402	62
Figure IV-6.	Minimized structure of the termolecular complex 401-402-415	64
Figure IV-7.	Observed acceleration of 401+402 vs. the amount of template 415	65
Figure IV-8.	Schematic representation of the replication cycle.....	66
Figure IV-9.	Bimolecular complex proposed for the fast reaction between 402 and 403	68
Figure IV-10.	The initial rate of the reaction between 401 and 404 vs. the amount of 401	69
Figure V-1.	Structures of the bis-receptors used as molecular templates.	80

Figure V-2.	Coupling of 501 and 502 in CHCl ₃	82
Figure V-3.	Observed initial rate ($10^{-6}\cdot\text{M}^{-1}\cdot\text{min}^{-1}$) of 501+502 vs. the amount of template 505f	83
Figure V-4.	Structures of molecules used in the binding studies.	84
Figure V-5.	Titration data of four UV-titrations.....	86
Figure V-6.	Preferred conformation of template 505c	87
Figure V-7.	Structures of the molecules used as catalyst and control compounds in the reaction of BuNH ₂ and 502	92
Figure V-8.	Schematic representation of the aminolysis catalysis by 517	95
Figure V-9.	Predicted structure of the complex between 517g and the reaction intermediate.	96
Figure VI-1.	The structure of DNA and PNA.....	109
Figure VI-2.	Minimized structure of the complex between 606 and ApA.....	111
Figure VII-1.	RNA hydrolysis by a bis-alkylguanidinium receptor.....	115
Figure VII-2.	A lanthanide complex effective in RNA hydrolysis.....	116
Figure VII-3.	Structure of the sequence-selective artificial hydrolytic ribonuclease.....	116
Figure VII-4.	Successful non-metal RNA-cleaving molecules.....	117
Figure VII-5.	Structure of the receptors screened for RNase activity.	118
Figure VII-6.	Autoradiographs of 20% denaturing polyacrylamide gels showing the partial cleavage of RNA-1 and RNA-2.....	120

List of Schemes

Scheme II-1. The synthesis of the dipyrazole cleft.....	35
Scheme II-2. The synthesis of the water-soluble bipyridyl cleft.....	37
Scheme IV-1. Synthesis of amine 403	60
Scheme IV-2. Synthesis of reference 'templates'.	61
Scheme V-1. Covalent coupling reaction which was used for the template studies.	79
Scheme V-2. Synthesis of the bis-receptors.	80
Scheme V-3. The hydrolysis reaction catalyzed by 505e and the structure of additives.....	90
Scheme V-4. Synthesis of receptors and control compounds.....	93
Scheme V-5. Covalent coupling reaction which was used for the studies with the catalytic receptors.	94
Scheme IV-1. The synthesis of the dimer	112

List of Tables

Table II-1.	Association constants of adenine derivatives	38
Table III-1.	List of catalytic rate constants.....	51
Table III-2.	List of second-order rate constants.....	52
Table VI-1.	Initial Rates of Amide formation.	67
Table V-1.	Observed rate accelerations in the coupling of 501+502	81
Table V-2.	Association energy of bis and mono receptors	85
Table V-3.	Rate accelerations observed in the hydrolysis of 502	91
Table V-4.	Observed rate accelerations in the butylaminolysis of 502 by 1 equiv of various catalysts	94

Chapter I. An Introduction to Molecular Recognition and Catalysis.

I.I Supramolecular Chemistry, Molecular Recognition and Catalysis

In order to explain and predict the behavior of molecules it is crucial to have an understanding of the intermolecular forces involved. Supramolecular chemistry¹ is the highly interdisciplinary field that studies and utilizes these interactions in settings as diverse as biology and physics. Molecular recognition² is the key to supramolecular chemistry since it deals with the transfer of information inherently present in chemical structures. This communication process controls supramolecular phenomena. Potential applications are still emerging,³ but due to the intense research effort in this field over the last few years progress has been made on several fronts. Some areas where applications are sought are the following:

- Synthesis guided by molecular recognition phenomena including self-assembly can yield compounds or materials with unprecedented structure and/or properties.
- A quantification of intermolecular forces can aid the rational design of drugs and deepen our understanding of biological processes.
- New diagnostic and analytical tools can be developed with applications in research and medicine.
- Selective receptors linked to solid supports can be used to effect convenient separations.
- The development of chemical devices such as sensors and switches is at hand. In more abstract terms: the use of recognition phenomena for signal (and thus information) generation, transfer, and detection is possible.
- The development of catalysis based on molecular recognition and using Nature's enzymes for inspiration, is progressing. This includes the design and synthesis of enzyme models as well as their development for practical selective catalytic processes.

The work described in this thesis fits the last category and is concerned with the development of catalytic processes based on molecular recognition. In other words,

(1) Lehn, J.-M. *Angew. Chem. Int. Ed. Engl.* **1990**, *29*, 1304.

(2) Rebek, J., Jr. *Angew. Chem. Int. Ed. Engl.* **1990**, *29*, 245

(3) Schneider, H.-J. *Angew. Chem. Int. Ed. Engl.* **1991**, *30*, 1417.

merging recognition and catalysis is the objective. The goal was not to exactly mimic a specific enzyme but rather their 'style' of enhancing reactions. Such catalysts fit a broader definition of enzyme models.⁴ The promise of model systems is their capacity to isolate catalytic parameters (ΔH^\ddagger , ΔS^\ddagger) and study them independently. In the next three sections examples from the literature are given. First, several types of high affinity receptors are shown, followed by catalytic systems that have been developed starting with these types of receptors. The last section of this chapter describes the thought processes on which the approach taken in this thesis was based.

I.2 Synthetic Receptors

The design of catalysts based on molecular recognition relies to a large extent on the types of intermolecular interactions involved. Over the last decade large numbers of synthetic host-guest systems have appeared in the literature. In several cases very high binding affinities have been achieved ($>10 \text{ kcal mol}^{-1}$), usually by combining a number of additive intermolecular interactions. A consequence of the choice of interactions is that the system operates only (or best) under specific conditions. Usually this means either in aqueous solutions or in organic solvents. This, of course, restricts the catalytic chemistry that can be achieved. In the next section examples from the literature are shown of high affinity synthetic host-guest systems. In this series several different intermolecular interactions or different combinations of interactions form the basis for the association.

Hydrogen bonds are weak in aqueous solution, yet they are very important in Nature communicating information transfer (e.g. in nucleic acid replication) and specificity in other chemical transformations. They can be important because they operate only in hydrophobic environments such as an enzyme active sites or interior of double stranded nucleic acids, where few competing water molecules are present. With synthetic systems their strength has been amplified using non-competitive organic solvents. Hamilton et al.⁵ have prepared a macrocyclic receptor, which binds barbiturates with 6 hydrogen bonds. With barbital it forms complex **101** (Figure I-1) with a binding energy of $8.4 \text{ kcal mol}^{-1}$ in CDCl_3 . Other systems have been prepared by Still et al.⁶ who have made several different types of basket

(4) (a) Reichwein, A. M.; Verboom, W.; Reinhoudt, D. N. *Recl. Trav. Chim. Pays-Bas*, **1994**, *113*, 343. (b) Kirby, A. *Angew. Chem. Int. Ed. Engl.* **1994**, *33*, 551.

(5) Chang, S. K.; Hamilton, A.D. *J. Am. Chem. Soc.* **1991**, *113*, 201.

(6) (a) Hong, J.-I.; Namgoong, S. K.; Bernardi, A.; Still, W. C. *J. Am. Chem. Soc.* **1991**, *113*, 5111. (b) Liu, R.; Still, W. C. *Tetrahedron. Lett.* **1993**, *16*, 2573. (c) Borchardt, A.; Still, W.C. *J. Am. Chem. Soc.* **1994**, *116*, 373. (d) Yoon, S. S.; Still, W. C. *J. Am. Chem. Soc.* **1993**, *115*, 823.

shaped receptors with amide groups as hydrogen bond donors and acceptors. The hosts are highly preorganized and also chiral, which has resulted in excellent enantioselective binding. Host **102** binds N-Ac-L-Thr-NHMe with a binding energy of >6.2 kcal mol⁻¹ which is over 3 kcal mol⁻¹ more than that for the corresponding D-enantiomer. The binding of the preferred enantiomer is believed to result from 3 hydrogen bonds. This host is also capable of binding organic soluble carbohydrates such as octyl glycosides with affinities of up to 5.1 kcal mol⁻¹. Using a combinatorial library screening method^{6c} several protected tripeptides were found to be good guests for a closely related derivative of **102**.

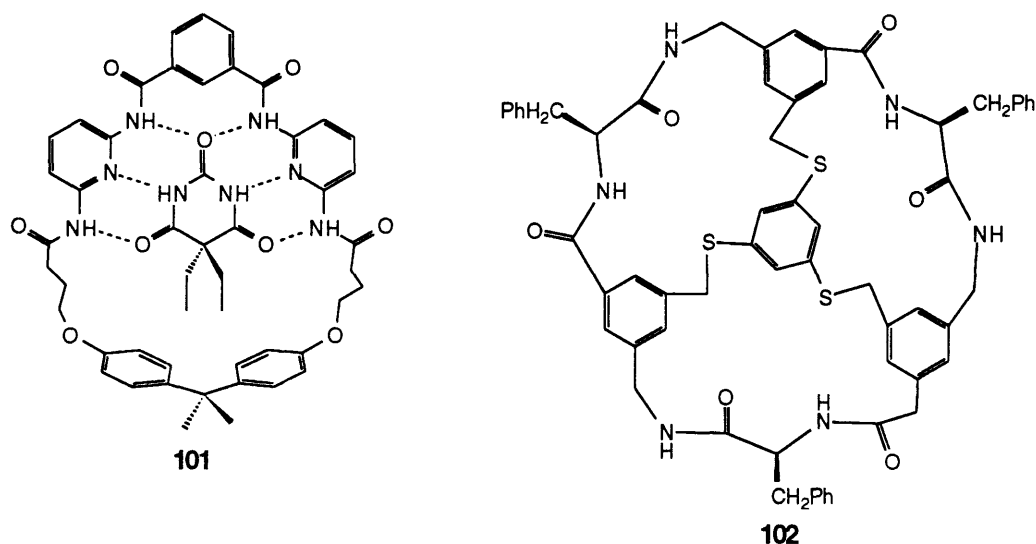


Figure I-1. Synthetic receptors developed by Hamilton and Still

Wilcox et al. have prepared a receptor containing two convergent carboxylic acid groups.⁷ This system was shown to be an effective host for several guests, e.g. 2 aminopyrimidine, bound by 4 hydrogen bonds as shown in complex **103** with an affinity of 4.7 kcal mol⁻¹ (Figure I-2). Zimmerman et al. have prepared a system reminiscent of tweezers⁸ (**4**) which is capable of binding 9-propyladenine with an affinity of 6.0 kcal mol⁻¹. This system combines two hydrogen bonds with π - π stacking⁹ from

(7) (a) Adrian, J. C., Jr.; Wilcox, C. S. *J. Am. Chem. Soc.* **1989**, *111*, 8055. (b) Adrian, J. C., Jr.; Wilcox, C. S. *J. Am. Chem. Soc.* **1991**, *113*, 678. (c) Wilcox, C. S. in *Frontiers in Supramolecular Organic Chemistry and Photochemistry*, Schneider, H. J.; Dürr, H., Eds.; VCH, Weinheim, Germany, 1991; pp 123-143.

(8) (a) Zimmerman, S. C.; Wu, W. *J. Am. Chem. Soc.* **1989**, *111*, 8054. (b) Zimmerman, S. C.; Wu, W.; Zeng, Z. *J. Am. Chem. Soc.* **1991**, *113*, 196.

(9) For a discussion on π - π interactions see Hunter, C. A.; Sanders, J. K. M. *J. Am. Chem. Soc.* **1990**, *112*, 5525.

two sides. Calculations suggested a roughly equal contribution of hydrogen bonds and aromatic stacking interactions.¹⁰

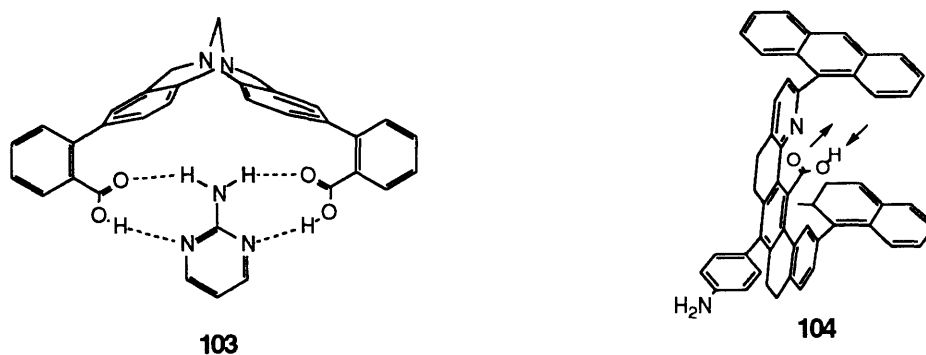


Figure I-2. Hosts of Wilcox and Zimmerman.

Diederich et al. have synthesized the macrobicyclic cyclophane **105** (Figure I-3).¹¹ In its unprotonated form this molecule was shown to bind pyrene in solvents that span almost the entire polarity spectrum. In water the binding energy was found to be 9.4 kcal mol⁻¹, whereas at the other extreme 1.3 kcal mol⁻¹ was measured in CS₂. A good correlation was found between binding affinity and the empirical solvent polarity parameter E_T(30)¹² in which factors like dielectric constant, polarizability and dipole moment are expressed.

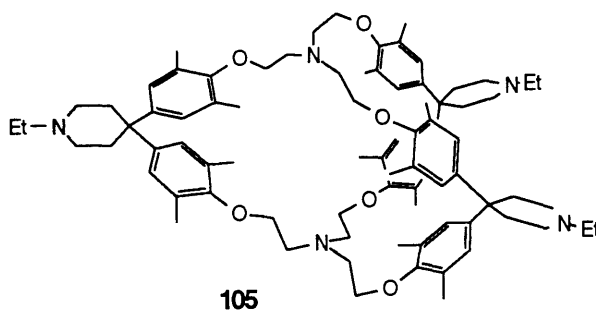


Figure I-3. Diederich's pyrene binder.

Separate correlations with solvent cohesion and solvent polarizability were not as good, but they showed a clear trend, nevertheless. The higher the solvent cohesion the stronger

(10) Blake, J. F.; Jorgensen, W. L. *J. Am. Chem. Soc.* **1990**, *112*, 7269.

(11) Smithrud, D. B.; Diederich, F. *J. Am. Chem. Soc.* **1990**, *112*, 339.

(12) Reichardt, C. *Solvents and Solvent Effects in Organic Chemistry*, 2nd ed.; VCH, Weinheim, Germany, 1988; pp 339-405

the binding due to releasing solvent molecules upon binding: the **solvophobic effect**. The higher the polarizability of the solvent, the less of an advantage complexation has and, accordingly, the lower the binding since both host and guest are polarizable units.

By linking two hydrophobic binding sites - cyclodextrins - with a spacer element, Breslow et al. have created hosts with a very high affinity for appropriate guests (Figure I-4).¹³ In aqueous solution host **106** binds **107** with a binding energy of 10.3 kcal mol⁻¹, compared to 6.5 kcal mol⁻¹ for a single cyclodextrin/naphtyl interaction. Surprisingly the difference was due to an increase in binding enthalpy instead of entropic factors, commonly associated with a chelate effect.

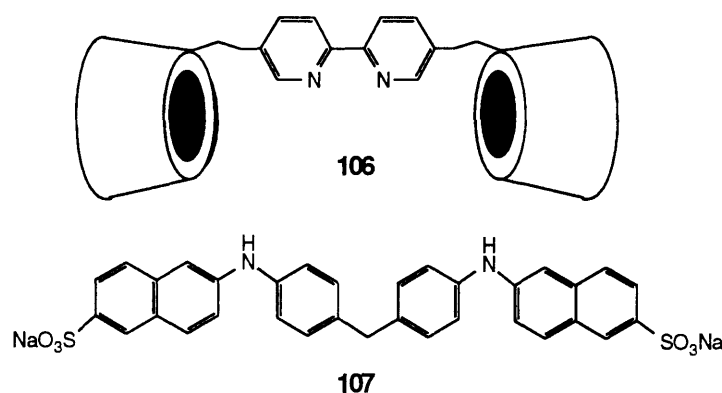


Figure I-4. Breslow's cyclodextrin dimer and guest.

Dougherty et al. used a hydrophobic cyclophane receptor as a tool to investigate **cation- π interactions** (Figure I-5).¹⁴ This type of interaction can be defined as the stabilizing force between a positive charge and the face of an aromatic ring. The contribution of these forces can be sizable as can be seen in the difference in binding energy to **108** (in water), between the charged **109** (8.4 kcal mol⁻¹) and the geometrically similar but neutral **110** (5.9 kcal mol⁻¹). The inherent effect is likely to be even larger, since **109** is much better solvated than **110**, a factor which would decrease its binding. The importance of this type of interaction in certain biological receptors has been proposed.¹⁴

(13) Zhang, B.; Breslow, R. *J. Am. Chem. Soc.* **1993**, *115*, 9353.

(14) (a) Kearney, P. C.; Mizoue, L. S.; Kumpf, R. A.; Forman, J. E.; McCurdy, A.; Dougherty, D. A. *J. Am. Chem. Soc.* **1993**, *115*, 9907, and references cited therein.

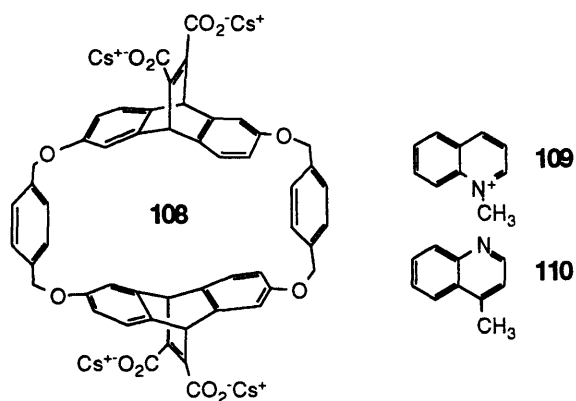


Figure I-5. Dougherty's receptor for the investigation of cation- π interactions.

Electrostatic interactions have also been utilized in synthetic supramolecular systems. The interaction between ions of opposite charge is strong, and can even be observed in a good solvating medium such as water. In Nature hydrogen bonds between charged partners frequently occur and usually add significant stabilization to ground and transition states. Lehn et al. have created an ATP receptor which functions in water (**111**, Figure I-6).¹⁵ The binding energy of the tetracationic macrocyclic portion of receptor to the tetra-anionic ATP is 6.5 kcal mol⁻¹. The acridine only adds about a factor of two to the binding constant by stacking interactions. Hamilton et al. have used a dicationic bis-acylguanidinium receptor to bind a mono anionic phosphodiester in CH₃CN with an affinity of 6.4 kcal mol⁻¹.¹⁶ The electrostatic interaction is part of a maximum of four hydrogen bonds, possibly as shown in **112**, which are responsible for the association.

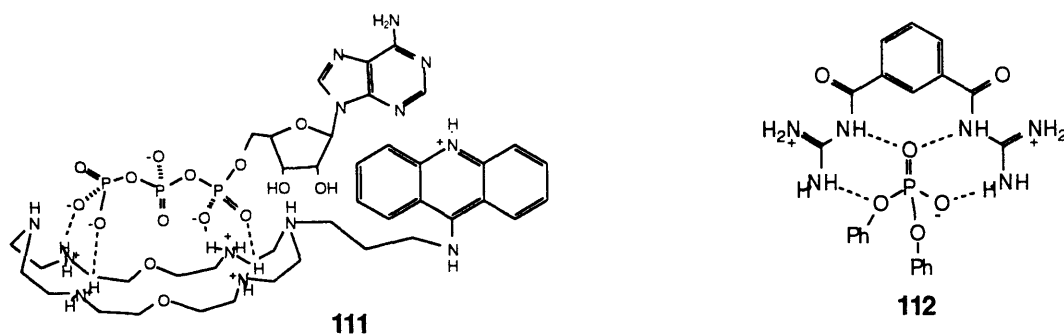


Figure I-6. Host-guest systems of Lehn and Hamilton that use electrostatic interactions.

(15) Hosseini, M. W.; Blacker, A. J.; Lehn, J.-M. *J. Am. Chem. Soc.* **1990**, *112*, 3896.

(16) Dixon, R. P.; Geib, S. J.; Hamilton, A. D. *J. Am. Chem. Soc.* **1992**, *114*, 365.

Metal-ligand binding has been used by Sanders et al. in the association of tripyridine **114** inside the tris-zinc-porphyrin system **113**, which occurs with a binding energy in CH_2Cl_2 of $13.6 \text{ kcal mol}^{-1}$ (Figure I-7). The binding energy of a single pyridine to a zinc-porphyrin is about 5 kcal mol^{-1} , illustrating that the interactions are largely additive.

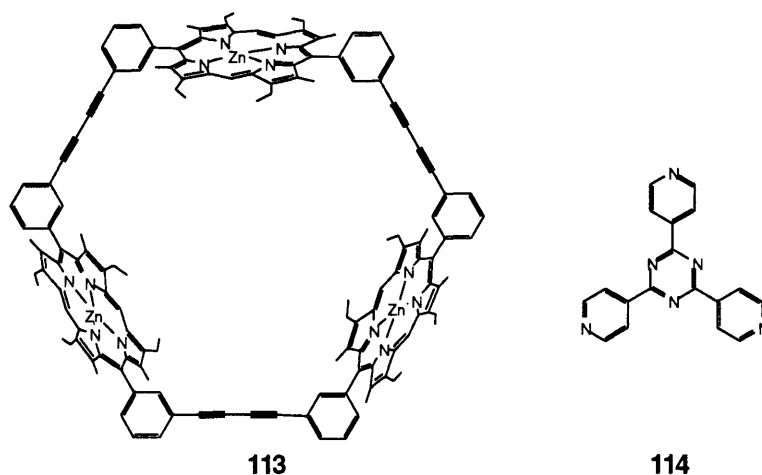


Figure I-7. Sanders' host and guest which associate through metal-ligand binding.

In summary, the use of several types of intermolecular interactions has produced a diverse array of high affinity synthetic receptors. They are based on hydrogen bonds, π -stacking, hydrophobic effects, cation- π interactions, ionic interactions and metal-ligand binding. Nature makes use of them simultaneously in many cases. In synthetic systems some of these interactions have been successfully combined e.g. hydrogen bonding and π -stacking or hydrophobic effects and cation- π interactions. However, the combination of hydrogen bonding and hydrophobic effects, important in enzymes, is still mostly undemonstrated. In part, this is a synthetic problem because it requires the preparation of a solvent shielded cavity internally lined with hydrogen bonding groups. For the development of enzyme models this is of importance because it would allow an enzyme model to work in water and have substrate recognition rather than shape-selectivity, and using all the available information in a structure.

I.3 Template Catalysis

A significant number of enzyme models catalyze reactions by bringing two reactants in close proximity. This reduces the activation entropy of the reaction, and catalysts of this

sort are considered to be a templates.¹⁷ The use of templates goes well beyond the field of enzyme models, since they have been used for synthetic purposes for a long time, mostly to effect difficult ring closures. One can consider template effects as the enhancement of chemical reactions by complementary surfaces. A more detailed discussion about template catalysis, its requirements, characteristics and limitations is in chapters IV and V of this thesis. In this section a few representative examples are shown that fit the general definition.

The first template is a very simple one, namely a Cu(I) ion. This metal ion has a preference for a tetrahedral coordination geometry e.g. with two substituted 1,10-phenanthroline units. Sauvage et al.¹⁸ took advantage of this by using phenanthroline units with phenolic substituents on the 2 and 9 position. Reacting the corresponding Cu(I) complex with an appropriate diiodide resulted in the formation of the interlocked system **115** in 27% yield (Figure I-8). Kelly et al. have applied template effects in the enhancement of an S_N2 reaction. The template consists of two linked receptor sites which can bind two different substrates simultaneously, using hydrogen bonds, in the termolecular complex **116**. The coupling rate of the substrates was enhanced 12-fold in the presence of one equiv. of the template in CDCl₃.

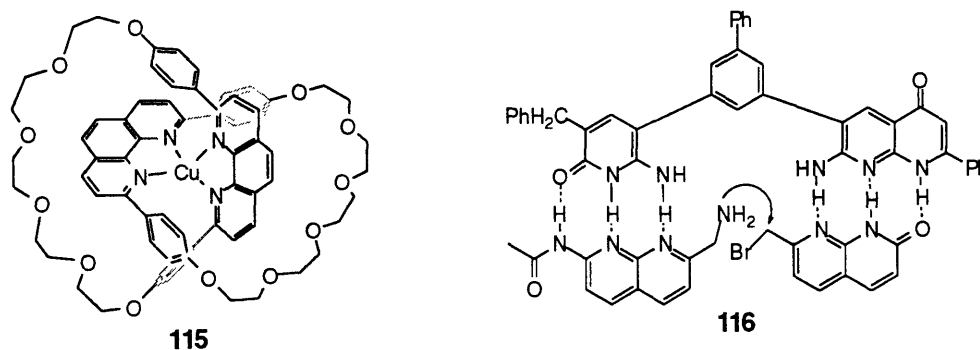


Figure I-8 Template catalysis applied in catenane formation and acceleration of an S_N2 reaction.

Sanders et al¹⁹ showed that their tris-porphyrin **113** was capable of catalyzing the Diels-Alder between diene **117** and dienophile **118** to give the exo-product **119** (exo

(17) For recent reviews see (a) Hoss, R.; Vögtle, F., *Angew. Chem. Int. Ed. Engl.* **1994**, *33*, 375; (b) Anderson, S.; Anderson, H. L.; Sanders, J. K. M. *Acc. Chem. Res.* **1993**, *26*, 469.

(18) Dietrich-Buchecker, C. O.; Sauvage, J.-P.; Kern, J.-M. *J. Am. Chem. Soc.* **1984**, *106*, 3043.

(19) (a) Walter, C. J.; Anderson, H. L.; Sanders, J. K. M. *J. Chem. Soc., Chem. Commun.* **1993**, 458. (b) Mackay, L. G.; Wylie, R. S.; Sanders, J. K. M. *J. Am. Chem. Soc.* **1994**, *116*, 3141. (c) Bonar-

selectivity > 95%, Figure I-9). In the absence of **113** the reaction yields (besides the exo-product) the endo-product. The initial rate was enhanced 1000-fold at 30 °C. This system suffers from product inhibition, since the product is bound more strongly than either of the starting materials. In order to circumvent this, a group transfer process is more attractive in comparison to a coupling reaction. A derivative of **113** was shown to be a catalysts in the acyl transfer reaction between alcohol **120** and acetylimidazole **121**, without product inhibition and with turn-over. This reaction was enhanced 16-fold by 0.05 equiv of the catalyst in toluene at 70 °C. That is, the transition state (or intermediate), a bimolecular complex, is bound better than the termolecular complexes of starting materials or products.

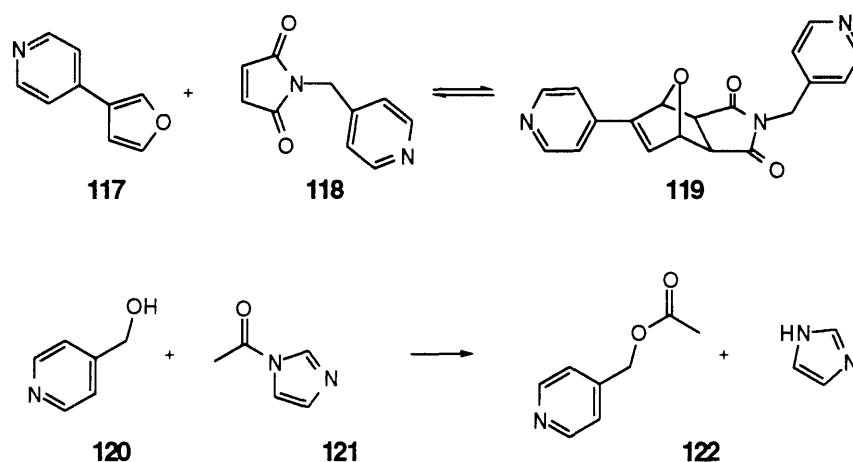


Figure I-9. Reactions catalyzed by Sanders' cyclic porphyrin trimer.

I.4 Other Enzyme models

Other types of enzyme models, which focus on different aspects of enzyme catalysis have also appeared. Transition states can be stabilized by reducing the activation entropy of a reaction as seen before in the template section,²⁰ but also by polar (or apolar) stabilization which reduce the activation enthalpy. In some model systems these effects operate simultaneously as they seem to do in actual enzymes. In other systems catalytic

Law, R. P.; Mackay, L. G.; Walter, C. J.; Marvaud, V.; Sanders, J. K. M. *Pure & Appl. Chem.* **1994**, 66, 803.

(20) Although the catalysis is dominated by entropic effects, some polar contribution due to moving a reaction from free solution into a cleft or receptor microenvironment can not be excluded.

effects can be largely attributed to polar stabilization. In this section a few successful model systems are presented and the nature of the catalysis is discussed.

Diederich et al²¹ have prepared the catalytic cyclophane **123** (Figure I-10). It contains a thiazolium ring and acts as a pyruvate-oxidase mimic. The initial rates of the oxidation of naphthalene-2-carbaldehyde to the corresponding acid in the presence of 0.08 equiv of **123** was over a 100-fold faster than with same amount of **124** (also present: potassium ferricyanide as the oxidizing agent in DMSO/water (3:2)). The enhancements were attributed to both entropic effects as well as apolar stabilization, due to moving the reaction to an apolar cavity. An apolar environment is accelerating for this system since the relevant transition states of the reaction are less polar than the ground states.

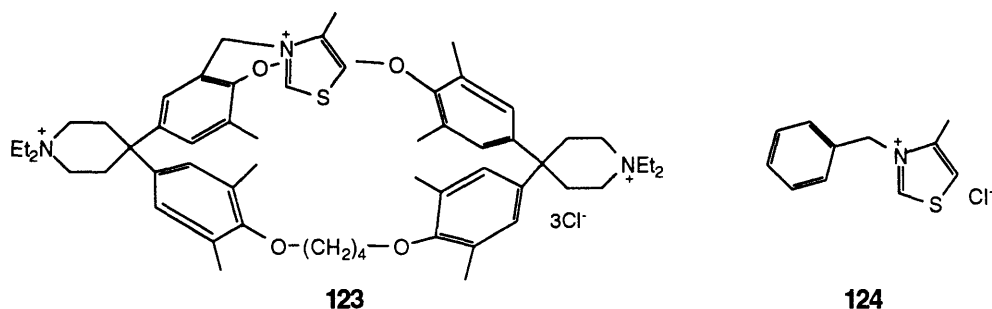


Figure I-10. A catalytic cyclophane and a reference compound.

Rebek et al.²² have shown the efficient use of convergent functional groups in the enhancement of enolization of quinuclidinone (Figure I-11). The substrate binds to the receptor in CDCl₃ with an affinity of 4.1 kcal mol⁻¹. The receptor (0.1 equiv) accelerates the enolization of quinuclidinone 60 times in wet CDCl₃ and saturation kinetics as well as competitive inhibition by related but unreactive substrates were observed. It was proposed that the acridine nitrogen acts as a general base whereas one of the carboxylic acid groups could act as a general acid, possibly in a concerted process as shown in **124**. The other carboxylic acid group would just be for binding to the ammonium function. Both entropic effects (bringing substrate and general base together) and polar transition state stabilization (due to the general acid) are likely as causes of the enhancements.

(21) Tam-Chang, S.-W.; Jiminez, L.; Diederich, F. *Helv. Chim. Acta.* **1993**, *76*, 2616.
(22) Wolfe, J.; Muehldorf, A.; Rebek, J., Jr. *J. Am. Chem. Soc.* **1991**, *113*, 1453.

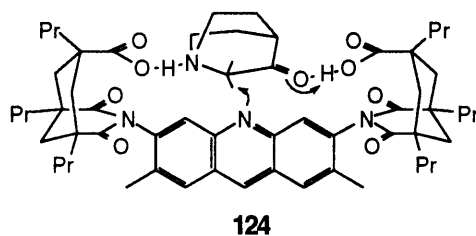


Figure I-11. A quinuclidinone enolization catalyst.

The cation- π interaction was used by Dougherty et al.²³ in the catalysis of the methylation of quinoline **125** (Figure I-12). In this reaction a positive charge builds up in the transition state which is stabilized by the cyclophane **108**. The intracomplex reaction was estimated to be 80-fold faster than the uncatalyzed reaction. Both the catalyzed and uncatalyzed reaction are bimolecular in nature. In the uncatalyzed reaction a methyl iodide molecule reacts with a molecule of quinoline, whereas in the catalyzed version the methyl iodide reacts with the quinoline-cyclophane complex. This implies that there is no entropic component to the catalysis which must therefore be caused by polar transition state stabilization alone.

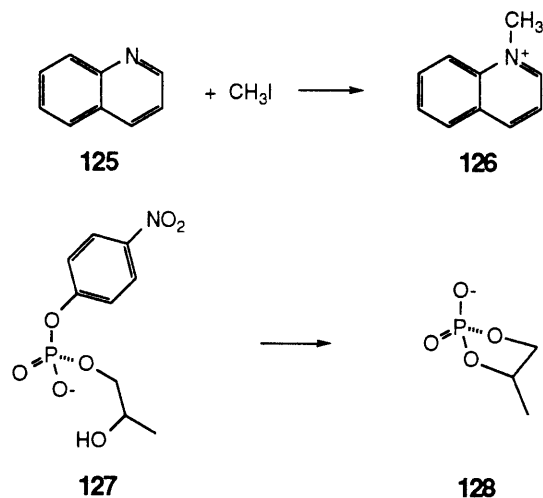


Figure I-12. Reactions catalyzed by model systems through polar transition state stabilization.

(23) McCurdy, A.; Jimenez, L.; Stauffer, D. A.; Dougherty, D. A. *J. Am. Chem. Soc.* **1992**, *114*, 10314.

Hamilton et al.²⁴ used their bis-acylguanidinium system **112** for catalysis of the intramolecular phosphoryl transfer of **127**. In CH₃CN 50 equiv. of **112** accelerated the reaction 290-fold. The receptor is complementary to the dianionic trigonal-bipyramidal intermediate which likely resembles the crucial transition state. Since the nucleophile is part of the substrate, an entropic contribution to the catalysis should be negligible. Again, the effects should be due to polar transition state stabilization.

I.5 Catalysis by Functionalized Adenine Receptors

At the outset of this work in the Rebek group, highly effective adenine receptors had recently been created.²⁵ The receptors contained a carbazole scaffold which was functionalized with two imide surfaces complementary to adenine. Adenine derivatives were bound by 6-7 kcal mol⁻¹ due to the incremental additive effects of hydrogen bonding and π -stacking. The geometry of the complex, as inferred from NMR data, is shown in Figure I-13. Molecular modeling suggests that this geometry is well defined, i.e. in order for all the favorable interactions to occur simultaneously (Watson-Crick and Hoogsteen base-pairing and stacking interactions) the adenine has to be positioned in a specific way. In this geometry substituents on the N9 of adenine and the carbazole nitrogen (R' and R'') are oriented in the same direction which led to the suggestion that productive chemistry should be possible between them. Many substituted adenine derivatives are known and functionalization of the carbazole also seemed possible. This was the starting point of the design of catalytic processes.²⁶

(24) Jubian, V.; Dixon, R. P.; Hamilton, A. D. *J. Am. Chem. Soc.* **1992**, *114*, 1120.

(25) Conn, M. M.; Deslongchamps, G; de Mendoza, J.; Rebek, J., Jr. *J. Am. Chem. Soc.* **1993**, *115*, 3548

(26) Portions of the work described in this thesis have already appeared in print or are scheduled to appear. (a) Pieters, R. J.; Rebek, J., Jr. *Recl. Trav. Chim. Pays-Bas*, **1993**, *112*, 330. (b) Tsao, B.; Pieters, R. J.; Rebek, J., Jr. *J. Am. Chem. Soc.* **1994**, in press. (c) Pieters, R. J.; Huc, I.; Rebek, J., Jr. *Angew. Chem. Int. Ed. Engl.* **1994**, *33*, 1579. (d) Pieters, R. J.; Huc, I.; Rebek, J., Jr. *Tetrahedron*, in press. (e) Huc, I.; Pieters, R. J.; Rebek, J., Jr. *J. Am. Chem. Soc.* **1994**, *116*, 10296. (f) Huc, I.; Pieters, R. J.; Rebek, J., Jr. *J. Am. Chem. Soc.* **1994**, *116*, 10592. In addition: (g) Pieters, R. J.; Huc, I.; Rebek, J., Jr. (Chapter V) has been submitted for publication.

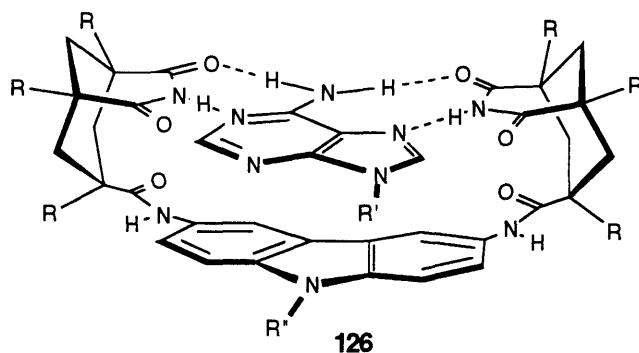


Figure I-13. The carbazole based adenine receptor used throughout this thesis for substrate binding.

Initial efforts were directed towards the creation of a metal center within the receptor as the center for catalysis (Chapter II). The development of a water-soluble version of the Kemp's imide modules²⁷ opened the way for use in this bio-relevant medium albeit with the sacrifice of a significant amount of binding energy. The use in the hydrolysis of phosphotriesters is described in Chapter III. To fully exploit the binding potential of the adenine receptors a return was made to organic solvents and catalytic coupling reactions were developed. In chapter IV the focus is on the information transfer of the catalysis, in the context of a replication cycle. In chapter V the catalysis itself was the focus and especially the exploration of the geometric and electronic/polar factors that determine the rate enhancements. In chapter VI and VII more biological aspects were explored. First, the linking of the adenine receptors to a peptide backbone for potential use with peptide nucleic acids (PNAs)²⁸ Secondly, some of the water-soluble receptors were tested for their ability to cleave RNA.

(27) Rotello, V. M.; Viani, E. A.; Deslongchamps, G.; Murray, B. A.; Rebek, J., Jr. *J. Am. Chem. Soc.* **1993**, *115*, 797.

(28) Nielsen, P. E.; Egholm, M.; Berg, R. H.; Buchardt, O. *Science*, **1991**, *254*, 1497.

Chapter II. Synthesis and Binding Studies of New Molecular Clefs for Recognition and Catalysis

II.1 Introduction

Molecular recognition is the key to most biological processes, and recent insights into molecular recognition phenomena have come from the design and synthesis of artificial receptors for biologically important targets. Placement of convergent functional groups in cleft like molecules¹ has resulted in highly effective receptors for nucleotides, barbiturates, ureas and peptides in their ground states. In enzymes, recognition of transition states is a crucial factor, and bringing recognition and catalysis closer together in space and time is the goal in the development of enzyme-like catalysis. In addition to convergent functional groups, Nature uses metal ions for both recognition and catalysis, and described here are synthetic systems that offer both features. These are due to a new class of adenine receptors which are well-suited for synthetic elaboration.²

The new receptors are based on a carbazole scaffold. They are substituted at the 3 and 6 positions with Kemp's triacid derivatives, which provide the imide hydrogen bonding surface complementary to adenine. The relative orientation of the surfaces is such that the Watson-Crick and Hoogsteen base-pairing can be simultaneous, and this results in very high binding affinities (Figure II-1).

(1) (a) Rebek, J., Jr. *Angew. Chem. Int. Ed Engl.* **1990**, *29*, 245. (b) Nowick, J. S.; Ballester, P.; Ebmeyer, F.; Rebek, J., Jr., *J. Am Chem. Soc.* **1990**, *112*, 8902. (c) Jeong, K.-S.; Tjivikua, T.; Muehldorf, A.; Deslongchamps, G.; Famulok, M.; Rebek, J., Jr. *J. Am. Chem. Soc.* **1991**, *113*, 201. (d) Chang, S. K.; Hamilton, A. D. *J. Am. Chem. Soc.* **1988**, *110*, 1318. (e) Famulok, M.; Jeong, K.-S.; Deslongchamps, G.; Rebek, J., Jr. *Angew. Chem. Int. Ed. Engl.* **1991**, *30*, 858. (f) Hong, J.-I.; Namgoong, S. K.; Bernardi, A.; Still, W. C. *J. Am. Chem. Soc.* **1991**, *113*, 5111. (g) Adrian, J. C., Jr.; Wilcox, C. S. *J. Am. Chem. Soc.* **1989**, *111*, 8055. (h) Zimmerman, S. C.; Zeng, Z.; Wu, W.; Reichert, D. E. *J. Am. Chem. Soc.* **1991**, *113*, 183. (i) Zimmerman, S. C.; Zeng, Z.; Wu, W. *J. Am Chem. Soc.* **1991**, *113*, 196.

(2) Conn, M. M.; Deslongchamps, G; de Mendoza, J.; Rebek, J., Jr. *J. Am. Chem. Soc.* **1993**, *115*, 3548.

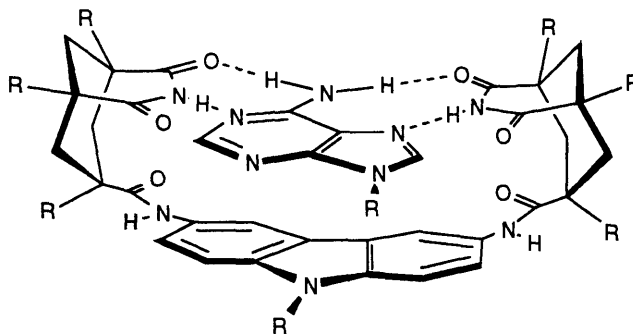
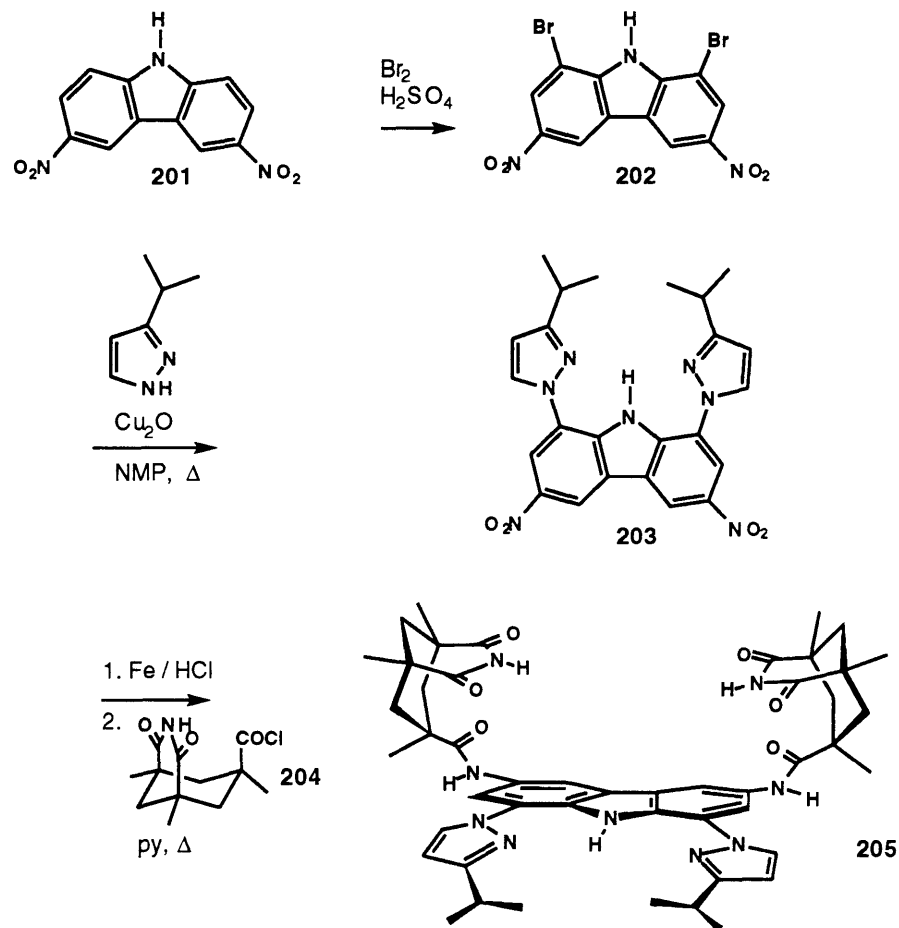


Figure II-1. The binding of adenine derivatives by diimide receptors.

The present study deals with further functionalization of the carbazole moiety for metal binding sites. An appropriately positioned metal ion should be able to catalyze a reaction of a bound adenine derivative and exhibit enzyme-like behavior; i.e. saturation kinetics and turnover. The reaction may be a biologically relevant reaction (e.g., a phosphate ester hydrolysis), or perhaps one without a biological counterpart. In this chapter are described the convergent modular synthesis of two such systems, and studies of their binding behavior in three solvents of different hydrogen bonding abilities. The structural details of the binding interactions are discussed.

II.2 Synthesis

In order to introduce a metal binding site to the carbazole based adenine chelators, we felt that further functionalization of carbazole was necessary. This was accomplished by treating 3,6-dinitrocarbazole **201** with bromine in conc. H_2SO_4 , which gave dibromide **202** in almost quantitative yield (Scheme II-1). The elaboration of the bromides to 5-membered ring heterocycles opened the way to a metal binding site resembling that of a porphyrin, except it has only three nitrogen donor atoms instead of four. The dibromide **202** was successfully coupled to 3(5)-isopropylpyrazole in an Ullmann fashion to give **203**. A large excess of the pyrazole had to be used, but it was possible to recycle this material. Reduction of the nitro groups with Fe and HCl followed by coupling of the resulting diamine with acid chloride **204** resulted in dipyrazole **205**. This product had a solubility of *ca.* 1mM in CHCl_3 .



Scheme II-1. The synthesis of the dipyrazole cleft.

Confirmation of the position of the isopropyl groups was obtained from a NOESY experiment on compound **206** (Figure II-2). The latter was obtained by reacting the diamine with pivaloylchloride. A clear NOESY cross peak was observed between a pyrazole hydrogen and a carbazole hydrogen, providing strong evidence for the structure shown.

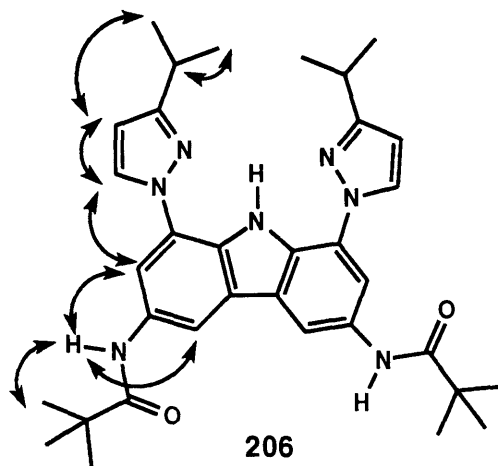


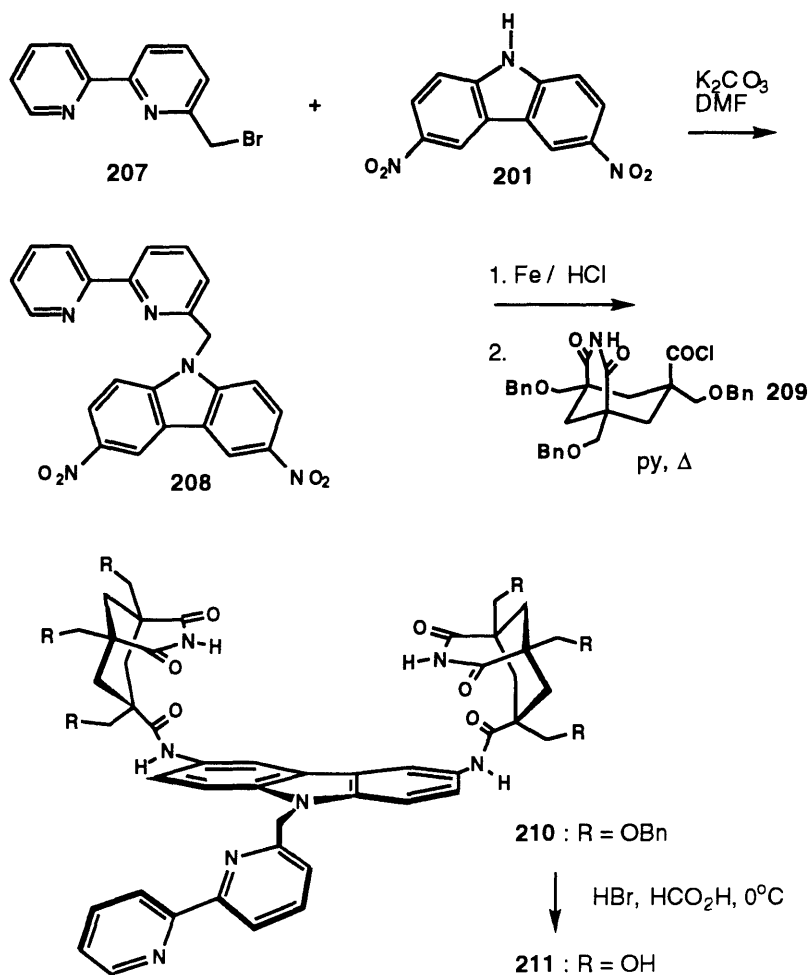
Figure II-2. Observed NOE signals for **206**.

A system bearing a 2,2'-bipyridine unit for the metal binding site was also synthesized. An important advantage of this system is that the coordination chemistry of 2,2'-bipyridine (bipy) systems is well established, and Cu^{2+} /bipy systems have been successful as catalysts for the hydrolysis of phosphate esters.^{3,4} A modular approach was taken in which 6-bromomethyl-2,2'-bipyridyl **207** was reacted with 3,6-dinitrocarbazole in the presence of K_2CO_3 (Scheme II-2). This gave a high yield of **208**; Fe and HCl were again used for the reduction of the nitro groups. Coupling of the diamine with acid chloride **209**, resulted in the organic soluble, receptor-ligand combination **210**. A water-soluble version was obtained by cleaving the benzyl groups by brief treatment with HBr according to a recently established protocol.⁵ The receptor-ligand **211** was thus obtained, and it showed a modest water solubility of 0.25 mM.

(3) Morrow, J. R.; Trogler, W. C. *Inorg. Chem.* **1989**, *28*, 2330

(4) (a) Rosch, M. A.; Trogler, W. C. *Inorg. Chem.* **1990**, *29*, 2409. (b) Modak, A. S.; Gard, J. K.; Merriman, M. C.; Winkeler, K. A.; Bashkin, J. K.; Stern, M. K. *J. Am. Chem. Soc.* **1991**, *113*, 283.

(5) Rotello, V. M.; Viani, E. A.; Deslongchamps, G.; Murray, B. A.; Rebek, J., Jr. *J. Am. Chem. Soc.* **1993**, *115*, 797.

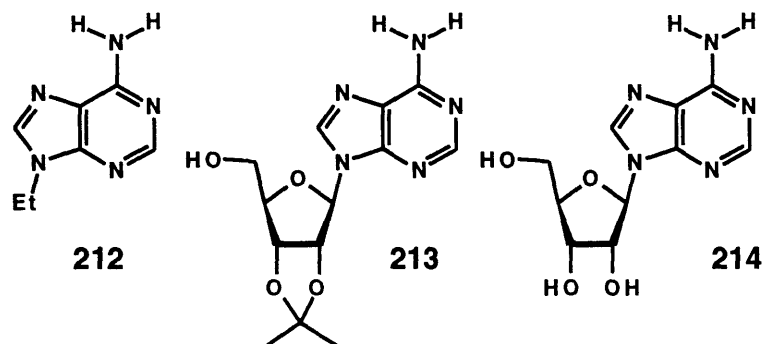


Scheme II-2. The synthesis of the water-soluble bipyridyl cleft

II.3 Binding Studies

Receptor **205** (0.5 mM) was titrated with 9-ethyladenine in CDCl_3 and gave a binding constant of about $1.5 \times 10^5 \text{ M}^{-1}$ (Table II-1). Measuring binding constants of this magnitude with NMR results in significant errors, and only the order of magnitude can be established. The imide hydrogen signal of the host is broad and found around 9.9 ppm suggesting that it is hydrogen bonded; the free imide resonance is usually observed at 7.6 ppm. Since the chemical shift was concentration independent this shift is believed to be the result of an intramolecular contact of the two imides. Molecular modeling using MacroModel and of CPK models support this surmise. On saturation of the host solution with 9-ethyladenine, the imide resonance shifts to 13.4 ppm. Significant broadening of the signal occurs in the early stages of the titration, but the imide signal sharpens as the

saturation point is reached. During the titration the amide and the carbazole NH signals shifted upfield (0.17 and 0.43 ppm respectively). The chemical shifts of the pyrazole hydrogens do not change significantly (< 0.05 ppm) during the titration, suggesting that they are not involved in the binding process.



K_a (M^{-1}), (δ imide of the complex)

Host	Solvent	Guest: 212	213	214
205	$CDCl_3^a$	1.5×10^5 (13.4)		
210	$CD_3COCD_3^a$	1.3×10^3 (13.6)	1.3×10^3 (13.1)	
211	H_2O^b	85 (13.0)		85 (12.1)

Table II-1. Association constants of adenine derivatives, obtained from NMR titrations. ^a At 23 °C. ^b In H_2O/D_2O 9:1, 10 mM sodium cacodylate buffer, ionic strength 50 mM (NaCl). pH 6.0, 10 °C

Receptor **210** was titrated with 9-ethyladenine in acetone- d_6 , instead of the usual $CDCl_3$, because the NMR spectrum of **210** in $CDCl_3$ showed only broad signals. In addition, it was of interest to see how much the binding affinity decreases when a more competitive solvent (for hydrogen bonds) was used. No evidence for an intramolecular imide contact was seen: the NH resonance was found at 9.5 ppm, which is the same value observed for systems with just one imide surface in that solvent. The binding constants for both 9-ethyladenine and 2'3'-isopropylidene-adenosine were found to be $1.3 \times 10^3 M^{-1}$. Similar base pairing was observed for either adenine derivative, the imide chemical shift moving from 9.5 to 13.6 and 13.1 ppm respectively. Aromatic stacking can also be inferred from upfield shifts of the carbazole H1 and H2. Very small changes (<0.1 ppm) were observed in the bipyridyl chemical shifts, suggesting that it had little involvement in the binding process. However H5 of the pyridine ring proximal to the carbazole is an

exception. In titration with 9-ethyladenine this proton moves 0.11 ppm upfield but with the adenosine **213** an upfield shift of 0.38 ppm was observed. It is possible that the more sterically demanding ribose unit of **213** restricts the rotation of the bipyridyl unit more than does the ethyl group of **212**. The consequence is that H5 of the pyridine spends a larger fraction of its time below the carbazole moiety (on the opposite face from the adenine), thus resulting in a larger upfield shift (Figure II-3).

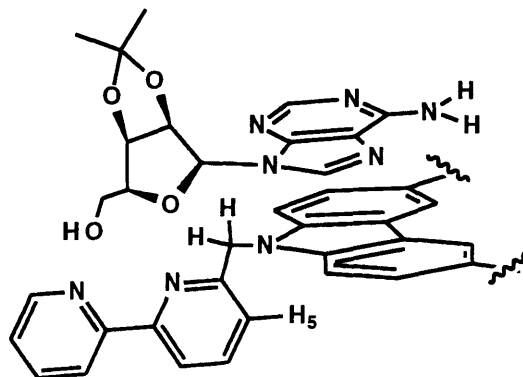


Figure II-3. Binding mode of **213** to **210**. Upon binding the rotation of the bipyridine unit is restricted, placing H5 underneath the carbazole aromatic system, resulting in an 0.38 ppm upfield shift.

For the titrations of **211** in water, a binomial peak suppression was used⁶ to observe the exchangeable protons. Titrations were performed in a buffer at pH 6 and 10 °C, and association constants of 85 M⁻¹ were measured for both 9-ethyladenine and adenosine. Base-pairing could be observed: the imide proton moved from 10.6 to 13.0 ppm (the calculated shift of the complex) for the 9-ethyladenine titration. This result indicates that the imide chemical shift of the base-paired complex is nearly solvent independent (Table II-1), at a value of approximately 13 ppm.

Despite this similarity of the overall binding of adenine derivatives in H₂O versus organic solvents, there are also considerable differences. This is not surprising since in organic solvents most of the association results from hydrogen bonding whereas in water the major part derives from hydrophobic effects. The most dramatic difference is the shift of the carbazole H4 signal. In water H4 of **211** shifts 0.33 ppm *upfield* upon saturation with 9-ethyladenine whereas in acetone-*d*₆ H4 of **210** shifts 0.37 ppm *downfield*. This is a difference between the two complexes of 0.7 ppm! One explanation is as follows: in

(6) (a) Hore, P. *J. Magn. Res.* **1983**, *54*, 539. (b) Hore, P. *J. Magn. Res.* **1983**, *55*, 283.

organic solvents the structure of the complex (as suggested by molecular modeling⁷) features one of the adenine NH bonds involved in bifurcated hydrogen bonding to the amide carbonyl (see Figure II-4, structure A) and an imide carbonyl (not shown). This binding mode brings the carbazole H4 into the magnetically deshielded area of the amide carbonyl, resulting in a downfield shift. This in contrast to H1 and H2 which shift upfield as expected due to stacking interactions. In water, stacking interactions are expected to determine the structure of the complex to a larger extent. The position for optimal stacking of two aromatic surfaces is believed to be an "offset" geometry⁸. Molecular modeling suggests that this geometry can best be accommodated by the reverse carbonyl position of the amide bond, which is now directed toward H2 (see Figure II-4, structure B).

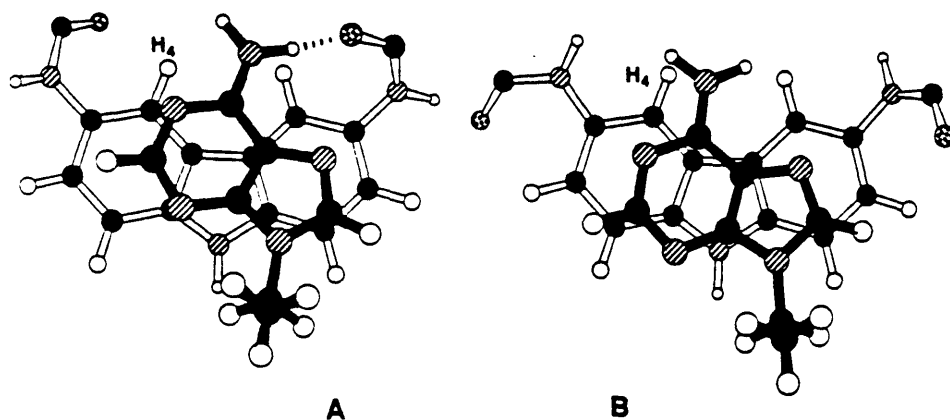


Figure II-4. Minimized structures of the complex of **212** with the diimide portion of **205**, **210** and **211**, with the amide carbonyl pointed towards (A) and away (B) from H4 of the carbazole (imides omitted for clarity).

II.4 Metal Ion Binding

The ability of **211** to bind Cu^{2+} was confirmed by a titration which was monitored by UV spectroscopy (Figure II-5). The spectrum of **211** consists of a simple superposition of the carbazole and the bipyridyl chromophores. On complexation of Cu^{2+} , a significant decrease in intensity at the absorption maximum of 282 nm is observed, accompanied by the appearance of shoulders at 297 and 318 nm. Two isosbestic points can be seen at 270

(7) Using the AMBER force field in the MACROMODEL program, W. C. Still, Columbia University.

(8) Hunter, C. A.; Sanders, J. K. M. *J. Am. Chem. Soc.* **1990**, *112*, 5525.

and at 293 nm. These observations are consistent with the coordination of Cu^{2+} to bipyridine.^{4b}

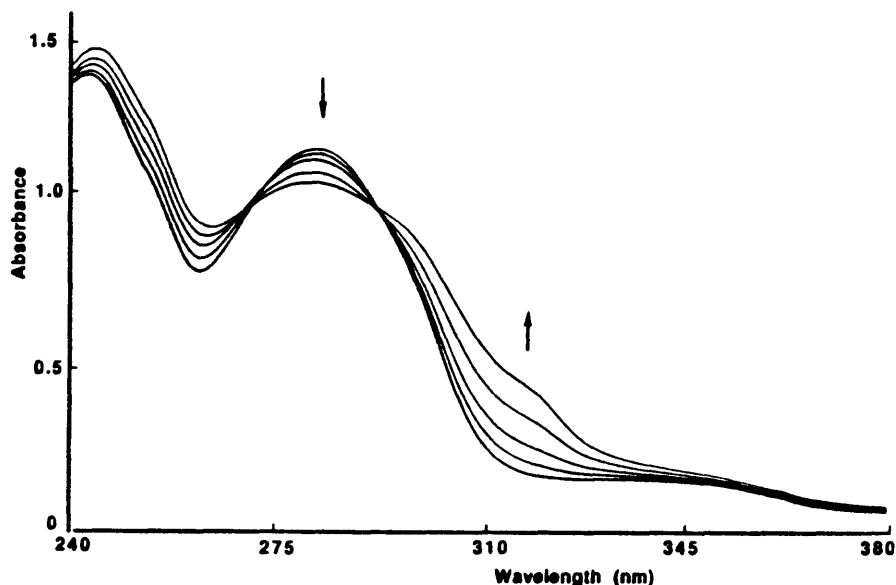


Figure II-5. Electronic absorption spectra of the titration of 211 (3.9×10^{-5} M) with 0.25 equiv portions of CuCl_2 in 20 mM HEPES buffer (pH 7.0).

II.5 Conclusions

New molecular clefts have been prepared in short, highly modular syntheses. They have been shown to bind to adenine derivatives in solvents of different hydrogen bonding ability. The design of these molecules permits a metal ion to be bound, and at least in one case, chelation of Cu^{2+} was shown to occur. Having both features present in one molecule now opens the possibility of enzyme-like behavior for recognition and catalysis. (See chapter III).

II.6 Experimental Section

General. Infrared spectra were obtained from a Mattson Sygnus 100 FT IR spectrophotometer and a Perkin Elmer 1600 FT IR spectrophotometer. ^1H NMR spectra were measured with Bruker WM-250 (250-MHz), AC-250 (250 MHz) and Varian XL-300 (300 MHz), Unity 300 (300MHz) and VXR-500 (500 MHz) spectrometers. UV-spectra were taken on a Hewlett Packard 8451A diode array spectrophotometer. High-resolution mass spectra were obtained with a Finnegan Mat 8200 instrument. For the FAB spectra 3-nitrobenzyl alcohol was used as the matrix. Melting points were taken on a Electrothermal 9100 melting point apparatus. Commercial-grade solvents were used

without further purification except for pyridine which was distilled from calcium hydride. 3(5)-isopropylpyrazole and 6-bromomethyl-2,2'-bipyridine were prepared according to the procedures of Thompson et al⁹ and Lehn et al¹⁰ respectively. Imide acid chlorides **204**¹¹ and **209**¹² as well as 3,6-dinitrocarbazole¹³ were prepared according to established procedures.

1,8-dibromo-3,6-dinitrocarbazole (202). To a solution of 3,6-dinitrocarbazole **201** (1.000 g, 3.891 mmol) in conc. H₂SO₄ (20 mL) was added Br₂ (2.0 mL, 39 mmol). The mixture was heated at 100 °C. After 15 min, more Br₂ (1.0 mL, 19 mmol) and H₂SO₄ (25 mL) were added, and the mixture was heated at 100 °C for another 2 h. After cooling the mixture was poured onto ice and the resulting yellow solid was filtered off, yielding 1.600 g (99%) of **202**: mp > 320 °C; IR (KBr) 3083, 1525, 1486, 1335, 1304, 1241, 1183 and 744 cm⁻¹; ¹H NMR (300 MHz, DMSO-*d*₆) δ 12.76 (s, 1H), 9.54 (d, 2H, J = 2.1 Hz), 8.57 (d, 2H, J = 2.1 Hz); HRMS m/e for C₁₂H₅Br₂N₃O₄, calcd. 412.8644, found 412.8648.

Dipyrazole (203). A mixture of dibromide **202** (1.752 g, 4.224 mmol), Cu₂O (3.362 g, 25.344 mmol) and 3(5)-isopropylpyrazole (13.94 g, 126.7 mmol) were heated together with 1-methyl-2-pyrrolidinone (10 mL) at reflux under argon for 18 h. The mixture was poured into H₂O (300 mL), after which EtOAc (450 mL) and THF (150 mL) were added. The layers were mixed and after separation the organic layer was washed with conc. NH₃ / sat. NaCl 1 : 2 (6 x 150 mL), followed by 10 % HCl / sat. NaCl 1 : 1 (4 x 150 mL). After further washings with a sat. NaHCO₃ solution (150 mL) and a sat. NaCl solution (150 mL), the solvent was removed. The residue was treated with hot hexane/EtOAc 1 : 1 (200 mL), cooled and the residual solid was filtered off yielding 718 mg (36%) of a greenish yellow solid : mp > 300 °C; IR (KBr) 3349, 2966, 1543, 1407, 1326, 1300 and 877 cm⁻¹; ¹H NMR (300 MHz, CDCl₃) δ 12.66 (s, 1H), 8.96 (d, 2H, J = 1.6 Hz), 8.48 (d, 2H, J = 1.8 Hz), 8.19 (d, 2H, 2.6 Hz), 6.50 (d, 2H, J = 2.8 Hz), 3.32 (septet, 2H, J = 7.0 Hz), 1.40 (d, 12 H, J = 7.0 Hz); HRMS m/e for C₂₄H₂₃N₇O₄, calcd. 473.1811, found 473.1808.

(9) Trofimenko, S.; Calabrese, J. C.; Domaille, P. J.; Thompson, J. S. *Inorg. Chem.* **1989**, *28*, 1091.

(10) Ziessel, R.; Lehn, J.-M. *Helv. Chim. Acta* **1990**, *73*, 1149.

(11) Askew, B.; Ballester, P.; Buhr, C.; Jeong, K.-S.; Jones, S.; Paris, K.; Williams, K.; Rebek J., Jr. *J. Am. Chem. Soc.* **1989**, *111*, 1082.

(12) Kato, Y.; Conn, M. M. *J. Am. Chem. Soc.* **1994**, *116*, 3279.

(13) Grotta, H. M.; Riggle, C. J.; Bearn, A. E. *J. Org. Chem.* **1964**, *29*, 2474.

Dipyrazole-diimide (205). A mixture of dinitro compound **203** (570 mg, 1.205 mmol), iron powder (1.344 g, 24.09 mmol) and conc. HCl (2.0 mL, 24 mmol) in EtOH / H₂O 3 : 1 (150 mL) was heated at reflux for 14 h. The EtOH was evaporated at reduced pressure and the aqueous residue was made alkaline with KOH. After addition of EtOAc/THF 1:1 (400 mL) the mixture was washed with a sat. NaCl solution (3 x 100 mL), dried on MgSO₄, filtered and concentrated to afford 441 mg (89%) of the gray brown solid diamine which was used without further purification in the next step: IR (KBr) 3349, 2966, 1543, 1407, 1326, 1300 and 877 cm⁻¹; ¹H NMR (300 MHz, CDCl₃) δ 10.78 (s, 1H), 7.92 (d, 2H, J = 2.4 Hz), 7.19 (d, 2H, J = 1.8 Hz), 6.92 (d, 2H, J = 1.8 Hz), 6.33 (d, 2H, J = 2.4 Hz), 3.70 (br.s., 4H), 3.22 (septet, 2H, J = 7.4 Hz), 1.37 (d, 12 H, J = 7.0 Hz). A solution of the diamine (52 mg, 0.126) and imide acid chloride **204** (71 mg, 0.277 mmol) in pyridine (10 mL) was heated under argon at reflux for 18 h. The solvent was removed and the residue was purified by radial chromatography over silica gel using MeOH / CH₂Cl₂ 1 : 19 resulting in 45 mg (42%) of a white solid : mp. 265 °C (dec.); IR (KBr) 3408, 2865, 1727, 1705, 1465 and 1199 cm⁻¹; ¹H NMR (300 MHz, DMSO-*d*₆) δ 11.38 (s, 1H), 10.57 (s, 2H) 9.38 (s, 2H), 8.37 (d, 2H, J = 2.1 Hz), 8.08 (s, 2H), 7.79 (s, 2H), 6.56 (d, 2H, J = 2.7 Hz), 3.20 (septet, 2H, J = 7.2 Hz), 2.74 (d, 4H, J = 15.0 Hz), 1.93 (d, 2H, J = 12.1 Hz), 1.44 (d, 2H, J = 13.1 Hz), 1.38-1.06 (m, 36H) including 1.34 (d, 12H, J = 6.6 Hz), 1.25 (s, 6H) and 1.15 (s, 12 H); HRMS (FAB) m/e for C₄₈H₅₈N₉O₆ (M + H) calcd. 856.4510, found 856.4507.

Dipyrazole (206). To a solution of the dipyrazolediamine (see synthesis of **205**, 80 mg, 0.1937 mmol) and NEt₃ (500 μL, 3.59 mmol) in CH₂Cl₂ (40 mL) at RT, was added dropwise trimethylacetyl chloride (100 μL, 0.812 mmol). After 15 min CH₂Cl₂ (20 mL) and water (50 mL) were added. After separating the layers, the organic portion was washed with 10% HCl (3 x 25 mL), sat. NaHCO₃ (3 x 25 mL) and brine (25 mL). After drying on MgSO₄, filtration and removal of the solvent 87 mg (77%) of an off-white solid was obtained: mp. 292-293 °C; IR (KBr) 3406, 2963, 1654, 1603, 1528, 1475, 1407, 1205, 846 and 757 cm⁻¹; ¹H NMR (300 MHz, CDCl₃) δ 11.33 (s, 1H), 8.05 (d, 2H, J = 2.6 Hz), 7.98 (d, 2H, J = 1.8 Hz), 7.92 (d, 2H, 1.8 Hz), 7.51 (s, 2H), 6.36 (d, 2H, J = 2.5 Hz), 3.21 (septet, 2H, J = 6.9 Hz), 1.39 (s, 18 H), 1.38 (d, 12H, J = 6.9 Hz); HRMS m/e for C₃₄H₄₃N₇O₂, calcd. 581.3478, found 581.3468.

Bipyridine (208). 3,6-dinitrocarbazole **201** (963 mg, 3.74 mmol) and K₂CO₃ (5.17 g, 37.4 mmol) were mixed in DMF (60 mL) and stirred for 10 min. 6-bromomethyl-2,2'-bipyridyl **207** (932 mg, 3.74 mg) was added all at once. The mixture was heated at

115 °C for 2 h and poured into H₂O (150 mL). The resulting precipitate was filtered, washed with H₂O and dried. Obtained was 1.547 g (97%) of a beige solid: mp. 281 - 282 °C; IR (KBr) 3422, 1603, 1584, 1512, 1477, 1335, 1313, 1102 and 756 cm⁻¹; ¹H NMR (300 MHz, DMSO-*d*₆) δ 9.55 (d, 2H, J = 2.5 Hz), 8.59 (d, 1H, J = 5.0 Hz), 8.45 (dd, 2H, J = 9.1 and 2.5 Hz), 8.24 (dd, 1H, J = 7.9 and 1.2 Hz), 8.06 (d, 2H, J = 9.1 Hz), 7.91 (dd, 1H, J = 7.7 and 7.7 Hz), 7.83 (d, 1H, J = 8.0 Hz), 7.77 (ddd, 1H, J = 7.6, 7.6 and 1.9 Hz), 7.42 (d, 1H, J = 7.6 Hz), 7.36 (ddd, J = 6.8, 5.0 and 1.6 Hz) and 6.05 (s, 2H); HRMS m/e for C₂₃H₁₅N₅O₄, calcd. 425.1124, found 425.1121.

Bipyridine-diimide (210). Dinitro compound **208** (630 mg, 1.48 mmol) was dissolved in EtOH/H₂O 2:1 (150 mL). Iron powder (496 mg, 8.88 mmol) and conc. HCl (250 μL, 3.0 mmol) were added and the mixture was heated at reflux with vigorous stirring for 14 h. Most of the EtOH was removed and the remaining aqueous mixture was made alkaline with KOH. The product was extracted into CH₂Cl₂ (250 mL), washed with a saturated alkaline EDTA solution (2 x 75 mL) and with brine (75 mL). The CH₂Cl₂ solution was dried on MgSO₄, filtered and concentrated to 3-4 mL. Hexane (20 mL) was added and the resulting precipitate was filtered and dried, resulting in 380 mg (70%) of the cream-colored solid diamine, which was used in the next step without further purification: ¹H NMR (300 MHz, CDCl₃) δ 8.70 (d, 1H, J = 3.9 Hz), 8.47 (d, 1H, J = 7.9 Hz), 7.86 (ddd, 1H, J = 7.7, 7.7 and 1.8 Hz), 7.56 (dd, 1H, J = 7.8 Hz), 7.36 (d, 2H, J = 1.9 Hz), 7.36 - 7.30 (m, 1H), 7.17 (d, 2H, J = 8.6 Hz), 6.85 (dd, 2H, J = 8.6 and 2.3 Hz), 6.64 (d, 1H, J = 7.7 Hz), 5.58 (s, 2H) and 3.60 (br.s., 4H). Imide acid chloride **209** (0.390 mmol, obtained from the corresponding carboxylic acid (217 mg, 0.390 mmol) by heating it under reflux in SOCl₂ for 2 h and concentrating it *in vacuo*), was mixed together with the diamine (71 mg, 0.195 mmol) and a catalytic amount of DMAP in dry pyridine (10 mL). The mixture was heated at 110°C for 14 h under argon. After removal of the solvent and radial chromatography over silica gel (2% MeOH in CH₂Cl₂) 134 mg (48%) of a slightly yellow solid was obtained: ¹H NMR (300 MHz, DMSO-*d*₆) δ 10.64 (s, 2H), 9.33 (s, 2H), 8.65 (d, 1H, J = 4.0 Hz), 8.26 (d, 1H, J = 7.9 Hz), 8.21 (d, 1H, J = 8.0 Hz), 8.17 (s, 2H), 7.91 (dd, 1H, J = 7.8 and 7.8 Hz), 7.77 (d, 1H, J = 8.0 Hz), 7.58 (d, 2H, J = 8.9 Hz), 7.44 (d, 2H, J = 9.0 Hz), 7.40-7.10 (m, 31 H), 6.88 (d, 1H, J = 7.7 Hz), 5.79 (s, 2H), 4.51 (s, 8H), 4.46 (s, 4H), 3.74 (d, 4H, J = 8.8 Hz), 3.48-3.36 (m, 8H), 2.56 (d, 4H, J = 14.6 Hz), 2.33 (d, 2H, J = 12.8 Hz) and 1.61 (d, 6H, J = 13.2 Hz); HRMS (FAB) m/e for C₈₉H₈₆N₇O₁₂ (M+H), calcd. 1444.6334, found 1444.6342.

Hexahydroxy cleft (211). Hexabenzoyloxy cleft **210** (158 mg, 0.109 mmol) was dissolved in formic acid (Fluka, 98%) and stirred at 0 °C. HBr gas was bubbled through the solution for 40 min. The solvent was removed *in vacuo* and the residue suspended in MeOH. For complete precipitation some Et₂O was added and the solid was filtered off. The solid was washed with a 20% NaHCO₃ solution followed by H₂O and dried. Obtained was 69 mg (70%) of an off-white solid: mp 145 °C; IR (KBr) 3424, 1701, 1098, 738 and 698 cm⁻¹; ¹H NMR (300 MHz, DMSO-*d*₆) δ 10.41 (s, 2H), 9.16 (s, 2H), 8.65 (d, 1H, J = 3.8 Hz), 8.28 (d, 1H, J = 8.5 Hz), 8.24 (d, 2H, J = 1.9 Hz), 8.21 (d, 1H, J = 8.0 Hz), 7.95 (ddd, 1H, J = 7.6, 7.6 and 1.9 Hz), 7.76 (dd, 1H, J = 7.7 and 7.7 Hz), 7.56 (d, 2H, J = 8.8 Hz), 7.45 (dd, 2H, J = 8.5 and 2.1 Hz), 7.44 - 7.40 (m, 1H), 6.83 (d, 1H, J = 7.9 Hz), 5.78 (s, 2H), 5.10 - 5.07 (m, 2H), 4.77 - 4.73 (m, 4H), 3.79 - 3.73 (m, 4H), 3.39 - 3.36 (m, 2H), 2.39 (d, 4H, J = 14.3 Hz), 2.19 (d, 2H, J = 12.3 Hz), 1.48 (d, 4H, J = 14.1 Hz) and 1.33 (d, 2H, J = 13.1 Hz); HRMS (FAB) *m/e* for C₄₇H₅₀N₇O₁₂ (M+H), calcd. 904.3518, found 904.3511.

NMR Titrations. NMR titrations in acetone-*d*₆ and CDCl₃ were performed on a host solution of around 1 mM in an NMR tube at 23 °C. Part of this host solution was used to prepare a guest solution of 5-20 mM. Aliquots of the guest solution were added and the 300 MHz-NMR spectra were recorded until the chemical shift of the host signal remained close to constant. Association constants were obtained by nonlinear least-squares fit of the 1:1 binding isotherm¹⁴. NMR titrations in water were obtained using the same constant host protocol, but at 10 °C. The solvent was H₂O/D₂O 9:1 with DSS as an internal standard, and contained 10 mM sodium cacodylate buffer (pH adjusted to pH 6.0 with HCl) and ionic strength = 50 mM (NaCl). The concentration of **211** was close to 0.25 mM and a binomial water peak suppression pulse sequence⁶ was used to record the spectra (500 MHz). For the 9-ethyl adenine titration in water association constants were corrected for guest dimerisation using the following equation¹⁵ :

$$[G]_t = [H]_t X^3 + (2K_d/K_a^2 - [G]_t - 2[H]_t - 1/K_a) X^2 + (2[G]_t + [H]_t + 1/K_a) X$$

$$\text{where } X = (\delta_{\text{obs}} - \delta_H) / (\delta_{\text{HG}} - \delta_H)$$

(14) K. A. Connors, *Binding Constants: the Measure of Molecular Complexation Stability*, Wiley, New York, 1987.

(15) The model was created by Dr. Brian Murray.

$[H]_t$ = total host concentration; $[G]_t$ = total guest concentration; K_a = the association constant; K_d = the dimerisation constant; (δ_{obs} , δ_H and δ_{HG} are observed chemical shift, and the chemical shift of the free host and the host-guest complex respectively). The K_d of 9-ethyladenine was determined by a separate experiment (13.8 M^{-1} at $10 \text{ }^\circ\text{C}$) and used for solving the equation.

UV-titration of 211 with CuCl_2 . 600 μL of the ligand solution (39 μM solution of **211** in 20 mM HEPES buffer at pH 7.0) was put in a quartz cuvette. Additions of a solution containing 39 μM of **211** and 0.31 mM of CuCl_2 were made until no further changes occurred in the UV-spectrum between 240 and 380 nm (*ca.* 1 equiv).

Chapter III. Hydrolysis of Phosphate Triesters by a Novel Cleft. Influence of Binding on Rate Acceleration.

III.1 Introduction

As part of a program of designing enzyme-like catalytic processes, we describe in this chapter efforts to combine the use of both recognition and catalytic elements in a novel receptor.¹ Previous work in this laboratory has shown that cleft-like receptors can be built efficiently and incrementally by convergent modular synthesis from Kemp's triacid^{2,3}. High affinity adenine receptors have been developed using two convergent imide surfaces for simultaneous Watson-Crick and Hoogsteen base pairing in addition to π -stacking to a carbazole scaffold. The carbazole nitrogen has provided a convenient handle for further functionalization. Here is described the incorporation of a metal-ligand complex in order to evaluate the effect of substrate binding on phosphate ester hydrolysis.⁴

The hydrolysis of phosphate esters is known to be promoted by transition metals, such as Cu^{2+} ^{5,6,7,8}, Zn^{2+} ^{5,6,9,10,11,12} and lanthanides.¹³ The activity of the metal-ligand complex depends on its exchange properties, its geometry, and also on the acidity of the coordinated water molecules. A pathway that is often quoted as being responsible for the catalytic activity of metal complexes includes simultaneous Lewis acid activation of the P-O bond (or C-O in case of amide or esters) and intracomplex attack of a metal bound hydroxide. These bound hydroxides can be available at near neutral pH due to the enhanced acidity of metal-bound water molecules. Promoting intracomplex hydrolysis of phosphate esters requires a geometry for the reaction complex in which the

-
- (1) Chapter I, this thesis.
 - (2) Rebek Jr., *J. Angew. Chem. Int. Ed. Engl.* **1990**, *29*, 245.
 - (3) Conn, M. M.; Deslongchamps, G.; de Mendoza, J.; Rebek Jr., *J. Am. Chem. Soc.* **1993**, *115*, 3548
 - (4) The kinetics and the quantitative analysis were performed by Dr. Belinda Tsao.
 - (5) Chin, *J. Acc. Chem. Res.* **1991**, *24*, 145-152.
 - (6) Rosch, M. A.; Trogler, W. C. *Inorg. Chem.* **1990**, *29*, 2409.
 - (7) Morrow, J. R.; Trogler, W. C. *Inorg. Chem.* **1988**, *27*, 3387.
 - (8) Morrow, J. R.; Trogler, W. C. *Inorg. Chem.* **1989**, *28*, 2330.
 - (9) Anslyn, E.; Breslow, R. *J. Am. Chem. Soc.* **1989**, *111*, 4473.
 - (10) Shelton, V. M.; Morrow, J. R. *Inorg. Chem.* **1991**, *30*, 4295.
 - (11) Breslow, R.; Huang, D.-L.; Anslyn, E. *Proc. Natl. Acad. Sci.* **1989**, *86*, 1746.
 - (12) Gellman, S. H.; Petter, R.; Breslow, R. *J. Am. Chem. Soc.* **1986**, *108*, 2388.
 - (13) Morrow, J. R.; Buttrey, L. A.; Shelton, V.; Berback, K. A. *J. Am. Chem. Soc.* **1992**, *114*, 1903.

coordinated hydroxide ion (or water) is *cis* with respect to the bound phosphate.¹⁰ To achieve such a geometry, the metal must have two adjacent coordination sites which are unoccupied. This geometry can be achieved using a Cu(II)-2,2'-bipyridine catalyst. Accordingly, this well-studied system was chosen as the catalytic unit to incorporate into the carbazole based adenine receptor. If the receptor is able to bring the catalyst and substrate together in the correct orientation, then enhanced rates of hydrolysis should result. The design, synthesis and binding studies of this cleft have been described in chapter I. In this chapter the mechanistic studies of the catalytic hydrolysis of phosphate triesters using the cleft are presented.

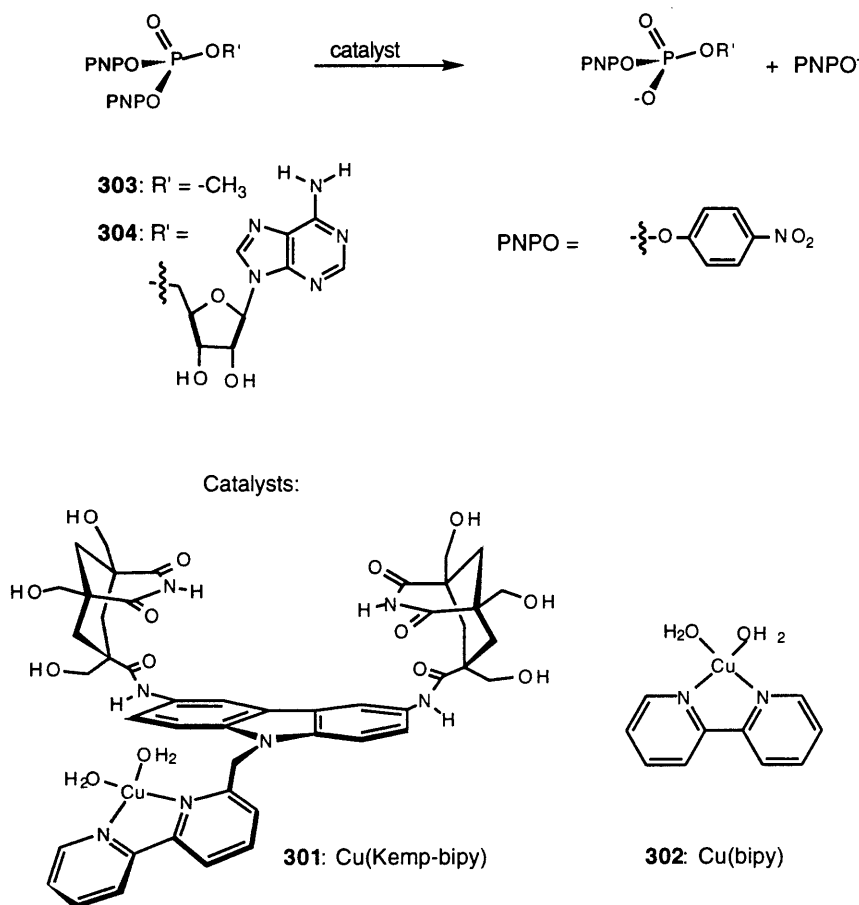


Figure III-1 The hydrolysis of the phosphate triesters.

III.2 Catalytic Hydrolysis

Hydrolysis of adenosine 5'-O,O-bis(p-nitrophenyl) phosphate **304** or bis(p-nitrophenyl) methyl phosphate **303** were studied using both the receptor Cu(Kemp-bipy) **301** and Cu(bipy) **302** as catalysts. The overall reaction is shown in

Figure III-1. The products of the reactions were analyzed by ^{31}P NMR. The chemical shifts of the products were compared to authentic samples of diesters. In both cases, no further hydrolysis to the corresponding phosphate monoesters took place.

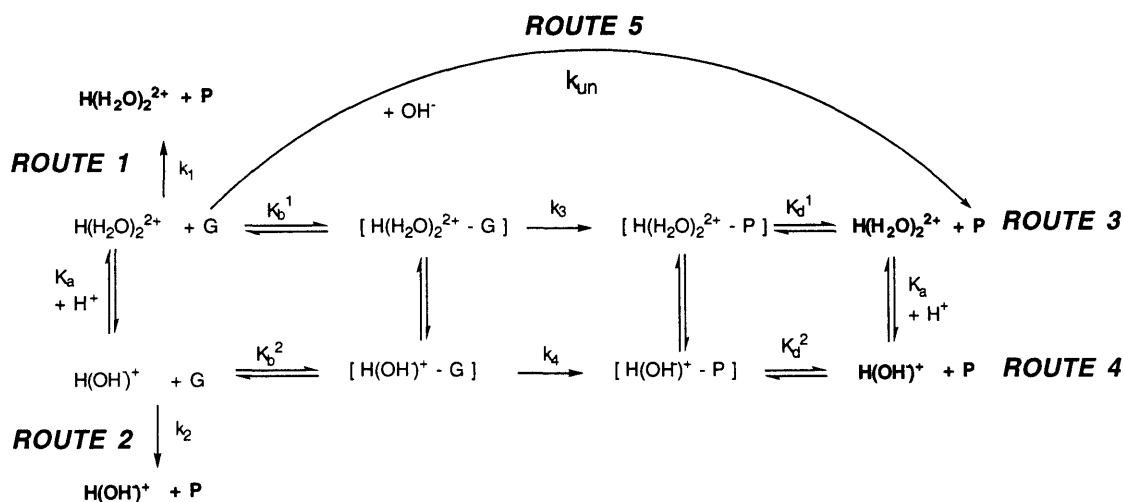


Figure III-2. The mechanism of hydrolysis of phosphotriesters **303** or **304** (denominated G) catalyzed by receptor/catalyst **301** or catalyst **302**. $\text{H}(\text{H}_2\text{O})_2^{2+}$ is $\text{Cu}(\text{Kemp-bipy})(\text{H}_2\text{O})_2^{2+}$ or $\text{Cu}(\text{bipy})(\text{H}_2\text{O})_2^{2+}$. $\text{H}(\text{OH})^+$ is $\text{Cu}(\text{Kemp-bipy})(\text{OH})^+$ or $\text{Cu}(\text{bipy})(\text{OH})^+$. P is the product.

All relevant association processes and reaction steps are presented in Figure III-2. Under the reaction conditions, the $\text{Cu}(\text{bipy})$ unit of catalysts **301** or **302** exists in two forms. Both the acidic, $\text{H}(\text{H}_2\text{O})_2^{2+}$, and basic forms, $\text{H}(\text{OH})^+$, are kinetically active.⁸ First of all, bimolecular reactions between the substrates, **303** or **304**, and the acidic, $\text{H}(\text{H}_2\text{O})_2^{2+}$, or basic, $\text{H}(\text{OH})^+$, components of the catalysts are described by routes 1 and 2. Routes 3 and 4 are operational only if formation of association complexes between the catalyst and the substrate is possible. In this case, the substrate can bind to either the acidic, $\text{H}(\text{H}_2\text{O})_2^{2+}$, or basic, $\text{H}(\text{OH})^+$ form of the catalyst. This would give the respective host-guest complexes with association constants K_b^1 and K_b^2 . These host-guest complexes can turn over to the respective host-product complexes with catalytic rate constants of k_3 and k_4 . Finally, there remains the specific-base catalyzed hydrolysis of the substrate as described by route 5.

The overall rate law can be written as follows:

$$\begin{aligned}
 \frac{dP}{dt} = & (k_1[\text{H}(\text{H}_2\text{O})_2^{2+}] + k_2[\text{H}(\text{OH})^+])[G] + k_3[\text{H}(\text{H}_2\text{O})_2^{2+} - \text{G}] \\
 & + k_4[\text{H}(\text{OH})^+ - \text{G}] + k_{un}[\text{OH}^-][G]
 \end{aligned} \quad (1)$$

Substituting the equilibrium expressions and mass balance equation into (1) and re-expressing it in terms of the total concentrations of host and guest gives after some simplification:

$$k_{obs} = \frac{(k_1 + k_3 K_b^1)[H^+] + (k_2 + k_4 K_b^2)K_a}{[H^+] + K_a} [H]_t + k_{un}[OH^-] \quad (2)$$

Assuming that the binding constants to both $H(H_2O)_2^{2+}$ and $H(OH^-)^+$ are the same, that is, $K_b^1 = K_b^2 \equiv K_b$, then, equation (2) simplifies to Equation (3).

$$k_{obs} = \frac{(k_1 + k_3 K_b)[H^+] + (k_2 + k_4 K_b)K_a}{[H^+] + K_a} [H]_t + k_{un}[OH^-] \quad (3)$$

Since Cu(bipy) **2** possesses no recognition element, both routes 3 and 4 in Figure 2 can be neglected and the rate expression simplifies to:

$$k_{obs} = \frac{k_1[H^+] + k_2 K_a}{[H^+] + K_a} [H]_t + k_{un}[OH^-] \quad (4)$$

The acid dissociation constant, K_a , for the catalyst **301** was determined by titration with known concentrations of NaOH ($pK_{a1} = 6.1 \pm 0.5$). The acid dissociation constant for Cu(bipy) at 25 °C ($pK_{a1} = 7.9$) determined by Gustafson and Martell¹⁴ was used for calculating various rate constants for Cu(bipy). Unlike Cu(bipy) which dimerizes with K_d of $1 \times 10^5 \text{ M}^{-1}$ at 25 °C, titrations of Cu^{2+} with ligand **301** indicated a 1:1 stoichiometry. The dimerization pathway was inhibited sterically. However, in the case of Cu(bipy), at concentrations higher than 10^{-5} M dimerization decreases the amount of active catalyst. This has been taken into account in calculating various rate constants.

To assure that the U-shaped cleft does not interfere with the catalytic Cu(bipy) group, both receptor **301** and Cu(bipy) **302** were evaluated as catalysts toward substrate **303**. The effect of binding was then investigated using substrate **304**.

According to equation (1), linear regression of a plot of k_{obs} vs. $[H]_t$ gives $\frac{(k_1 + k_3 K_b)[H^+] + (k_2 + k_4 K_b)K_a}{[H^+] + K_a}$ as the slope and the background first-order rate constant, $k_{un}[OH^-]$, as intercept. Then a plot of the slope vs. $[H^+]$ gives the catalytic rate

(14) Gustafson, R. L.; Martell, A. R.; *J. Am. Chem. Soc.* **1959**, *81*, 525

constants, k_3 and k_4 and the binding constant, K_b . The various rate constants are presented in Table III-1.

Substrate	Catalyst	k_1 ($M^{-1}s^{-1}$)	k_2 ($M^{-1}s^{-1}$)	k_3 (s^{-1})	k_4 (s^{-1})
303	302	0.75	1.2		
303	301	0.75	1.76		
304	302	0.5 ± 0.09	1.2 ± 0.7		
304	301	0.5 ± 0.09	1.2 ± 0.7	0.08 ± 0.002	0.7 ± 0.05

Table III-1. List of catalytic rate constants for hydrolysis of bis(p-nitrophenyl) methyl phosphate **303** and adenosine O,O-bis(p-nitrophenyl) phosphate **304** catalyzed by Cu(Kemp-bipy) **301** and Cu(bipy) **302** at 25 °C. Where, Substrate **3** is MeO-P(O)-OPNP₂, Substrate **304** is Ad-OP(O)-OPNP₂, k_{un} is $1 M^{-1}s^{-1}$; $pK_{a1} = (6.2 \pm 0.5)$ for Cu(Kemp-bipy) **301**; $pK_{a1} = (7.9)$ for Cu(bipy) **302**. Studies were performed at 25 °C from pH 6 to 9.5 with buffer concentrations ranging from 0.01 to 0.09M.

Within the pH range under investigation, the copper-hydroxo species, $H(OH)^+$ is always more active than the copper-diaqua species, $H(H_2O)_2^{2+}$, that is, $H(OH)^+$ dependent terms, k_2 and k_4 , are always larger than $H(H_2O)_2^{2+}$ dependent terms, k_1 and k_3 . The second-order rate constants for the hydrolysis of adenosine 5'-O,O-bis(p-nitrophenyl) phosphate **304** catalyzed by Cu(Kemp-bipy) **301** and calculated association constants at different pH's are listed in Table III-2.

It is seen from Table III-1 that the second-order rate constants, k_1 and k_2 , describing routes 1 and 2 are similar for both receptor **301** and Cu(bipy) **302**. Therefore, it may be assumed that receptor **301** is as catalytically active as Cu(bipy) **302** and that incorporation of a rigid binding domain does not affect its catalytic ability. This also allowed us to substitute values for k_1 and k_2 obtained using Cu(bipy) **302** into equation (1) in order to determine rate constants, k_3 and k_4 , describing routes 3 and 4.

pH	K_b (M^{-1})	k_3K_b ($M^{-1}s^{-1}$)	k_4K_b ($M^{-1}s^{-1}$)	Rel. rate k_3K_b / k_1	Rel. rate k_4K_b / k_2
6	75	6	52.5	12	44
7.5	24	1.9	16.8	3.8	14
8.5	13	1.0	9.1	2.0	7.6
9.5	9.4	0.8	6.6	1.6	5.5

Table III-2. List of second-order rate constants and calculated association constants for the hydrolysis of adenosine 5'-O,O-bis(p-nitrophenyl) phosphate **304** catalyzed by Cu(Kemp-bipy) **301** at various pH. Substrate is Ad-OP(O)-OPNP₂ **304** and catalyst is Cu(Kemp-bipy) **304**. Studies were performed at 25 °C with buffer concentrations ranging from 0.01 to 0.09M and ionic strength 0.1M.

The data of Table III-2 shows that the affinity of adenosine phosphate **304** towards receptor **301** is strongly pH dependent. At lower pH, where binding is more significant, routes 3 and 4 in Figure III-2 dominate. As binding becomes weaker at high pH, the receptor begins to behave like Cu(bipy) **302** itself. The decrease of binding affinity upon increasing pH can be attributed to the deprotonation of the imide on receptor **301**. The pK_a of the imide is 9.6 at 25 °C.^{15,16} As pH approaches the pK_a of the imide, complex formation is discouraged.

III.3 Influence of binding.

Productive binding involves the correct positioning of the reactive groups and enhances rates of reactions. Molecular modeling using MacroModel suggested that binding of the adenine portion of **304** to the receptor of **301** would position the 5'-phosphate ester in close proximity to the bipy unit (see Figure III-3).

(15) Kortum, G.; Vogel, W.; Andrussov, K.; "Dissociation Constants of Organic Acids in Aqueous Solutions", Plenum Press, New York, 1961.

(16) Flaschka, H. A.; Barnard Jr., A. J.; Sturock, P. E.; "Quantitative Analytical Chemistry", Barnes and Noble, New York, 1969.

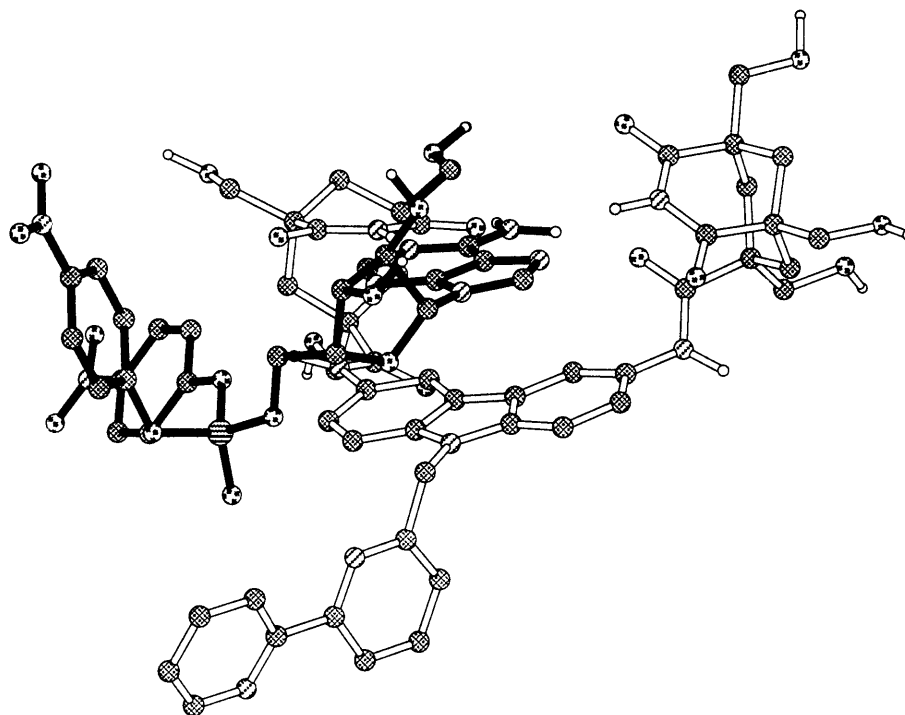


Figure III-3 Minimized structure of the host-guest complex between **304** (darkened structure) and metal free **301** using the program "MacroModel".

The proximity of the phosphate moiety to the Cu(bipy) unit allowed facile coordination to the metal. The hydrolysis reaction presumably followed the double-activation pathway proposed by Trogler and Morrow.⁷ A coordinated phosphate intermediate is formed, followed by intramolecular hydrolysis by reaction with cis-coordinated water or hydroxide.

Contributions of binding towards rates of hydrolysis of adenosine phosphate **304** can be interpreted using the relative rates shown in Table III-2. A maximum of 44-fold was found when comparing the intracomplex versus the unbound rate constants. It is also apparent that the optimum pH for maximal rate enhancement is at pH 6. The limit of rate enhancement depends not only on the affinity of Cu(Kemp-bipy) **301** for adenosine phosphate **304** but also on the concentration of the copper hydroxo species. This is implicated as the active catalyst at alkaline pH.⁷ While the concentration of the copper hydroxo species increases with increasing pH, the binding affinity of the imide cleft decreases. These opposing effects, thus, determine the optimum pH for rate acceleration to be 6.

III.4 Conclusions

Described here is the first attempt to use a molecular receptor based on directional hydrogen bonds in aqueous solution as a substrate binder for a transition metal catalyst. Hydrogen bonding in the competitive solvent water is weak but can be achieved when combined with hydrophobic binding to aromatic surfaces.^{1,17} Although the adenine affinity of the receptor used in this work ranks among the highest known in organic solvents, in water only moderate affinity ($K_b \sim 100$ at 10 °C) remains.¹ Water is the most biorelevant solvent and therefore a successful enzyme model should exhibit substrate recognition (involving also H-bonding) and catalysis in this solvent. An assay was developed to evaluate the influence of recognition on the catalytic hydrolysis of phosphotriesters. Although phosphotriesters as models for RNA are of limited value,¹⁸ they do allow the evaluation of the geometric constraints involved in metal catalyzed hydrolysis reactions and their higher reactivity compared to phosphodiester allows for kinetics within a more convenient time window.

In this work a modest rate enhancement was obtained from the kinetic analysis. The results are supported by the magnitude and pH dependence of the kinetic association constants, which are in good agreement with values obtained from binding studies.¹ Moreover, the geometry similar to the one required for intracomplex catalysis here, has resulted in 10^3 fold rate enhancements in aminolysis reactions.¹⁹ Interpreting kinetic data from a system with many equilibria and reaction pathways requires caution. Due to the complexity of the system several uncertainties remain. The lower pKa of the copper bound water molecules of Cu(Kemp-bipy) as compared to Cu(bipy) may give the former a certain advantage. In addition the degree of Cu(bipy) dimerization, although accounted for in the analysis, possibly complicates matters. The most serious limitation of the system is the low substrate affinity of the receptor, which in several of the experiments is less than 1% saturated with the adenosine-phosphotriester. Accordingly, it was not possible to access its true catalytic potential.

(17) Rotello, V. M.; Viani, E. A.; Deslongchamps, G.; Murray, B. A.; Rebek Jr., J. *J. Am. Chem. Soc.* **1993**, *115*, 797.

(18) Even activated phosphodiester were recently shown to be a poor model for RNA: Bashkin, J. K.; Jenkins, L. A. *J. Chem. Soc. Dalton. Trans.* **1993**, 3631.

(19) Chapter IV, this thesis.

The observation that high association constants are not required for use of artificial systems as RNA- hydrolysis catalysts,²⁰ induces optimism about potential application of this system. It even has the advantage of specific (adenine) recognition, and Cu(bipy) has already been shown to hydrolyze RNA at neutral pH.²¹ Efforts towards this goal are described in Chapter VII.

III.5 Experimental Section

General. All chemicals were purchased from Aldrich Chemical Company and were used without further purification. MES, HEPES, TAPS and CHES buffers were purchased from Sigma Chemical Company. Ultraviolet-visible spectra were taken on a Perkin-Elmer Lambda II spectrophotometer equipped with a Haake D1 circulating water bath. Data were collected using the program "PECSS", Perkin Elmer Computer Software System. Nonlinear regressions were performed using the program "Systat 5.2". pH titrations were performed with SPER scientific Digital pH meter. The concentrations of NaOH was determined by titration with standardized HCl. UV-cuvettes, supracil grade with 10 mm pathlength, were purchased from Hellma Cells, Inc. ¹H and ³¹P NMR spectra were obtained on Varian XL-300 or Varian UN-300 spectrometers. All ¹H chemical shifts were reported in ppm and were referenced to residual solvents. ³¹P chemical shifts were reported in ppm with external reference of 85% H₃PO₄ in DMSO-*d*₆ at 0 ppm.

Synthesis. Synthesis of receptor Kemp-bipy has been described previously.¹ The synthesis of bis(p-nitrophenyl) chlorophosphate and adenine 5'-O,O-bis(p-nitrophenyl) phosphate **304** were according to established procedures.^{22,23}

Kinetics. Buffers used were within pH range of 6 to 9.5. Concentrations of buffers were 0.01 - 0.09 M with ionic strength of 0.1M (NaNO₃). Stock solutions of Cu(NO₃)₂ (1.6 x 10⁻³ M) and bipyridine (3.5 x 10⁻² M) in respective buffers; receptor **301** (0.01M), bis(p-nitrophenyl) methyl phosphate **303** (4.2 x 10⁻³M) and adenosine 5'-O,O-bis(p-nitrophenyl) phosphate **304** (2.433 x 10⁻³ M) in anhydrous methanol were

(20) (a) Smith, J.; Ariga, K.; Anslyn, E. V.; *J. Am. Chem. Soc.* **1993**, *115*, 362. (b) Kneeland, D. M.; Ariga, K.; Lynch, V. M.; Huang, C.-Y.; Anslyn, E. V.; *J. Am. Chem. Soc.* **1993**, *115*, 10042.

(21) Modak, A. S.; Gard, J. K.; Merriman, M. C.; Winkeler, K. A.; Bashkin, J. K.; Stern, M. K.; *J. Am. Chem. Soc.*, **1991**, *113*, 283.

(22) Murayama, A.; Jastorff, B.; Cramer, F.; Hettler, H.; *J. Org. Chem.* **1971**, *36*, 3029.

(23) Eckstein, F.; Simonson, L. P.; Bar, H. P.; *Biochemistry*, **1974**, *13*, 3806.

prepared. A 1:1 mixture of $\text{Cu}(\text{NO}_3)_2$ and receptor **301** or bipyridine were used to give the corresponding $\text{Cu}(\text{Kemp-bipy})$ **301** or $\text{Cu}(\text{bipy})$ **302** respectively. Binding of Cu^{2+} to ligand **301** was confirmed by UV-titrations.¹ To a cuvette containing 0.1 to 1 equiv of $\text{Cu}(\text{Kemp-bipy})^{2+}$ **301** or $\text{Cu}(\text{bipy})^{2+}$ **302** in the appropriate buffers was added 1 equiv of phosphate solution, **303** or **304**. The total volume in the cuvette was 1 mL and the total concentration of phosphate was kept constant at 7.0×10^{-5} or 3.5×10^{-5} M. The total concentrations of catalysts varied between 3.5×10^{-6} to 7.0×10^{-5} M. The rate of hydrolysis was determined by spectrophotometrically at 400 nm which corresponds to the release of p-nitrophenolate. Rate constants were determined by fitting to first-order rate equations.

Product analysis. Reaction mixtures from 10 to 20 kinetic runs were combined. Cu^{2+} was removed by cation exchange using Sephadex SP-C25 column, Na^+ form, 1.5 x 10 cm and H_2O as eluant. Water was then removed by rotary evaporation and products were analyzed by ^{31}P NMR. ^{31}P NMR ($\text{DMSO}-d_6$, reference to 85% H_3PO_4 in $\text{DMSO}-d_6$): δ -12.306 (bis(p-nitrophenyl) methyl phosphate), -12.928 (mono-(p-nitrophenyl) methyl phosphate sodium salt), -123.859 (adenosine 5'-O,O-bis-(p-nitrophenyl) phosphate), -93.066 (adenosine 5'-O-(p-nitrophenyl) phosphate sodium salt).

Molecular Modeling. All molecular modeling was performed on a Silicon Graphics 4D30G+ with MacroModel 3.5X. The conformations of the complexes were derived by minimization using the MULT routine and TNCG algorithm, all-atom AMBER* force field and GB/SA continuum water solvation.

Chapter IV. Reciprocal Template Effects in Bisubstrate Systems: A Replication Cycle

IV.1 Introduction

The enhancement of chemical reactions by complementary surfaces - template effects - is widespread in biological and chemical processes.¹ Nucleic acid replication is the paradigm example: one strand acts as a template for the other.² The complementarity is both physical -size and shape- and chemical. The chemical effects result from several intermolecular forces as hydrogen bonding, π - π interactions or metal ligand binding. Examples of all of these in synthetic systems have been reported.³ The enhancement caused by a template can result in selectivity: the formation of one product at the expense of another. Template effects have made cyclizations possible which are otherwise hard to achieve. Stoddart and Sauvage provide excellent examples in the synthesis of interlocked molecules.^{3d,3i} The Rebek group has earlier reported the use of hydrogen bonds and π -stacking as the source of (self)-complementarity in replication systems.⁴ In this chapter reciprocal templating effects in bisubstrate coupling reactions are reported.⁵ The reciprocal nature arises from the fact that in a set of two reactions, the product of one template enhanced reaction is a template for the other, and the choice of template and substrate is arbitrary. The role the templates play in a single templated reaction is schematically depicted in Figure IV-1, where the template binds two reagents simultaneously. This promotes an otherwise bimolecular reaction to a unimolecular (or intracomplex) one and leads to enhanced coupling rates by reducing activation entropies.

(1) For recent reviews see (a) Hoss, R.; Vögtle, F., *Angew. Chem. Int. Ed. Engl.* **1994**, *33*, 375; (b) Anderson, S.; Anderson, H. L.; Sanders, J. K. M. *Acc. Chem. Res.* **1993**, *26*, 469.

(2) For a recent experimental study of reciprocal effects in nucleic acid chemistry see Sievers, D.; von Kiedrowski, G. *Nature* **1994**, *369*, 221.

(3) (a) Walter, C. J.; Anderson, H. L.; Sanders, J. K. M. *J. Chem. Soc., Chem. Commun.* **1993**, 458. (b) Kelly, T. R.; Zhao, C.; Bridger, G. J. *J. Am. Chem. Soc.* **1989**, *111*, 3744. (c) Kelly, T. R.; Bridger, G. J.; Zhao, C. *J. Am. Chem. Soc.* **1990**, *112*, 8024. (d) Dietrich-Buchecker, C. O.; Sauvage, J. P.; Kern, J. M. *J. Am. Chem. Soc.* **1984**, *106*, 3043. (e) Mock, W. L.; Irra, T. A.; Wepsiec, J. P.; Adhya, M. *J. Org. Chem.* **1989**, *54*, 5302. (f) von Kiedrowski, G.; Wlotzka, B.; Helbing, J.; Matzen, M.; Jordan, S. *Angew. Chem. Int. Ed. Engl.* **1991**, *30*, 423; (g) Terfort, A.; von Kiedrowski, G. *Angew. Chem. Int. Ed. Engl.* **1992**, *31*, 654. (h) Goodwin, J.T.; Lyn, D. G. *J. Am. Chem. Soc.* **1992**, *114*, 9197; (i) Amabilino, D. B.; Ashton, P. R.; Tolley, M. S.; Stoddart, J. F.; Williams, D. J. *Angew. Chem. Int. Ed. Engl.* **1993**, *32*, 1297.

(4) (a) Nowick, J. S.; Feng, Q.; Tjivikua, T.; Ballester, P.; Rebek, J., Jr. *J. Am. Chem. Soc.* **1991**, *113*, 8831. (b) Park, T.-K.; Feng, Q.; Rebek, J., Jr. *J. Am. Chem. Soc.* **1992**, *113*, 4529.

(5) The work in this chapter has been carried out in collaboration with Ivan Huc.

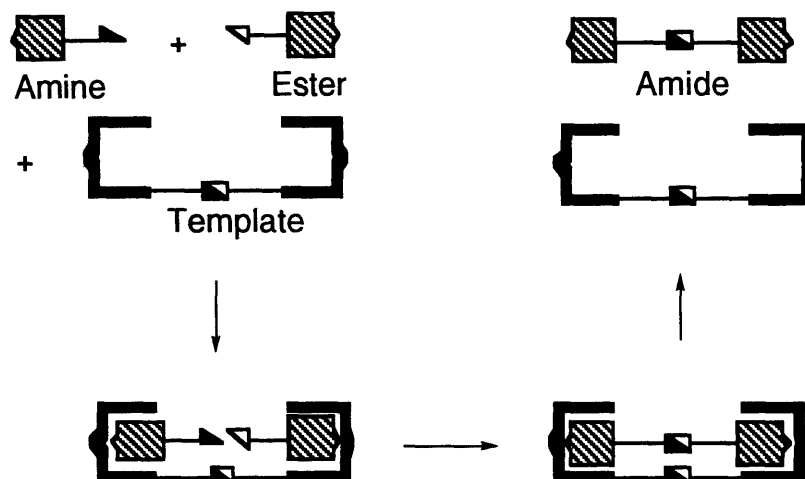


Figure IV-1 Schematic representation of a template enhanced coupling reaction.

The complementarity on which the current work relies is the binding of adenine derivatives by previously reported scorpion shaped receptors.⁶ The association involves the chelation of the purine nucleus of adenine by two imides attached to a carbazole surface. The imides provide simultaneous Watson-Crick and Hoogsteen base pairing while the carbazole stacks to the purine (Figure IV-2). High binding affinities between these two components ($K_a = 10^4 - 10^5 \text{ M}^{-1}$) are observed in organic solvents, and precise positioning of the adenine in the diimide pocket is expected.

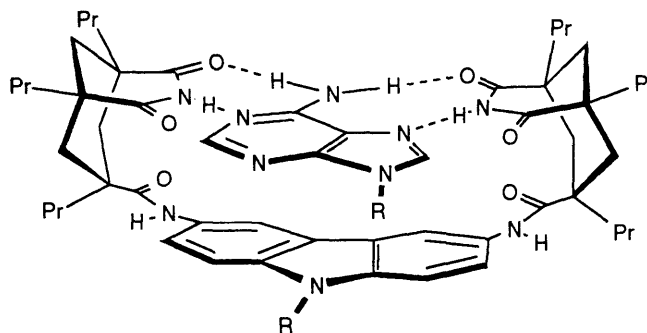


Figure IV-2 The binding of adenine derivatives by diimide receptors.

Both the carbazole portion of the receptor and the ribose portion of adenosine are well suited for synthetic elaboration. They can be outfitted with complementary chemically reactive functions - amine nucleophiles and active ester electrophiles - for covalent

(6) (a) Conn, M. M.; Deslongchamps, G; de Mendoza, J.; Rebek, J., Jr. *J. Am. Chem. Soc.* **1993**, *115*, 3548. (b) Chapter II, this thesis.

coupling reactions. Two amines and two active esters were prepared (Figure IV-3) and the template effects of their coupling products were systematically evaluated.

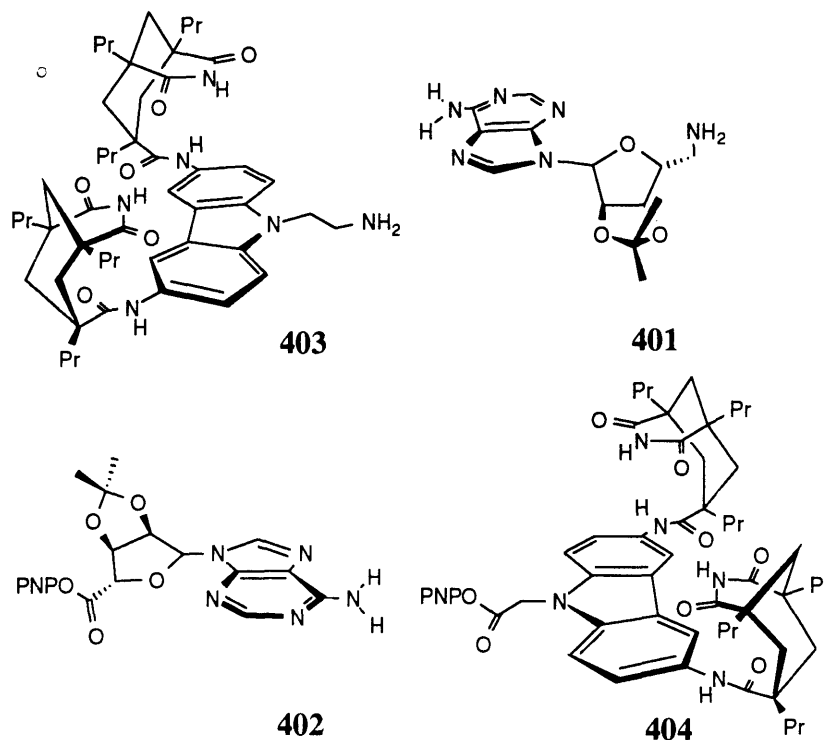


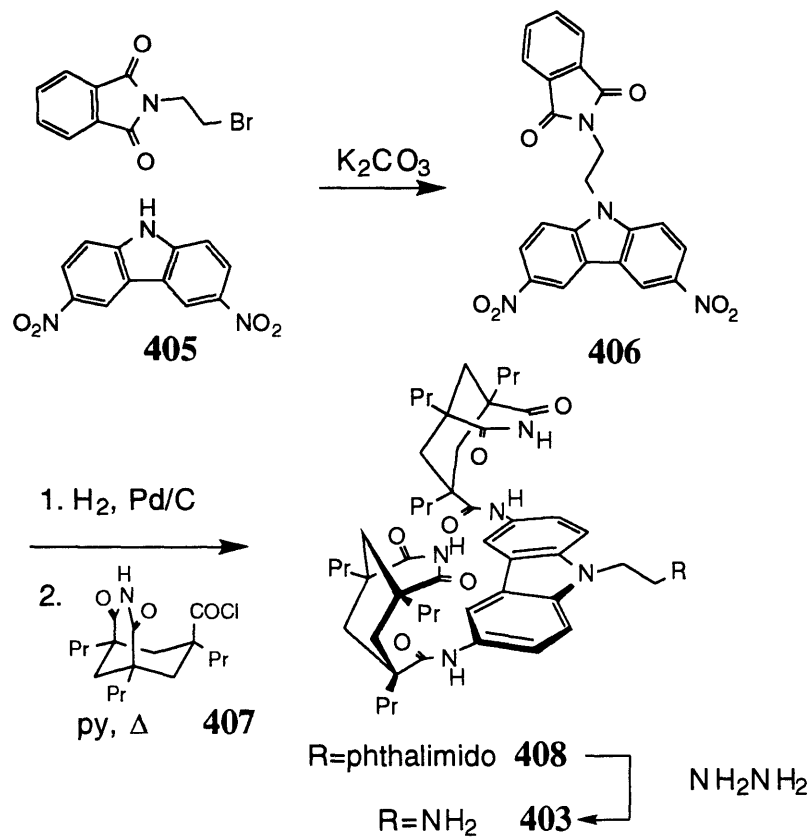
Figure IV-3. Structures of amines and active esters.

IV.2 Synthesis

The two p-nitrophenylesters **402** and **404** (Figure IV-3) were prepared from their corresponding carboxylic acids^{6a,7} using p-nitrophenol and the coupling reagent EDC. Amine **401** was prepared according to a published procedure,⁸ and amine **403** was made from 3,6-dinitrocarbazole in four steps (Scheme IV-1). This involved coupling **405** to N-(2-bromoethyl)-phthalimide to give **406**. Hydrogenation of the nitro groups, followed by acylation of the resulting amines with Kemp's imide acid chloride **407** gave **408**. Cleavage of the phthalimide with hydrazine resulted in **403** in 52% overall yield.

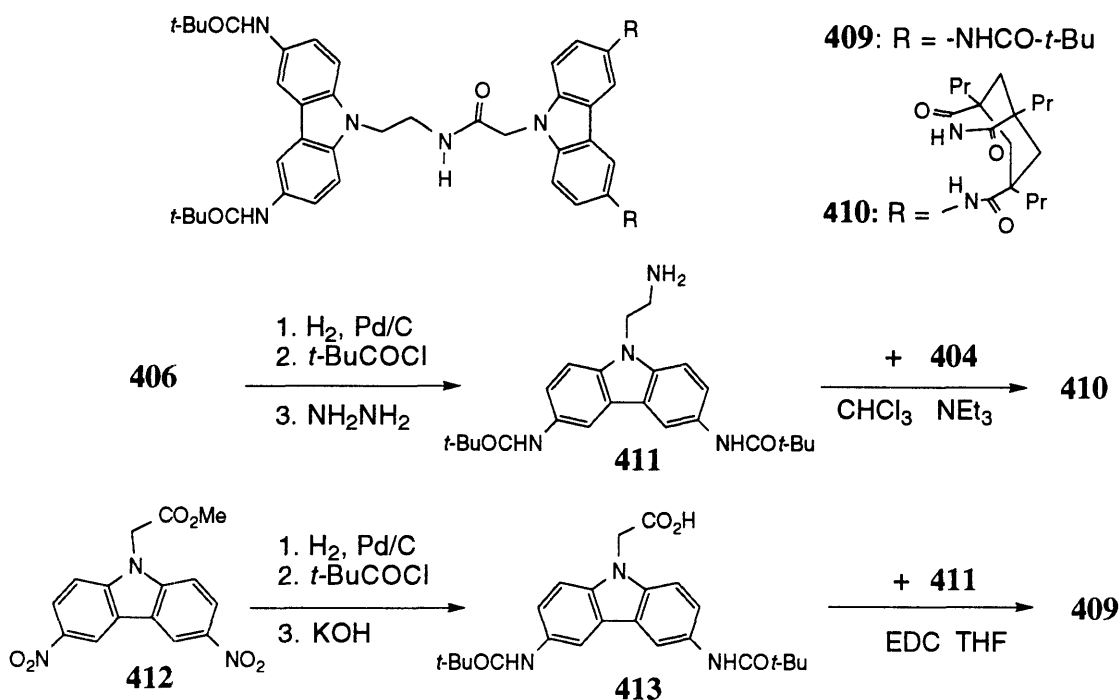
(7) Schmidt, R.S.; Schloz, U.; Schwille, D. *Chem. Ber.* **1968**, *101*, 590.

(8) Kolb, M.; Danzin, C.; Barth, J.; Claverie, N. *J. Med. Chem.* **1982**, *25*, 550.



Scheme IV-1 Synthesis of amine **403**.

Two reference templates **409** and **410**, containing many of the structural features of template **415** (*vide infra*) but lacking two recognition sites and one recognition site, respectively, were prepared according to Scheme IV-2. Hydrogenation of dinitro compound **406**, followed by acylation of the diamine with pivaloyl chloride and subsequent hydrazinolysis gave amine **411**. Coupling of this amine to active ester **404** gave **410**. Hydrogenation of dinitro compound **412**^{6a} followed by acylation as before, then by saponification of the ester resulted in acid **413**. This acid was coupled to amine **411** with EDC to give **409**.



Scheme IV-2. Synthesis of reference 'templates'.

IV.3 Template Effects

Coupling reactions in CHCl_3 were carried out at $25\text{ }^\circ\text{C}$, and monitored spectrophotometrically following the release of *p*-nitrophenol. The results are summarized in Table IV-1. The first reaction studied was the coupling between **401** and **402**. At equimolar concentrations of 0.05 mM in CHCl_3 , in the presence of triethylamine, the coupling proceeds with an initial rate of $1.5 \times 10^{-8}\text{ M min}^{-1}$ (Figure IV-5) to give the product amide **414** (Figure IV-4). The reaction was then run in the presence of 1 equiv of **415**, which is the product of the reaction between **403** and **404** (*vide infra*). Compound **415** accelerated the coupling reaction between **401** and **402** by a factor of ten. This acceleration is reduced when competitive binders are present: the product **414** (1 equiv), which can be bound by **415** at both ends (see chapter 5), reduces the acceleration to three-fold whereas a large amount of 9-ethyladenine (10 equiv), which can only recognize a single end of the structure, lowers the acceleration to two-fold. The rate of the uncatalyzed reaction is unaffected by these compounds. The reference compound **409**, which lacks both receptor sites, had no effect on the rate of the reaction. Compound **410**, having one receptor site, slightly *reduces* the initial coupling rate (by about 25%).

This is presumably due to the fact that its bound reagents are less accessible for reaction with reagents in solution.

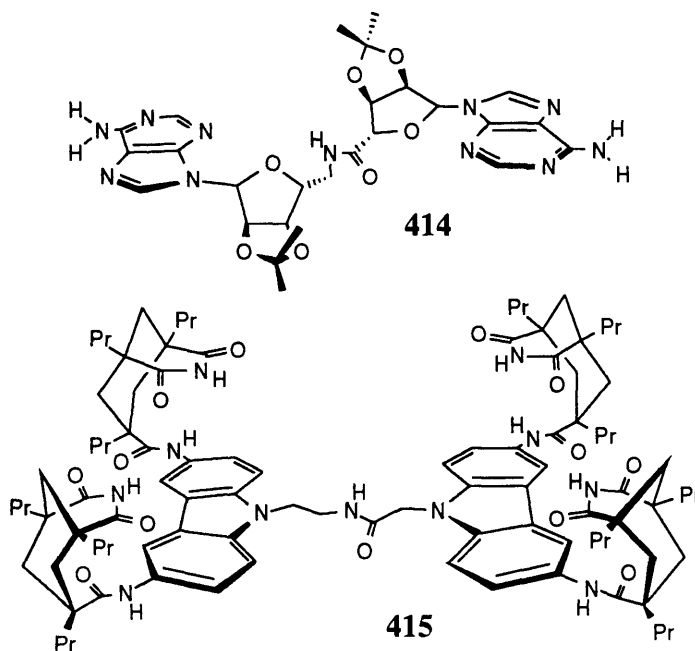


Figure IV-4. Structures of coupling products/templates.

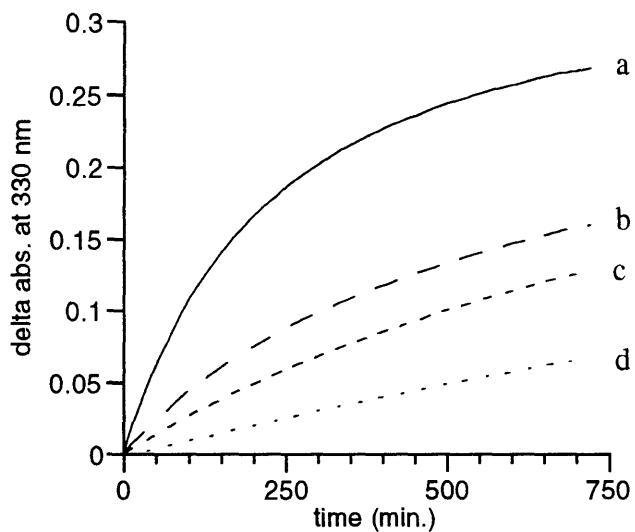


Figure IV-5. Absorption increases at 330 nm over time for the reaction between 401 and 402 (both at 0.05 mM) in CHCl_3 at 25 °C with 4 mM N_3Et and with (a) 1 equiv of 415; (b) 1 equiv of 415 + 1 equiv of 414; 1 equiv of 415 + 10 equiv of 9-ethyladenine; (d) no additives (background).

IV.4 Solvent Effects.

The acceleration of the coupling between **401** and **402** as caused by **415** was shown to be solvent dependent. At the same concentrations and temperature, the 10-fold acceleration in CHCl₃ increased to 13-fold when CCl₄ was used. In chlorobenzene a 9-fold acceleration was measured, whereas in THF and CH₃CN no rate enhancements were observed. These results parallel the binding affinity of the adenine receptors in these solvents. Although the receptors do bind adenine derivatives in e.g. THF, the binding constant is too low to result in significant association under the dilute reaction conditions. In CCl₄ the adenine affinity is expected to be even higher than in the weakly competitive CHCl₃. The observed acceleration probably reflects this enhanced affinity.

IV.5 Molecular Modeling

All the results above are consistent with a termolecular complex that is responsible for the observed rate enhancements. A more accurate description is that this complex represents the first intermediate on the reaction coordinate from starting materials to products. The rate determining step is the breakdown of the tetrahedral intermediate. A successful template stabilizes the crucial transition state more than the ground state, but nevertheless it must bind the starting materials to begin with. See chapter V for a discussion on template effects. To evaluate (qualitatively) the viability of a termolecular complex of template and two starting materials, a computer minimization was carried out. The three components were docked together and the complex was minimized using the AMBER^{*9} force field and GB/SA CHCl₃ solvation¹⁰ in MacroModel v. 3.5.¹¹ A minimized structure is shown in Figure IV-6. The modeling suggests that both adenosine derivatives can be accommodated simultaneously by **415**, and that the binding permits, in a C-shape backbone conformation, a close proximity of the two reactive groups.

(9) (a) Weiner, S. J.; Kollman, P. A.; Case, D. A.; Singh, U. C.; Alagona, G.; Profeta, S., Jr.; Weiner, P. *J. Am. Chem. Soc.* **1984**, *106*, 765; (b) Weiner, S. J.; Kollman, P. A.; Nguyen, D. T.; Case, D. A. *J. Comput. Chem.* **1990**, *11*, 440; (c) McDonald, D. Q.; Still, W. C. *Tetrahedron Lett.* **1993**, *33*, 7743.

(10) Still, W. C.; Tempczyk, A.; Hawley, R. C.; Hendrickson, T. *J. Am. Chem. Soc.* **1990**, *112*, 6127.

(11) Still, W. C., Columbia University, New York; Mohamadi, F.; Richards, N. G. J.; Guida, W. C.; Liskamp, R.; Lipton, M.; Caufield, C.; Chang, G.; Hendrickson, T.; Still, W. C. *J. Comput. Chem.* **1990**, *11*, 440.

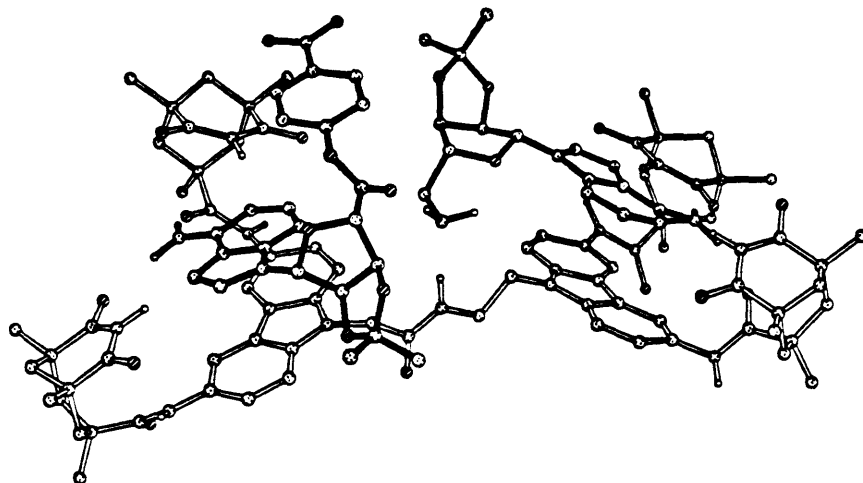


Figure IV-6. Minimized structure of the termolecular complex **401-402-415**. Carbon-bound hydrogens are not represented for clarity. The minimization was carried out with the trimethyl version of the Kemp's imide amide modules.

IV.6 Simulation vs. Experiment

More support for the mechanism came from experiments in which the concentration of added template was varied. Increasing the amount of **415** also increased the initial coupling rates to a maximum acceleration observed at 2 equiv. Further addition resulted in *lower* coupling rates (Figure IV-7); the two reactive components become increasingly separated as complexes on different template molecules. In support of this interpretation, some simulations were carried out to see how the concentration of the productive termolecular complex varies with the amount of added template. The concentration of the complex should be proportional to the rate enhancements.

Calculations were based on the assumption that the template binds each substrate independently and with the same intrinsic affinity K . This is reasonable for an S-shaped overall conformation of the template, and perhaps less likely for the C-shaped conformation required for reaction. If $[T]_{tot}$ represents the total concentration of Template, $[S]_{tot}$ the sum of the total concentrations of the Substrates and $[R]$, $[RS]$ and $[S]$ the concentrations of free and occupied Receptor sites and free Substrate respectively, combining the three following equations:

$$[R] + [RS] = 2[T]_{tot} \quad [S] + [RS] = [S]_{tot} \quad K = \frac{[RS]}{[R][S]}$$

gives [S] as a solution of:

$$[S]^2 + \left(2[T]_{\text{tot.}} - [S]_{\text{tot.}} + \frac{1}{K} \right) [S] - \frac{[S]_{\text{tot.}}}{K} = 0$$

The fraction of occupied receptor sites is:

$$\frac{[RS]}{2[T]_{\text{tot.}}} = \frac{K[S]}{1 + K[S]}$$

And therefore, the concentration of termolecular complex is calculated by substitution of [S] into:

$$[TS_2] = [T]_{\text{tot.}} \left(\frac{K[S]}{1 + K[S]} \right)^2$$

When the concentrations of amine and esters are equal, the concentration of productive complex (containing one of each reagent) is $[TS_2]/2$. Using these calculations the solid line in Figure IV-7 was produced. The line shows that the calculated concentration of productive termolecular complex varies in the same way with template concentration as does the experimentally observed rate acceleration, supporting the proposed mechanism. The best fit was obtained when a K_a of 14000 M^{-1} ($\Delta G = -5.7 \text{ kcal mol}^{-1}$) was used in the calculation. This number is in good agreement with the experimentally observed association constants for similar receptor systems.^{6a}

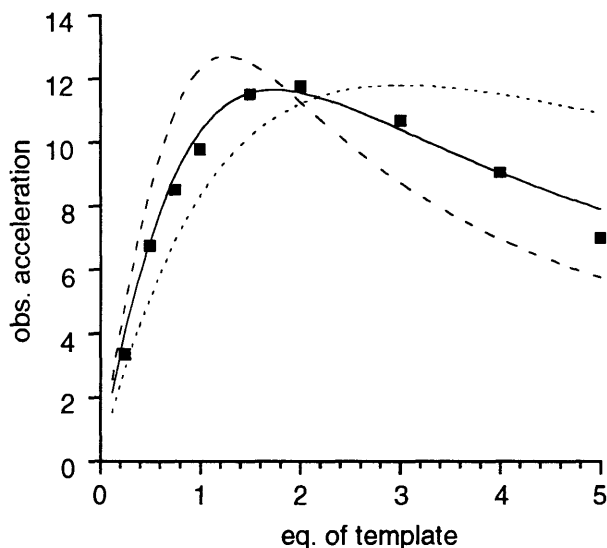


Figure IV-7. Observed acceleration of **401+402** vs. the amount of template **415** (■), (0.05 mM of each reagent, 4 mM NEt_3 in CHCl_3 at 25°C). Calculated concentration of productive complex (**401-402-415**) (solid line) for an affinity receptor-adenine of 14000 M^{-1} under the same conditions. Calculated concentration for $K=5000 \text{ M}^{-1}$ (dotted line), and for $K=45000 \text{ M}^{-1}$ (dashed line). Note that no vertical scale is represented for the calculated data, as the scale is different for each line.

IV.7 Reciprocal Template Effects

The availability of the four molecules of Figure IV-3 allowed us to evaluate several other reactions involving template effects. The first reaction was the coupling of **403** and **404** to give **415**. For this reaction an initial rate of $4.3 \times 10^{-9} \text{ M min}^{-1}$ was measured (Table IV-1). Addition of one equiv of **414** increased the initial coupling rate five-fold. Both product (**415**) and 9-ethyladenine acted as competitive inhibitors; both reduced the acceleration while having no significant effect on the background reaction rate. The acceleration is again likely due to a termolecular complex complementary in structure to the one shown in Figure IV-6, but this time the "outside" amide is formed instead of the "inside" one. This system is related to the previous one in a special way, since the product of one reaction is a template for the other: *These reciprocally templated reactions formally represent a replication cycle.*

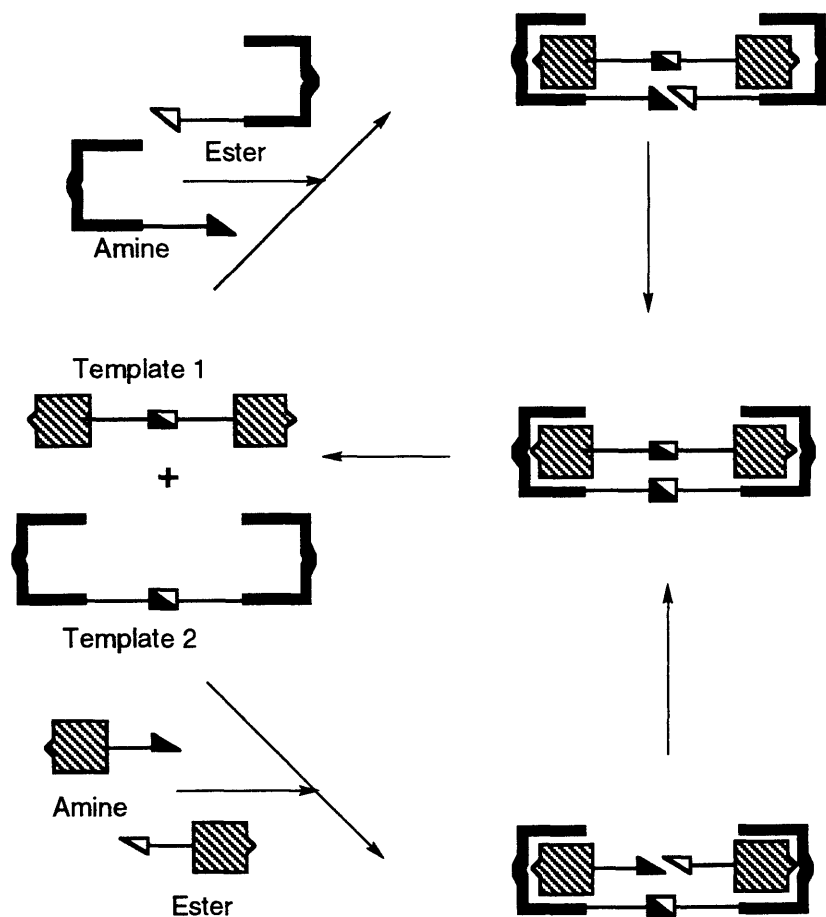


Figure IV-8. Schematic representation of the replication cycle.

reaction*	Concentration (mM)					Init. rate (10 ⁻⁹ M/min)**
	[14]	[15]	[9-Et- Ad.]	[9]	[10]	
1+2	-	-	-	-	-	15
1+2	0.05	-	-	-	-	16
1+2	-	0.05	-	-	-	150
1+2	0.05	0.05	-	-	-	42
1+2	-	0.05	0.5	-	-	30
1+2	-	-	0.5	-	-	15
1+2	-	-	-	0.05	-	15
1+2	-	-	-	-	0.05	11
3+4	-	-	-	-	-	4.3
3+4	0.05	-	-	-	-	23
3+4	-	0.05	-	-	-	4.3
3+4	0.05	0.05	-	-	-	13
3+4	0.05	-	0.5	-	-	15
3+4	-	-	0.5	-	-	4.8
3+2	-	-	-	-	-	53000
3+2	-	-	0.5	-	-	14000
1+4	-	-	-	-	-	2200
1+4	-	-	0.5	-	-	600

Table VI-1. Initial Rates of Amide formation. *Both components are present at 0.05 mM in CHCl₃ + 4 mM NEt₃ at 25 °C. **Values are averaged from multiple independent runs. Standard deviations are ±15%.

IV.8 Bimolecular Coupling Reactions

The remaining coupling combinations of the starting materials (Figure IV-3) are the reactions between **401** and **404** and between **402** and **403**. These reactions involve complementary bimolecular components and are both about three orders of magnitude faster than those previously discussed (Table IV-1). The high rates are due to the association of the two reaction partners, resulting in complexes in which the reactive groups are almost always in close proximity¹² (see Fig. IV-9 for **402-403**). This conclusion is supported by the observation, in both cases, of saturation kinetics, i.e. increasing the concentration of the amine results eventually in a maximum velocity (see Fig. IV-10 for **401** and **404**).

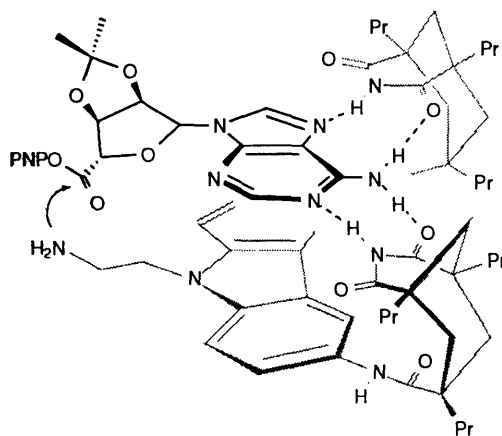


Figure IV-9. Bimolecular complex proposed for the fast reaction between **402** and **403**.

The products of these coupling reactions are "folded shut" as intramolecular complexes. In the ¹H NMR spectrum (CDCl₃, room temperature), the two imide protons give separate signals around 13-ppm; one results from base pairing to the adenine in the Watson-Crick mode and the other binds in the Hoogsteen fashion. Dilution studies on the coupling product of **401** and **404** showed that the chemical shift of these bound protons is concentration independent. Additional support for intramolecular association came from Vapor Pressure Osmometry (VPO). The apparent molecular weight of observed for a

(12) For related systems see: (a) Tecilla, P.; Hamilton, A. D. *J. Chem. Soc., Chem. Commun.* **1990**, 1232. (b) Göbel, M. W.; Bats, J. W.; Dürner, G. *Angew. Chem. Int. Ed. Engl.* **1992**, *31*, 207. (c) Lehn, J. M.; Sirlin, C. *J. Chem. Soc., Chem. Commun.* **1978**, 949. (d) Cram, D. J.; Katz, H. E. *J. Am. Chem. Soc.* **1983**, *105*, 135. (e) G. L. Trainor, Breslow, R. *J. Am. Chem. Soc.* **1981**, *103*, 154.

3 mM solution in CHCl_3 is 833, 72% of the actual value (1154.6), using a related receptor as a reference.¹³

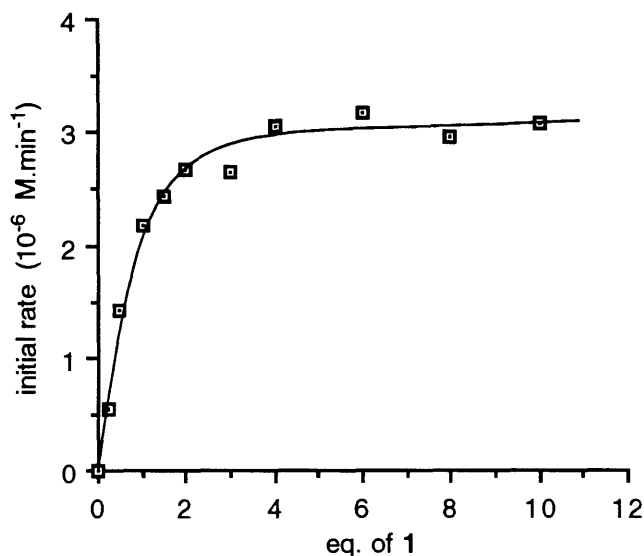


Figure IV-10. The initial rate of the reaction between **401** and **404** vs. the amount of **401**. $[\mathbf{404}] = 5 \cdot 10^{-5} \text{ M}$, $[\text{NEt}_3] = 4 \cdot 10^{-3} \text{ M}$ in CHCl_3 at 25°C . Line is drawn for visual guidance only.

IV.9 Conclusion

Covalent coupling reactions have been accelerated by up to 13-fold with a bisubstrate template. The presence of a termolecular complex involved in the catalysis was supported by the observation of 1) competitive inhibition, 2) the lack of activity of "no recognition templates", 3) solvent dependence, 4) molecular modeling and 5) the correlation between experiment and simulation. The rate enhancements here are comparable to those observed by Kelly^{3b,c} in reaction templates for bimolecular $\text{S}_{\text{N}}2$ reactions and are considerably larger than those observed in template effects involving **self-complementary** structures.⁴ The reciprocal templating effects of **414** and **415** represent a replication cycle. Whether these cycles are generally more efficient than the minimalist self-complementary replicators is the subject of ongoing research. The large accelerations in bimolecular systems due to association of both reaction components

(13) The accuracy of the VPO method is notoriously poor as the technique works optimally for non-associating molecules. Systems with polar functionality tend to give higher-than-theoretical molecular weights due to nonspecific aggregation, see Seto, C. T. ; Whitesides, G. M. *J. Am. Chem. Soc.* **1993**, *115*, 905.

shows the potential advantages of molecular recognition in catalysis as well as in stoichiometric reactions.

IV.10 Experimental Section

General. Infrared spectra were obtained from a Perkin Elmer 1600 FT IR spectrophotometer. ^1H NMR spectra were measured with Bruker WM-250 (250-MHz), AC-250 (250 MHz) and Varian XL-300 (300 MHz), Unity 300 (300MHz). UV measurements were taken on a Perkin Elmer Lambda 2 spectrophotometer. High-resolution mass spectra were obtained with a Finnegan Mat 8200 instrument. For the FAB spectra 3-nitrobenzyl alcohol was used as the matrix. Melting points were taken on a Electrothermal 9100 melting point apparatus. Commercial-grade solvents were used without further purification

Adenosine active ester (402). In 5 mL of anhydrous THF were mixed: 2',3'-O-isopropylidene-adenosine-5'-carboxylic acid⁷ (100 mg, 0.311 mmol), 4-nitrophenol (169 mg, 4 eq), EDC (265 mg, 4.5 eq) and DMAP (11 mg, 0.3 eq). The initial suspension slowly turned into a homogeneous solution and a sticky white solid separated on the flask walls (EDC-urea). The solution was stirred for 48 h at room temperature. It was then decanted, and the solvent was removed. The residue was dissolved in CH_2Cl_2 and subjected to a flash chromatography on a (short) silica gel column. The eluting solvent (EtOAc) was pushed through quickly to avoid product decomposition on silica gel. The residue was redissolved in a minimal EtOAc and Et_2O was added until no more precipitation occurred. The white solid was filtered off and dried. Yield 102 mg (74%); mp 118-122 °C. IR (KBr) 3322, 3164, 1756, 1639, 1594, 1526, 1349, 1207, 1099, 1074 and 864 cm^{-1} . ^1H NMR (300 MHz, CDCl_3) δ 8.20 (d, 2H, $J = 9.3$ Hz), 8.19 (s, 1H), 7.00 (d, 2H, $J = 9.0$ Hz), 6.28 (s, 1H), 6.09 (br.s., 2H), 5.90 (d, 1H, $J = 5.4$ Hz), 5.57 (d, 1H, $J = 6.0$ Hz), 5.10 (s, 1H), 1.66 (s, 3H), 1.47 (s, 3H). HRMS (EI) m/e calcd for $\text{C}_{19}\text{H}_{18}\text{N}_6\text{O}_8$: 442.1237; found 442.1234.

Carbazole diimide active ester (404). In 2 mL of anhydrous THF were mixed: the appropriate acid^{6a} (50 mg, 0.058 mmol), 4-nitrophenol (32 mg, 4 equiv), EDC (50 mg, 4.5 eq) and DMAP (2 mg, 0.3 equiv). The initial suspension slowly turned into a homogeneous solution and a sticky white solid adhered to the flask (EDC-urea). The solution was stirred for 48 h at room temperature. It was then decanted off, and the solvent was removed. The residue was dissolved in CH_2Cl_2 and subjected to a flash

chromatography on a (short) silica gel column. The eluting solvent (EtOAc) was pushed through quickly to avoid product decomposition on silica gel. The residue was redissolved in a little ether and hexane was added until total precipitation of a white solid which was filtered off and dried. Yield 38 mg (67%) of pure product; mp 235 °C (dec.). IR (KBr) 3380, 3225, 3959, 2933, 2871, 1698, 1526, 1490, 1466, 1346 and 1203 cm^{-1} . ^1H NMR (300 MHz, $\text{DMSO-}d_6$) δ 10.37 (s, 2H), 9.17 (s, 2H), 8.31 (d, 2H, $J = 7.0$ Hz), 8.13 (s, 2H), 7.59 (d, 2H, $J = 8.8$ Hz), 7.54 - 7.45 (m, 4H), 5.66 (s, 2H), 2.67 (d, 4H, $J = 14.0$), 2.02 (d, 2H, $J = 12.7$ Hz), 1.90 - 1.70 (m, 4H), 1.55 - 1.00 (m, 26H), 0.97 - 0.75 (m, 18H).

Phthalimide (406). N-(2-bromoethyl)-phthalimide (1.482 g, 4.77 mmol), 3,6-dinitrocarbazole **405** (300 mg, 1.17 mmol), and K_2CO_3 (1.612 g, 11.66 mmol), were mixed in DMF (7mL) and heated at 110 °C. A yellow precipitate formed slowly, and after 1 h the mixture was poured into H_2O (100 mL). The solid was filtered off, washed with H_2O , EtOH and dried to give 437 mg (87%) of a yellowish solid; mp . 330 °C. IR (KBr) 1706, 1602, 1586, 1509, 1475, 1336, 1313, 1225, 1131, 1103, 719 cm^{-1} ; ^1H NMR (300 MHz, $\text{DMSO-}d_6$) δ 9.45 (d, 2H, $J = 2.2$ Hz), 8.28 (dd, 2H, $J = 9.2$ and 2.3 Hz), 7.78 (d, 2H, $J = 9.2$ Hz), 7.80 - 7.65 (m, 4H), 4.85 (t, 2H, $J = 5.3$ Hz), 4.03 (t, 2H, $J = 5.3$ Hz). HRMS (EI) m/e calcd for $\text{C}_{22}\text{H}_{14}\text{N}_4\text{O}_6$: 430.0913; found: 430.0912.

Phthalimide (408). Dinitro compound **406** (400 mg, 0.930 mmol) was dissolved in DMF (150 mL). Pd/C (10%, 350 mg) was added and a H_2 balloon was connected. After stirring at room temperature for 14 h the catalyst was filtered off through celite and the solvent was removed, to give 315 mg (92%) of the cream-colored amine. ^1H NMR (300 MHz, $\text{DMSO-}d_6$) δ 7.78 (s, 4H), 7.05 (d, 2H, $J = 8.9$ Hz), 7.03 (d, 2H, $J = 2.1$ Hz), 6.62 (dd, 2H, $J = 8.5$ and 2.0 Hz), 4.62 (br.s., 4H), 4.39 (t, 2H, $J = 6.2$ Hz), 3.89 (t, 2H, $J = 6.1$ Hz). The diamine (312 mg, 0.843 mmol), imide acid chloride **407** (605 mg, 1.77 mmol) and a catalytic amount of DMAP were dissolved in pyridine (12 mL) and heated at reflux for 3 h. The solvent was removed and the residue was dissolved in CH_2Cl_2 , washed with a saturated NaHCO_3 solution (30 mL), dried on MgSO_4 , filtered and concentrated. The product was purified through column chromatography over silica gel (2% MeOH in CH_2Cl_2) to give 543 mg (60% from **406**) of a beige solid; mp 197 °C. IR (KBr) 3380, 2958, 1713, 1489, 1466, 1396, 1310, 1191, 803, 719 cm^{-1} . ^1H NMR (300 MHz, $\text{DMSO-}d_6$) δ 10.38 (s, 2H), 9.12 (s, 2H), 8.09 (s, 2H), 7.78 (s, 4H), 7.37 (2, 4H), 4.65 - 4.55 (m, 2H), 4.00 - 3.90 (m, 2H), 2.65 (d, 4H, $J = 13.9$ Hz), 2.02 (d, 2H, $J = 12.5$ Hz), 1.86 - 1.70 (m, 4H), 1.55 - 1.00 (m, 26 H), 0.95 - 0.72 (m, 18H). HRMS (FAB) m/e calcd for $\text{C}_{58}\text{H}_{73}\text{N}_6\text{O}_8$ (M + H): 981.5490; found: 981.5486.

Amine (403). Phthalimide **408** (540 mg, 0.550 mmol) was dissolved in MeOH (25 mL). Hydrazine (520 μ L, 16.6 mmol) was added and the mixture was stirred at room temperature for 14 h. The solvent was removed and CH_2Cl_2 (50 mL) was added to the residue. The insoluble part was filtered off and the filtrate was concentrated to give 462 mg (99%) of an off-white solid; mp 196 $^\circ\text{C}$ (dec.). IR (KBr) 3378, 2958, 1699, 1488, 1466, 1200 and 803 cm^{-1} . ^1H NMR (300 MHz, $\text{DMSO}-d_6$) δ 10.36 (s, 2H), 9.13 (s, 2H), 8.12 (s, 2H), 7.50 - 7.36 (m, 4H), 4.35 - 4.25 (m, 2H), 2.91 - 2.82 (m, 2H), 2.66 (d, 4H, $J = 13.4$ Hz), 2.02 (d, 2H, $J = 12.7$ Hz), 1.85 - 1.70 (m, 4H), 1.57 - 1.00 (m, 26 H), 0.95 - 0.73 (m, 18 H). HRMS (FAB) m/e calcd for $\text{C}_{50}\text{H}_{71}\text{N}_6\text{O}_6$ ($M + \text{H}$); 851.5435 found: 851.5428.

Amine (411). Dinitro compound **406** (158 mg, 0.367 mmol) was dissolved in DMF (100 mL). Pd/C (10%, 150 mg) was added and a H_2 balloon was connected. After stirring at room temperature for 14 h the catalyst was filtered off through celite and the solvent was removed. The diamine was dissolved in CH_2Cl_2 (25 mL). Trimethylacetyl chloride (271 μ L, 2.20 mmol) and NEt_3 (307 μ L, 2.20 mmol) were added and the mixture was stirred for 1 h. CH_2Cl_2 (40 mL) was added, and the mixture was washed with a saturated NaHCO_3 solution (30 mL). After drying on MgSO_4 , filtration and removal of the solvent, the diamide was purified using column chromatography over silica gel (5 % MeOH in CH_2Cl_2), to give 135 mg (68%) of a beige solid; ^1H NMR (300 MHz, CDCl_3) δ 8.23 (d, 2H, $J = 2.0$ Hz), 7.82 - 7.77 (m, 2H), 7.71 - 7.66 (m, 2H), 7.48 (dd, 2H, $J = 8.6$ and 2.0 Hz), 7.41 (s, 2H), 7.39 (d, 2H, $J = 8.6$ Hz), 4.53 (t, 2H, $J = 6.8$ Hz), 4.08 (t, 2H, $J = 6.7$ Hz), 1.36 (s, 18 H). This diamide (122 mg, 0.227 mmol) was dissolved in 5 mL MeOH and 20 mL THF. Hydrazine (214 μ L, 6.8 mmol) was added and the mixture was stirred for 14 h. The solvent was removed and the residue treated with CH_2Cl_2 (25 mL). The resulting suspension was filtered and the filtrate concentrated to obtain 76 mg (56 % from **6**) of an off-white powder; mp 227 - 229 $^\circ\text{C}$. IR (KBr) 3346, 3277, 2957, 1650, 1536, 1488, 1317, 1216 and 791 cm^{-1} . ^1H NMR (300 MHz, CDCl_3) δ 8.23 (d, 2H, $J = 2.2$ Hz), 7.54 (dd, 2H, $J = 8.9$ and 2.2 Hz), 7.45 (br. s, 2H), 7.37 (d, 2H, $J = 8.8$ Hz), 4.35 (t, $J = 6.0$ Hz), 3.18 (t, $J = 6.0$ Hz), 1.37 (s, 18 H). HRMS (EI) m/e calcd for $\text{C}_{24}\text{H}_{32}\text{N}_4\text{O}_2$: 408.2525; found: 408.2527.

Acid (413). Dinitro compound **412**^{6a} (247 mg, 0.88 mmol) was dissolved in DMF (30 mL). Pd/C (10%, 30 mg) was added and a H_2 balloon was connected. After stirring at room temperature for 15 h. the mixture was filtered through celite and the filtrate was concentrated. Trituration with Et_2O solidified the diamine which was dried under vacuum. The solid and NEt_3 (3 equiv) were dissolved in anhydrous CH_2Cl_2 (5 mL) at

0 °C and trimethylacetyl chloride (0.32 mL, 3 equiv) was added dropwise. After 3 h at room temperature, a sat. NaHCO₃ solution (10 mL) was added and the mixture was stirred for 1 h. The layers were separated and the organic phase was concentrated. The residue was dissolved in a mixture of THF (30 mL), EtOH (90 mL), and aqueous NaOH (1 N, 30 mL) and stirred at room temperature for 30 min. The mixture was acidified to pH 1 with conc. HCl and the solvent was removed. The crude material was triturated with water, filtered, washed with water and dried under vacuum to yield **413** as an off-white solid (339 mg, 91% from **412**). mp 176 - 178 °C. IR (KBr) 3296, 2960, 1722, 1662, 1523, 1491, 1201 and 792 cm⁻¹. ¹H NMR (300 MHz, DMSO-*d*₆) δ 12.48 (br s, 1H), 9.20 (s, 2H), 8.33 (d, J = 1.8 Hz, 2H), 7.54 (dd, J = 8.8 and 1.8 Hz, 2H), 7.43 (d, J = 8.7 Hz, 2H), 5.14 (s, 2H), 1.26 (s, 18H). HRMS (EI) m/e calcd for C₂₄H₂₉N₃O₄: 423.2158; found: 423.2157.

Amide (409). Amine **411** (25 mg, 0.061 mmol), acid **413** (26 mg, 0.061 mg), EDC (23 mg, 0.123 mmol) and NEt₃ (9 μL, 0.06 mmol) were mixed together in THF (10 mL) and stirred for 14 h. After filtration and concentration of the filtrate the residue was purified using radial chromatography over silica gel (10 % MeOH in CH₂Cl₂). Obtained was 39 mg (78%) of a white solid; mp 230 °C (dec.). IR (KBr) 3349, 2960, 1659, 1530, 1488, 1310, 1202 and 798 cm⁻¹. ¹H NMR (300 MHz, CDCl₃) δ 8.21 (s, 2H), 8.17 (s, 2H), 8.02 (d, 2H, J = 2.2 Hz), 7.99 (d, 2H, J = 1.8 Hz), 7.21 (dd, 4H, J = 8.4 and 1.7 Hz), 6.68 (d, 2H, J = 8.8 Hz), 6.59 (d, 2H, J = 8.9 Hz), 4.74 (br. t, 1H), 4.55 (s, 2H), 4.19 (t, 2H, J = 6.2 Hz), 3.77 - 3.66 (m, 2H), 1.51 (s, 18 H), 1.50 (s, 18 H). HRMS (EI) m/e calcd for C₄₈H₅₉N₇O₅: 813.4578; found: 813.4581.

Aminolysis products. Equimolar amounts of amine and PNP ester were mixed in CHCl₃ in the presence of NEt₃ (80 equiv) at room temperature. After completion of the reaction the solvent and NEt₃ were removed and the product was purified using radial chromatography over silica gel.

Amide (414): mp 161 - 165 °C. IR (KBr) 3425, 1644, 1599, 1384, 1212 and 1088 cm⁻¹. ¹H NMR (300 MHz, CDCl₃) δ 8.17 (s, 1H), 8.03 (s, 1H), 7.95 - 7.85 (m, 1H), 7.74 (s, 1H), 7.69 (s, 1H), 6.43 (br. s, 2H), 6.39 (br. s, 2H), 5.98 (d, 1H, J = 3.3 Hz), 5.84 (d, 1H, J = 2.4 Hz), 5.33 (dd, 1H, J = 6.2 and 2.0 Hz), 5.24 - 5.15 (m, 2H), 4.89 (dd, 1H, J = 6.3 and 4.8 Hz), 4.80 (d, 1H, J = 1.6 Hz), 4.04 (dd, 1H, 8.0 and 4.2 Hz), 3.84 - 3.72 (m, 1H), 3.37 - 3.25 (m, 1H), 1.63 (s, 3H), 1.59 (s, 3H), 1.36 (s, 3H), 1.32 (s, 3H). HRMS (EI) m/e calcd for C₂₆H₃₁N₁₁O₇: 609.2408; found: 609.2410.

Amide (415): mp 245 °C (dec). IR (KBr) 3380, 2958, 1700, 1528, 1489, 1466 and 1197 cm^{-1} . ^1H NMR (300 MHz, DMSO- d_6) δ 10.37 (s, 2H), 10.35 (s, 2H), 9.16 (s, 2H), 9.14 (s, 2H), 8.42 - 8.35 (m, 1H), 8.16 (s, 4H), 7.53 - 7.42 (m, 6H), 7.31 (d, 2H, $J = 8.8$ Hz), 4.86 (s, 2H), 4.41 - 4.30 (m, 2H), 3.48 - 3.37 (m, 2H), 2.67 (d, 8H, $J = 13.3$ Hz), 2.03 (d, 4H, $J = 12.5$ Hz), 1.86 - 1.70 (m, 8H), 1.60 - 1.05 (m, 52H), 0.95 - 0.75 (m, 36H). HRMS (FAB) m/e calcd for $\text{C}_{100}\text{H}_{136}\text{N}_{11}\text{O}_{13}$ (M + H): 1699.0319; found: 1699.0310.

Coupling product of 402 and 403: IR (KBr) 3384, 2958, 2932, 2871, 1698, 1466, 1207, 869 and 798 cm^{-1} . ^1H NMR (300 MHz, DMSO- d_6) δ 10.74 (s, 2H), 9.10 (s, 2H), 8.25 (s, 1H), 8.14 (d, 2H, $J = 1.5$ Hz), 7.84 (s, 1H), 7.73 - 7.66 (m, 1H), 7.40 (dd, 2H, $J = 8.8$ and 2.0 Hz), 7.33 (br. s, 2H), 7.27 (d, 2H, $J = 8.8$ Hz), 6.31 (d, 1H, $J = 1.9$ Hz), 5.32 - 5.22 (m, 2H), 4.47 (d, 1H, $J = 1.9$ Hz), 4.08 - 3.88 (m, 2H), 3.27 - 3.10 (m, 2H), 2.68 (d, 4H, $J = 13.9$ Hz), 2.04 (d, 2H, $J = 12.4$ Hz), 1.88 - 1.71 (m, 4H), 1.54 - 1.02 (m, 32H), 0.95 - 0.72 (m, 18 H). HRMS (FAB) m/e calcd for $\text{C}_{63}\text{H}_{84}\text{N}_{11}\text{O}_{10}$ (M + H): 1154.6403; found: 1154.6408.

Coupling product of 401 and 404¹⁴: IR (KBr) 3377, 3214, 2959, 1700, 1696, 1647, 1533, 1468, 1201 cm^{-1} ; ^1H NMR (300 MHz, DMSO- d_6) δ 10.69 (s, 2 H), 9.12 (s, 2 H), 8.31 (s, 2 H), 8.13 (d, 2 H, $J = 1.6$ Hz), 8.05 (s, 1 H, amide), 7.39 (m, 4 H), 7.30 (s, 1 H), 7.27 (s, 1 H), 6.15 (d, 1 H, $J = 2.9$ Hz), 5.42 (m, 1 H), 4.95 (s, 2 H), 4.91 (m, 1 H), 4.21 (m, 1 H), 3.4 (m, 2 H), 2.68 (d, 4 H, $J = 13.5$ Hz), 2.04 (d, 2 H, $J = 12.7$ Hz), 1.8 (m, 4 H), 1.54 (s, 3 H), 1.51 (m, 4 H), 1.4-1.0 (m, 22 H), 1.31 (s, 3 H), 0.88 (t, 12 H, $J = 6.9$ Hz), 0.80 (t, 6 H, $J = 7.2$ Hz); HRMS (FAB) m/e calcd for $\text{C}_{63}\text{H}_{84}\text{N}_{11}\text{O}_{10}$ (M+H), 1154.6403; found, 1154.6408.

Amide (410). This compound was prepared according to the above mentioned aminolysis procedure from **404** and **411**. Isolated yield 94 %; mp 225 °C. IR (KBr) 3381, 2959, 2933, 2872, 1700, 1527, 1489, 1310, 1199 and 802 cm^{-1} . ^1H NMR (300 MHz, DMSO- d_6) δ 10.36 (s, 2H), 9.21 (s, 2H), 9.15 (s, 2H), 8.38 (d, 2H, $J = 1.8$ Hz), 8.35 (m, 1H), 8.12 (d, 2H, $J = 1.8$ Hz), 7.60 (dd, 2H, $J = 8.8$ and 1.8 Hz), 7.45 (m, 4H), 7.23 (d, 2H, $J = 8.8$ Hz), 4.80 (s, 2H), 4.37 (m, 2H), 3.48 - 3.37 (m, 2H), 2.67 (d, 4H, $J = 13.3$ Hz), 2.03 (d, 2H, $J = 12.5$ Hz), 1.86 - 1.70 (m, 4H), 1.60 - 1.05 (m, 44H), 0.95 - 0.75 (m, 18H). HRMS (FAB) m/e calcd for $\text{C}_{74}\text{H}_{98}\text{N}_9\text{O}_9$ (M + H): 1239.7488; found: 1256.7492.

(14) M. M. Conn, Ph.D. thesis, Massachusetts Institute of Technology, 1994.

Aminolysis Kinetics. Typically, CHCl_3 solutions of the amine (125 μL , 0.4 mM), NEt_3 (125 μL , 32 mM) and other additives (template, inhibitors), were mixed together in a quartz cuvet (1 cm pathlength). The volume was adjusted to 875 μL with CHCl_3 , and the solution of active ester was added (125 μL , 0.4 mM). The cuvet was closed with a teflon cap, shaken and quickly transferred to the temperature controlled ($25\text{ }^\circ\text{C} \pm 0.1\text{ }^\circ\text{C}$) compartment of the spectrometer. The reaction was periodically monitored at 330 nm. The data were collected using the PECSS software package v. 4.2 (Perkin-Elmer). The reactions were generally followed to at least 80% completion. Initial rates were determined from the first 10% of reaction. Reactions were run in duplicate or triplicate and numbers were averaged. Reactions were run with and without amine nucleophile to ensure the p-nitrophenol release was due to aminolysis rather than hydrolysis from residual water or undetected impurity.

Product analysis A product analysis was performed by taking two solutions with both 0.1 mM **401** and **402** (in CHCl_3 (20 mL) + 8 mM NEt_3). One of these also contained 0.1 mM **415**, which lead to an 8-fold initial rate acceleration as determined spectrophotometrically. After 72 h. the solvents and NEt_3 were removed and the residues were redissolved in $\text{DMSO-}d_6$ and analyzed by ^1H NMR. In both cases **414** was the only observed product.

Vapor Pressure Osmometry. The molecular weight determinations were performed on a Wescan Model 233 vapor pressure osmometer. Standards were measured at 1, 3, 6 and 10 mM and molecular weights determined at 3 mM in HPLC grade glass-distilled CHCl_3 (Aldrich). There is a $\pm 20\%$ margin of error for the measurements.

Chapter V. Template Effects and Polar Transition State Stabilization in Catalysis of Organic Reactions

V.1 Introduction

Bio-organic chemistry continues to be inspired by Nature's ability to catalyze reactions. For many bimolecular reactions gathering of substrates inside an enzyme's active site, reduces large entropic barriers that are paid for by the binding energy of the substrates.¹ Reactions can be enhanced by this phenomenon alone, that is, by complementary surfaces orienting reactants favorably for reaction. Any catalyst of this sort is a template, and several synthetic model systems using various intermolecular forces for binding and recognition are available.² The acceleration in rate with these catalysts is due to the reduction of *activation entropy* (ΔS^\ddagger). Another feature of enzyme catalysis involves selective polar (or apolar) stabilization of the highest energy transition state.³ This reduces the *activation enthalpy* (ΔH^\ddagger) of the reaction of bound substrates. Model systems that exhibit this feature are rarer, but the promise of model systems⁴ is their capacity to isolate catalytic parameters (ΔH^\ddagger , ΔS^\ddagger) and study them independently.

Advances in the field of molecular recognition have yielded many synthetic host-guest systems, but combining recognition with catalysis has proven especially challenging.⁵

(1) Page, M. I.; Jencks, W. P. *Proc. Natl. Acad. Sci. U.S.A.* **1971**, *68*, 1678.

(2) (a) Anderson, S.; Anderson, H. L.; Sanders, J. K. M. *Acc. Chem. Res.* **1993**, *26*, 469. (b) Hoss, R.; Vögtle, F., *Angew. Chem. Int. Ed. Engl.* **1994**, *33*, 375. (c) Sievers, D.; von Kiedrowski, G. *Nature* **1994**, *369*, 221. (d) Walter, C. J.; Anderson, H. L.; Sanders, J. K. M. *J. Chem. Soc., Chem. Commun.* **1993**, 458. (e) Kelly, T. R.; Zhao, C.; Bridger, G. J. *J. Am. Chem. Soc.* **1989**, *111*, 3744. (f) Kelly, T. R.; Bridger, G. J.; Zhao, C. *J. Am. Chem. Soc.* **1990**, *112*, 8024. (g) Dietrich-Buchecker, C. O.; Sauvage, J. P.; Kern, J. M. *J. Am. Chem. Soc.* **1984**, *106*, 3043. (h) Mock, W. L.; Irra, T. A.; Wepsiec, J. P.; Adhya, M. *J. Org. Chem.* **1989**, *54*, 5302. (i) von Kiedrowski, G.; Wlotzka, B.; Helbing, J.; Matzen, M.; Jordan, S. *Angew. Chem. Int. Ed. Engl.* **1991**, *30*, 423.; (j) Terfort, A.; von Kiedrowski, G. *Angew. Chem. Int. Ed. Engl.* **1992**, *31*, 654. (k) Goodwin, J.T.; Lyn, D. G. *J. Am. Chem. Soc.* **1992**, *114*, 9197; (l) Amabilino, D. B.; Ashton, P. R.; Tolley, M. S.; Stoddart, J. F.; Williams, D. J. *Angew. Chem. Int. Ed. Engl.* **1993**, *32*, 1297. (m) Nowick, J. S.; Feng, Q.; Tjivikua, T.; Ballester, P.; Rebek, J., Jr. *J. Am. Chem. Soc.* **1991**, *113*, 8831. (n) Park, T.-K.; Feng, Q.; Rebek, J., Jr. *J. Am. Chem. Soc.* **1992**, *113*, 4529. (o) Chapter IV, this thesis.

(3) (a) Pauling, L. *Nature (London)* **1948**, *161*, 707. (b) Kraut, J. *Science*, **1988**, *242*, 533.

(4) (a) Reichwein, A. M.; Verboom, W.; Reinhoudt, D. N. *Recl. Trav. Chim. Pays-Bas*, **1994**, *113*, 343. (b) Kirby, A. *Angew. Chem. Int. Ed. Engl.* **1994**, *33*, 551.

(5) For successful examples see: (a) McCurdy, A.; Jimenez, L.; Stauffer, D. A.; Dougherty, D. A. *J. Am. Chem. Soc.* **1992**, *114*, 10314. (b) Jubian, V.; Dixon, R. P.; Hamilton, A. D. *J. Am. Chem. Soc.* **1992**, *114*, 1120. (c) Breslow, R.; Graff, A. *J. Am. Chem. Soc.* **1993**, *115*, 10988. (d) Tam-Chang, S.-W.; Jimenez, L.; Diederich, F. *Helv. Chim. Acta.* **1993**, *76*, 2616. (e) Lehn, J.-M.; Sirlin,

Receptors with high binding affinities are now available⁶ and high binding affinities are often the result of multiple additive interactions that lead to a well-defined geometry of the complex. Such a complex is a good starting point for the design of catalysts, since catalysis is very dependent on the three dimensional positioning of functionality.⁷ Hydrogen bonds are particularly useful in molecular recognition since their directional nature is likely to produce predictable binding geometries. High affinities however, require organic solvents since hydrogen bonds are weak in aqueous solutions. For catalytic purposes this is not a disadvantage. Poor solvation of polar functionality in organic solvents (as in enzyme active sites) raises their chemical potential. This chapter describes the efforts to explore separately the passive template effects and more active polar transition state stabilization by acids and bases as observed in covalent coupling reactions of amines and active esters as well as hydrolysis reactions⁸

For substrate binding, as before, the carbazole based adenine receptors were used. The recognition event involves the chelation of the purine nucleus of adenosines by synthetic receptors based on Kemp's triacid and a carbazole spacer element.⁹ High affinities of these receptors for adenine in non-polar solvents result from the additive incremental effects of hydrogen-bonding and aromatic stacking. Chelation of the purine nucleus between the imide functions results in an unambiguous geometry of the complex, allowing the position of reactive groups to be predicted with some confidence.

V.2 Template Catalysis in Bisubstrate Systems.

The reaction studied involved the aminolysis of an unusually reactive p-nitrophenyl (PNP) ester **501** by amino-adenosine **502** in CHCl₃ (Scheme V-1). The ester **502** is

C. New. J. Chem. **1987**, *11*, 693. (f) Wolfe, J.; Muehldorf, A.; Rebek, J., Jr. *J. Am. Chem. Soc.* **1991**, *113*, 1453.

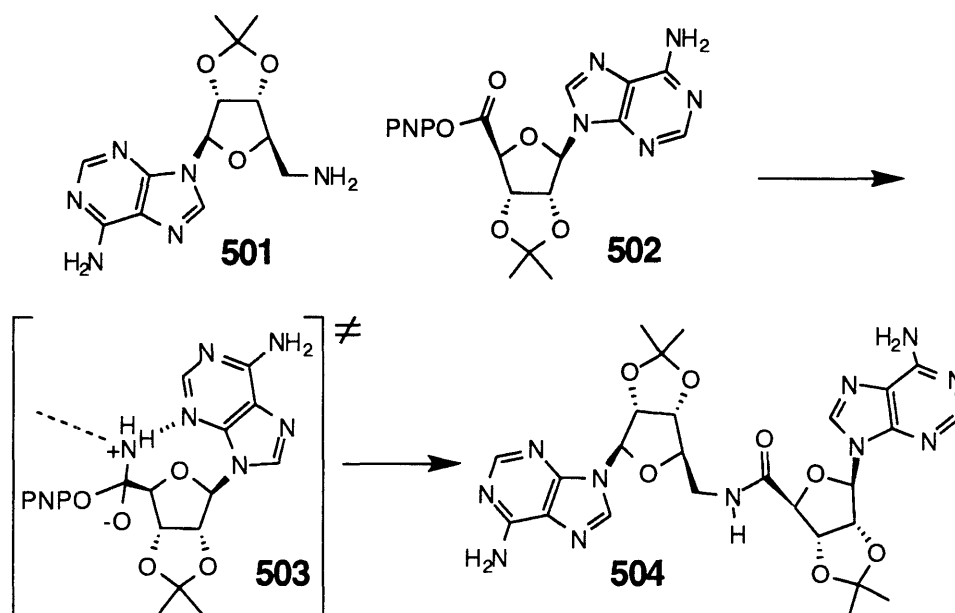
(6) (a) Adrian, J. C., Jr.; Wilcox, C. S. *J. Am. Chem. Soc.* **1989**, *111*, 8055. (b) Zimmerman, S. C.; Wu, W.; Zeng, Z. *J. Am. Chem. Soc.* **1991**, *113*, 196. (c) Kelly, T. R.; Kim, M. H. *J. Am. Chem. Soc.* **1994**, *116*, 7072. (d) Smithrud, D. B.; Diederich, F. *J. Am. Chem. Soc.* **1990**, *112*, 239. (e) Zhang, B.; Breslow, R. *J. Am. Chem. Soc.* **1993**, *115*, 9353. (f) Yoon, S. S.; Still, W. C. *J. Am. Chem. Soc.* **1993**, *115*, 823. (g) Chang, S. K.; Hamilton, A.D. *J. Am. Chem. Soc.* **1991**, *113*, 201. (h) Kearney, P. C.; Mizoue, L. S.; Kumpf, R. A.; Forman, J. E.; McCurdy, A.; Dougherty, D. A. *J. Am. Chem. Soc.* **1993**, *115*, 9907. (i) Jeong, K.-S.; Tjivikua, T.; Muehldorf, A.; Deslongchamps, G.; Famulok, M.; Rebek, J., Jr. *J. Am. Chem. Soc.* **1991**, *113*, 201.

(7) Knowles, J. R. *Nature*, **1991**, *350*, 121.

(8) The work in this chapter has been carried out in collaboration with Ivan Huc.

(9) (a) Conn, M. M.; Deslongchamps, G.; de Mendoza, J.; Rebek, J., Jr. *J. Am. Chem. Soc.* **1993**, *115*, 3548. (b) Chapter II, this thesis.

about 10^3 times more reactive than p-nitrophenyl acetate under the same conditions. It is possible that intramolecular stabilization of the tetrahedral intermediate **503** by hydrogen bonding to the purine N3 nitrogen is the cause (about which more, later).



Scheme V-1 Covalent coupling reaction which was used for the template studies.

A series of carbazole derivatives **505a-h** bearing two receptor sites separated by various spacers was prepared (Figure V-1). The synthetic pathways used are shown in Scheme V-2. Two distinct routes were used. The first uses alkylation of 3,6-dinitrocarbazole, followed by hydrogenation of the resulting tetranitro compound and coupling of the tetra-amine with the Kemp's imide acid chloride **506**. The other uses an Ullmann coupling of aryl bromides to carbazole followed by nitration to get to the tetranitro compounds. The only unsymmetrical template **505g** was made from a coupling of two different pieces as described earlier.²⁰

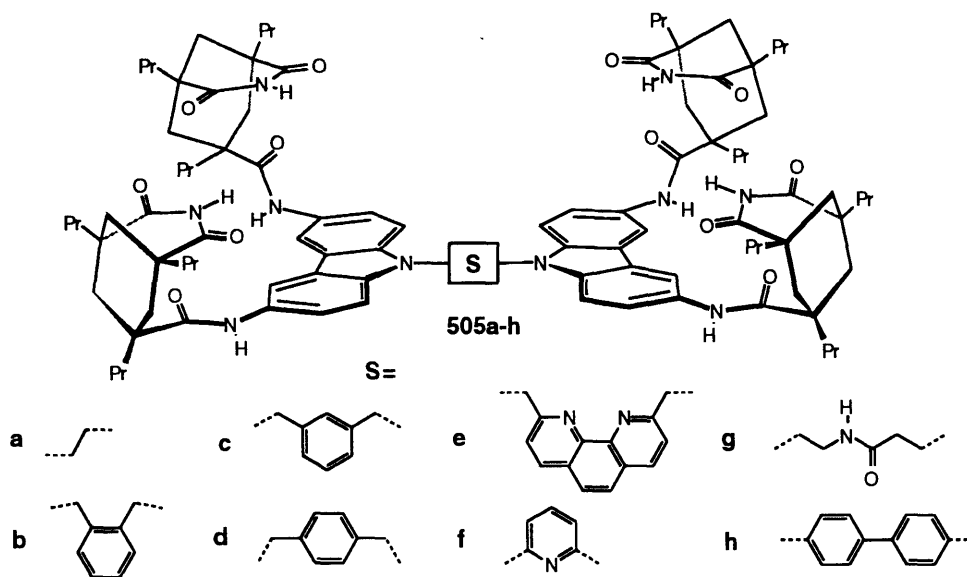
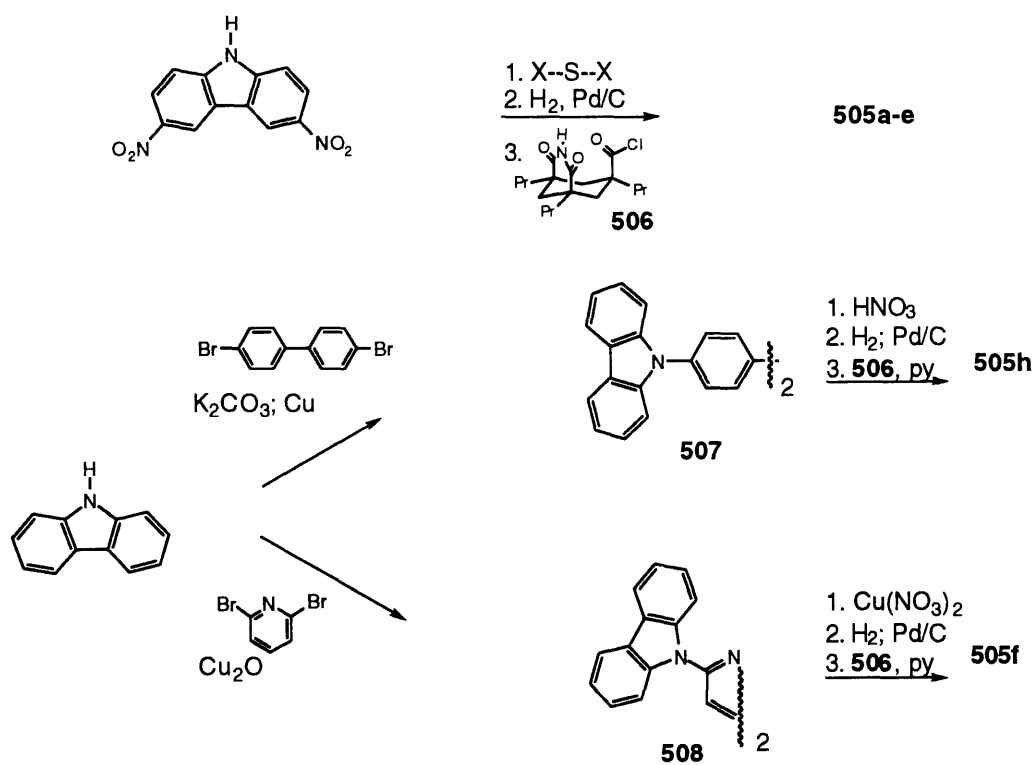


Figure V-1 Structures of the bis-receptors used as molecular templates.



Scheme V-2 Synthesis of the bis-receptors.

The effect of these molecules (1 equiv) on the coupling rate of **501** and **502** varied considerably: from no effect to an acceleration of 160-fold (Table V-1). Within experimental errors, compounds **505h** and **505d** had no or little effect on the reaction rate. Significant catalytic activity was observed for **505c** and **505g**. The distance between the receptor sites for both these templates does not differ much from **505h**, but they are more flexible (their spacers have fewer bonds fixed in a coplanar arrangement) and more conformations can be accommodated. Rate accelerations over one hundred fold were observed with **505b** and **505f**. The spacers of these two templates are slightly shorter than the previous ones and the bound reagents are likely to be held in closer proximity. They are also more rigid. While this feature was a drawback for the longer spacers, it becomes an advantage when the distance and shape are appropriate for a productive complexation. The rigidity of **505f** is obvious: it has only two rotatable bonds. And the poor flexibility of **505b** arises from restricted and coupled rotations of its four single bonds. Finally, the shortest spacer of **505a** does not lead to a larger acceleration. Here, negative cooperativity between the two binding events may be the cause. The very short distance between the receptor sites may accommodate the two substrates only when the backbone is in an S-shaped conformation i.e. the reactive functions diverge, rather than converge, and inhibition of the reaction is expected

Entry	Template:	Rate Acceleration:
1	505h	1
2	505d	1.2
3	505c	5.4
4	505g	10
5	505b	116
6	505f	160
7	505a	31

Table V-1. Observed rate accelerations in the coupling of **501+502** (both at 0.05 mM) in the presence of 1 equiv of potential templates and 4 mM NEt₃ in CHCl₃ at 25 °C.

The template activity of **505f** was studied in more detail. The 160-fold acceleration was reduced to 10-fold if 10 equiv of competitive binder 9-ethyladenine were added (Figure V-2). Similarly, addition of one equiv of the coupling product reduces the initial rate acceleration to 7-fold; a feature which precludes efficient turnover in this system.

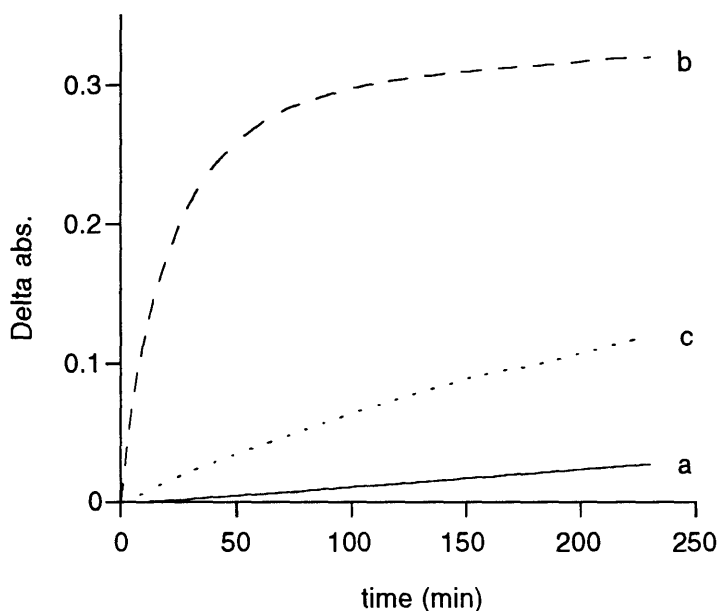


Figure V.2. Coupling of **501** and **502** in CHCl_3 with (a) no additives; (b) 1 equiv of **505f**; (c) 1 equiv of **505f** + 10 equiv of 9-ethyladenine.

Support for the presence of a termolecular complex (**501-502-505f**) as responsible for the observed accelerations was obtained in experiments where more than 1 equiv of **505f** was added. For concentrations of **505f** beyond 1 equiv, the reaction rate *decreases*; the reagents are separated on different template molecules (Figure V-3). This decrease is characteristic of the termolecular nature of the mechanism, and should be expected in all such systems at high template concentrations.

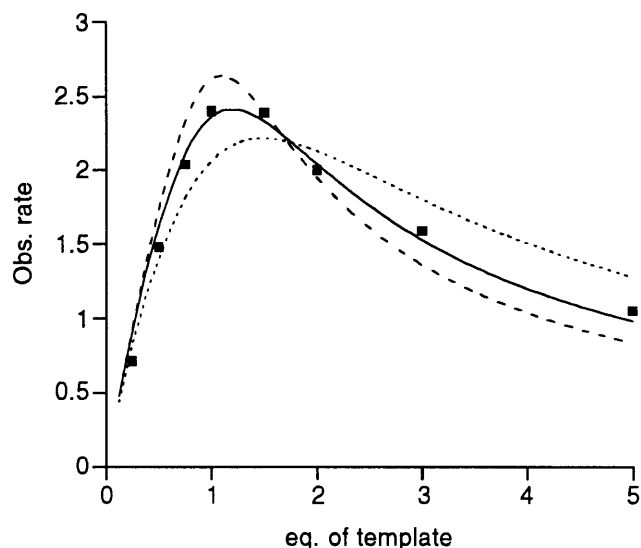


Figure V-3 Observed initial rate ($10^{-6}\cdot\text{M}^{-1}\cdot\text{min}^{-1}$) of **501+502** vs. the amount of template **505f** (■). Calculated concentrations of productive complex (**501.502.505f**) using different binding affinities: $\Delta G = 6.6 \text{ kcal mol}^{-1}$ (solid line), $5.9 \text{ kcal mol}^{-1}$ (dotted line) and $7.2 \text{ kcal mol}^{-1}$ (dashed line) Note that no vertical scale is represented for the calculated data as the scale is different for each line.

V.3 Binding studies

For templates to be effective they must be able to accommodate all the species they encounter along the reaction coordinate.^{2a} One frequently observed phenomenon is that they are highly complementary to the product, causing - as is the case for our system - product inhibition and no turnover.¹⁰ In order to evaluate if there was a correlation between rate acceleration and binding to the product, the appropriate binding studies were conducted. Since the product of the coupling reaction **504** has a structure similar to the tetrahedral intermediate **503**, and the corresponding transition state of its decomposition is rate determining, such a correlation seemed likely. Besides the similarity, the intermediate **503** also differs from **504** because its tetrahedral carbon orients the two purines differently, a feature which might be reflected in the binding affinity to the templates.

(10) This is a problem with covalent coupling reactions which can be circumvented by using group transfer reactions where the products bind with similar affinity than the starting materials. See: Mackay, L. G.; Wylie, R. S.; Sanders, J. K. M. *J. Am. Chem. Soc.* **1994**, *116*, 3141

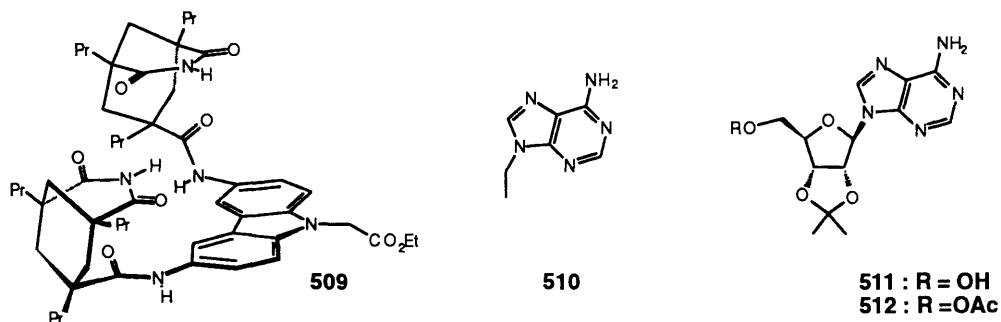


Figure V-4. Structures of molecules used in the binding studies.

The binding constants of the molecules involved are very high and UV-spectroscopy was necessary for our studies of affinity. The single adenine-receptor interactions have been previously determined by ^1H NMR titrations.^{9a} This is not an ideal method because the high affinities (6-7 kcal/mol) require low host concentrations in order to obtain reliable data.¹¹ With ^1H NMR, relatively high concentrations are required for data collection whereas with UV-spectroscopy the relevant data can be conveniently obtained at lower concentrations. On the other hand, UV does not give the structural information that ^1H -NMR does. However, in the case at hand, this information was already available from previous work.⁹ Stacking interactions of the aromatic moieties of our host and guest with our receptors is well established, and changes in the UV spectra on complexation were anticipated. Binding of an adenine derivative to the receptor resulted in a bathochromic shift of the carbazole absorption bands and the largest absorbance increase was observed at 312 nm. Three adenine derivatives **510**, **511**, and **512** were selected and their binding constants with the single receptor **509** were determined (Figure V-4). Next the three templates **505b**, **505d** and **505g** were titrated with **504**. Their corresponding rate acceleration factors in the aminolysis were 116, 1.2 and 10, respectively. These figures are compared with affinities in Table V-2. At 330 nm, the wavelength at which the aminolysis kinetics were measured, no absorbance changes due to enhanced binding occurred. The increases in absorbance at 312 nm when titrating the bis-receptors with **504** (entry 4-6) were roughly twice as those found in the single adenine-receptor interaction (entry 1-3). This suggests that both receptors are involved in the binding process (see Figure V-5). This notion is supported by the magnitude of the binding constants. The free energy of binding of adenine derivatives to receptor **509**, is about 6 to 7 kcal mol⁻¹. The ribose containing **511** and **512** both bind a little stronger

(11) Wilcox, C. S. in *Frontiers in Supramolecular Organic Chemistry and Photochemistry*, Schneider, H. J.; Dürr, H., Eds.; VCH, Weinheim, Germany, 1991, pp 123-143.

than does 9-ethyladenine **510**, perhaps benefiting from more van der Waals contacts. Binding of **504** by the bis-receptors was much stronger, in fact almost too strong to accurately measure with these techniques. It was clear however, that **505b** was the best receptor by over an order of magnitude. Since it was also the best catalyst in the aminolysis reaction there does indeed seem to be a correlation between product binding and catalytic efficiency in this system. On the other hand, the correlation is not perfect; the binding constants for templates **505d** and **505g** are very similar, yet **505d** is basically not a catalyst whereas **505g** is capable of accelerating the coupling reaction ten-fold.

Entry	Receptor	Guest	$-\Delta G$ (kcal mol ⁻¹)
1	509	510	6.0
2	509	511	6.9
3	509	512	6.6
4	505b	504	9.8
5	505d	504	8.0
6	505g	504	8.3

Table V-2 Association energy of bis and mono receptors as obtained from UV-titrations in CHCl₃ at 25 °C.

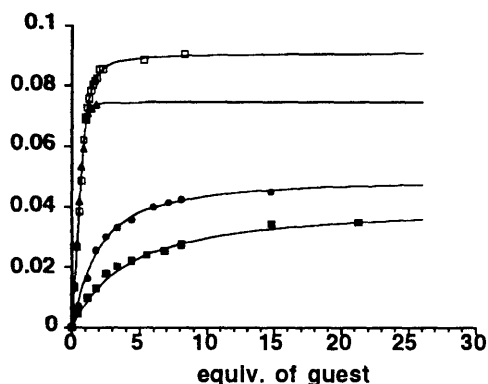
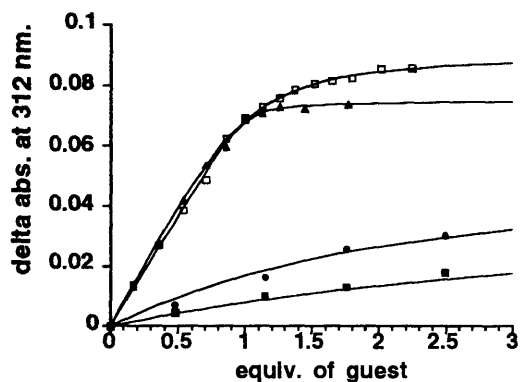


Figure V-5 Titration data and calculated lines of four of the titrations displayed with two different [guest] scales: (□) 505g + 504, (▲) 505b + 504, (●) 509 + 512, (■) 509 + 510. The concentrations of all hosts (mono and bis-adenine receptors) was 1×10^{-5} M. Solvent CHCl_3 , 25 °C.

V.4 Conformational Preferences Templates

The conformation of the free adenine receptors is mostly determined by intramolecular hydrogen bonding between the two imides on a given carbazole. This actually forms a small energetic barrier for the adenine binding. It is deduced from the ^1H NMR spectrum of the bis-imides in CDCl_3 , where the signal of the imide hydrogen appears at 10.8 ppm. This can be compared to 7.6 ppm for a typical "free" imide in this solvent.^{9a} Addition of adenines results in a downfield shift of this signal to over 13 ppm. Most spectra of the

adenine receptors show only broad signals likely due to additional intermolecular aggregation.

The bis receptor **505c** formed a notable exception to this usual pattern. The ^1H NMR spectrum of the free receptor is extremely sharp with an imide signal at 7.6 ppm. The receptor apparently folds itself into a sandwich conformation in which the carbazoles are stacked (Figure V-6). Two of the three different hydrogens on the benzene ring can be found at a typical chemical shift (7.2 and 7.3 ppm), whereas the aromatic hydrogen which is in *between* the carbazoles is shifted about 3 ppm *upfield* to 4.1 ppm. Its presence near the shielding faces of the aromatics is likely to be the cause. The signals of carbazole H1 and H4 are found at about 0.5 ppm more upfield than in comparable carbazole compounds, and in the UV spectrum of **505c** the main absorption band of carbazole appears at 293 nm vs 286 nm for **505b** and **505d**. Both observations are consistent with some degree of intramolecular aromatic stacking. The sandwich conformation does not allow the intramolecular imide contacts. Surprisingly, the stacking apparently provides enough stabilization to prevent imide-imide contacts since the unbound imide chemical shift is found at 7.6 ppm. It can not be excluded however that the amide bonds to the Kemp's imide units are hydrogen bonded to each other and provide additional stability to the conformation shown. Adenine binding is still possible because with the addition of adenines the imide signal moves to 13 ppm as usual. The template **505c** is only a modest catalyst for the coupling reaction. It is unlikely that the template can accommodate the compact tetrahedral intermediate **503** in the seemingly preorganized sandwich conformation. Rather, it may be advantageous for a different reaction.

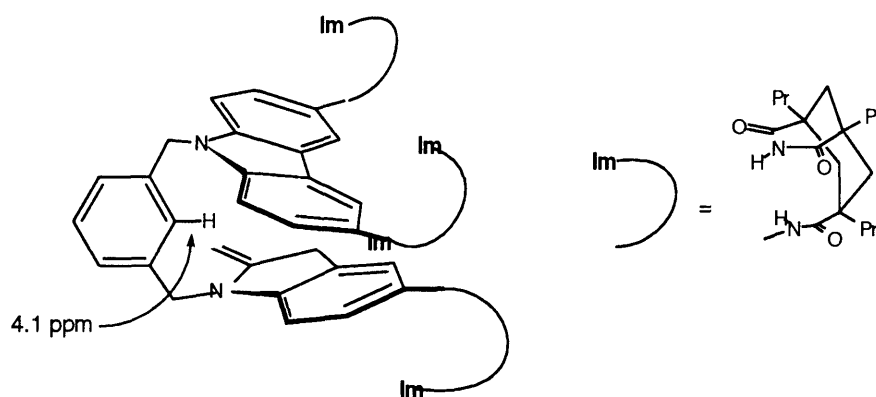


Figure V-6. Preferred conformation of template **505c**.

V.5 Discussion Template Catalysis

A template catalyzed reaction can be summarized as follows: (1) The template is able to bind the substrates. (2) It has a higher binding affinity for the highest transition state than the starting materials. (3) It is complementary to all intermediates and other transition states along the reaction coordinate (otherwise new kinetic barriers are created). A template either accelerates a reaction or changes its normal (uncatalyzed) course in favor of a different product. In the present system a 160-fold rate enhancement has been achieved in an aminolysis reaction with a stoichiometric amount of template. No functional groups are present to stabilize the zwitterionic components of the tetrahedral intermediate. The template possibly prevents the dissociation of the tetrahedral intermediate back to its free components, by binding to the adenine units. If the breakdown of the tetrahedral intermediate to product is indeed rate determining as commonly assumed¹² for aminolysis reactions in organic solvents, than that means that a breakdown back to starting materials is more favorable than a breakdown to product. Another interpretation of the role of the template may than be that it is increasing the partitioning of the tetrahedral intermediate and thus increasing the odds of product formation.

No matter what the provenance of the effects is, the net result is that an otherwise bimolecular reaction is promoted to a unimolecular (intracomplex) one. However, bringing two reagents in close proximity is not enough. This is shown by the lack of activity of **505d** and **505h**, i.e. not all of the three above mentioned criteria are fulfilled. The geometrical factors of a template are of crucial importance in satisfying these conditions. The variable elements in the series of potential templates **505a-h** are: (1) the relative orientation of the two receptor sites induced by the spacer and the overall *shape* of the molecule; (2) the *distance* between the receptor sites associated with this shape; (3) the *rigidity* of the molecule, or its propensity to stay or not to stay in a particular conformation corresponding to a shape and a distance.

Molecular Modeling suggests that **505a-h** can all accommodate the tetrahedral intermediate **503** in their cavities, but with conformations of the purines at the anomeric carbon that do not all allow the intramolecular stabilization of the ammonium ion by the purine N3. Thus, the ineffective templates prevent the reaction from proceeding along the

(12) (a) Su, C.-W.; Watson, J. W. *J. Am. Chem. Soc.* **1974**, *96*, 1854. (b) Menger, F. M.; Vitale, A. C. *J. Am. Chem. Soc.* **1973**, *95*, 4931. (c) Thea, S.; Cevasco, G.; Guanti, G.; Petrillo, G. *Gaz. Chim. It.* **1988**, *118*, 607. (d) Hogan, J. C.; Gandour, R. D. *J. Org. Chem.* **1992**, *57*, 55.

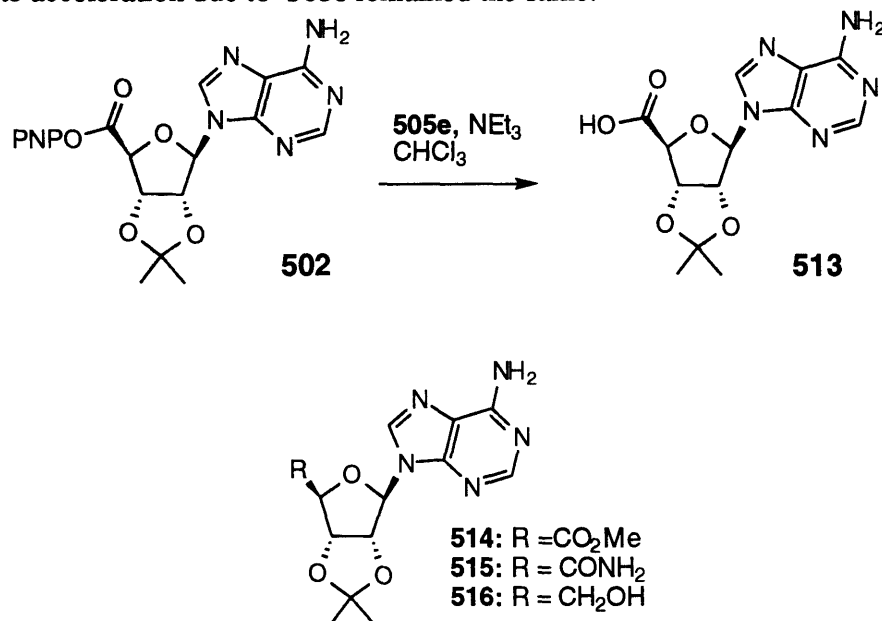
most favorable reaction coordinate; they cause a new kinetic barrier. Only a few of the conformations of the tetrahedral intermediate result in a fast reaction rate, and only the templates complementary to these conformations can substantially accelerate the reaction. In other words, only templates that obey all three criteria will be catalysts. Our binding studies support this conclusion. Similar binding constants to the reaction product for **505d** and **505g** are not paralleled by similar catalytic activity. The relatively flexible **505g** is capable of accommodating not only the product but also the reactive intermediates and transition states along the reaction coordinate. A consequence of this promiscuity is also that **505g** is only a modest catalyst. With **505d** one must conclude that its ability to bind the product is accidental and not accompanied by a similar ability to bind the crucial intermediates and transition states.

The observed initial rates with various amounts of **505f** correlated well with the calculated concentration of termolecular complex (**501-502-505f**, Figure V-3).²⁰ The fit was optimum for an association energy of 6.6 kcal mol⁻¹, consistent with the binding studies of the adenine/receptor interaction. At 0.05 mM of each substrate, the receptor sites are not fully saturated with guests. With this binding energy, the calculated initial value of [(**501-502-505f**)] is 1.15 x 10⁻⁵ M for 1 equiv of **505f**, which leads to a corrected accelerating factor for the template mediated reaction of 700-fold. An alternative description is based on effective molarity. At 1 equiv of template the initial rate is 2.4 x 10⁻⁶ M min⁻¹ and a termolecular complex concentration of 1.15 x 10⁻⁵ M can be calculated as before, which gives a "k_{cat}" of 0.21 min⁻¹. The background initial rate of 1.5 x 10⁻⁸ M min⁻¹ and the initial concentrations of the reactants give k_{uncat} = 6.0 M⁻¹min⁻¹. The ratio of k_{cat}/k_{uncat} gives an effective concentration of 35 mM which can be compared to the 0.05 mM reactant concentration (a 700-fold increase in concentration).

V.6 Catalyzed Hydrolysis in CHCl₃

In our studies of the template effects it was continually determined if the observed spectrophotometric increase (release of p-nitrophenolate) was due to aminolysis rather than hydrolysis. This was accomplished by running the reactions with and without amine **501**. No catalyzed hydrolysis was observed except with with **505e**, where almost the entire observed reaction was due to hydrolysis (Scheme V-3). The catalyzed hydrolysis was about 100 times faster than the very slow background hydrolysis. When the water content of the CHCl₃ was increased to about 15-20 mM (by using a 1:1 ratio of "wet" and

"dry" CHCl_3 as defined by Wilcox et al¹³), the observed rates increased about four times but the rate acceleration due to **505e** remained the same.



Scheme V-3. The hydrolysis reaction catalyzed by **505e** and the structure of additives.

The fact that binding was involved in the hydrolysis is supported by several observations. (1) No catalyzed hydrolysis was observed by 2,9-dimethyl-1,10-phenanthroline (neocuproine). (2) Competitive inhibition was observed with adenine derivatives containing non-protic functional groups. (3) A plot of rate acceleration vs. $[\mathbf{505e}]$ curves downward, i.e. exhibits saturation behavior. A possibility is that the catalytic effect of **505e** is due to the ability of the phenanthroline nitrogens to bind water and due to their basicity they possibly also assist the water molecule in the attack. This type of binding by 1,9-disubstituted 1,10-phenanthroline derivatives is well established¹⁴ and also reflects the fact that neocuproine is sold only as the hydrate.

Intrigued by the fact that only one of the two binding sites was being used, experiments were conducted to evaluate the effect of other adenine derivatives as cocatalysts. The results are summarized in Table V-3. Addition of two equivalents of ester **514** resulted in a reduction of the acceleration to 80-fold, presumably due to competitive binding. However, when **515** and **516** (proton or hydrogen bond donors) were added, accelerations were observed, overriding the competitive inhibition. The

(13) Adrian, J. C., Jr.; Wilcox, C. S. *J. Am. Chem. Soc.* **1991**, *113*, 678

(14) Keipert, S. J.; Knobler, C. B.; Cram, D. J. *Tetrahedron*, **1987**, *43*, 4861.

carboxylic acid **513**, which in the presence of excess NEt_3 is likely to be an ammonium carboxylate ion pair, slows the catalyzed hydrolysis reaction by ten-fold. Part of this is due to nonspecific changes in solvation, since the same amount of benzoic acid also slows down the reaction by a factor of two. Since the substituents that were varied are constrained to converge on to the reaction center, it is tempting to ascribe their impact to transition state stabilization. The rate limiting step in the hydrolysis is likely to be the attack by H_2O , which results in a build up of negative charge in the transition state. The fact that proton sources, which can stabilize such a charge are accelerating, while the repulsive negative charge of the carboxylate is counter productive is consistent with this picture.

Entry	equiv of 505e	Additive (2 equiv):	Rate Acceleration:
1	-	-	1
2	1	-	100
3	1	514	80
4	1	515	200
5	1	513	10
6	1	516	130

Table V-3. Rate accelerations observed in the hydrolysis of **502** (0.05 mM) in the presence of several additives and 4 mM NEt_3 , in CHCl_3 containing 15-20 mM H_2O , at 25 °C.

V.7 Catalysis by Functional Groups

As previously stated, an alternative approach to template catalysis is the selective polar (or apolar) stabilization of the highest transition state by an array of complementary functional groups. In order to achieve this the position and orientation of the reaction center must be known and subject to control. The adenine receptor was used to position a purine-containing reactant, an electrophile, for reaction with an external reactant, an amine. Several derivatives of the receptors were made which position a functional group in various orientations and their effects on the reaction rates were evaluated. It is well established for aminolysis reactions of active esters that molecules that can stabilize the

ammonium group of the tetrahedral intermediate (hydrogen bond acceptors), or help its deprotonation (bases, tautomeric catalysts) accelerate these reactions in organic solvents.¹² That is, the breakdown, rather than the formation of the tetrahedral intermediate is rate determining. If the ammonium portion of the zwitterionic intermediates loses a proton, expulsion of the negatively charged leaving group will lead to a neutral amide, rather than a high energy protonated one.

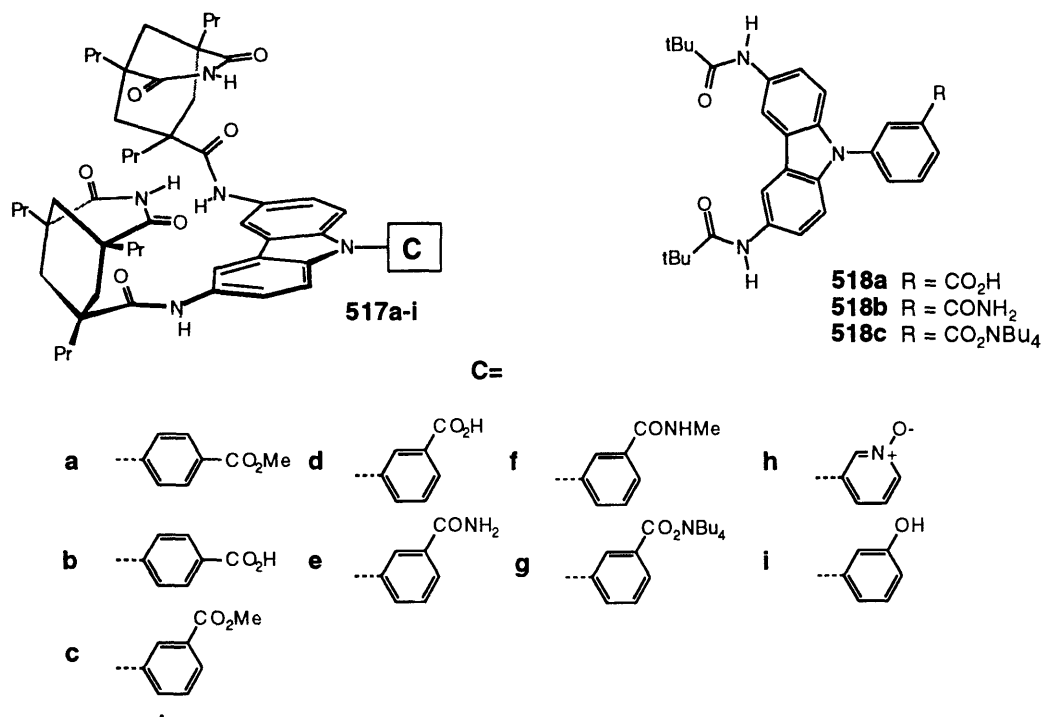
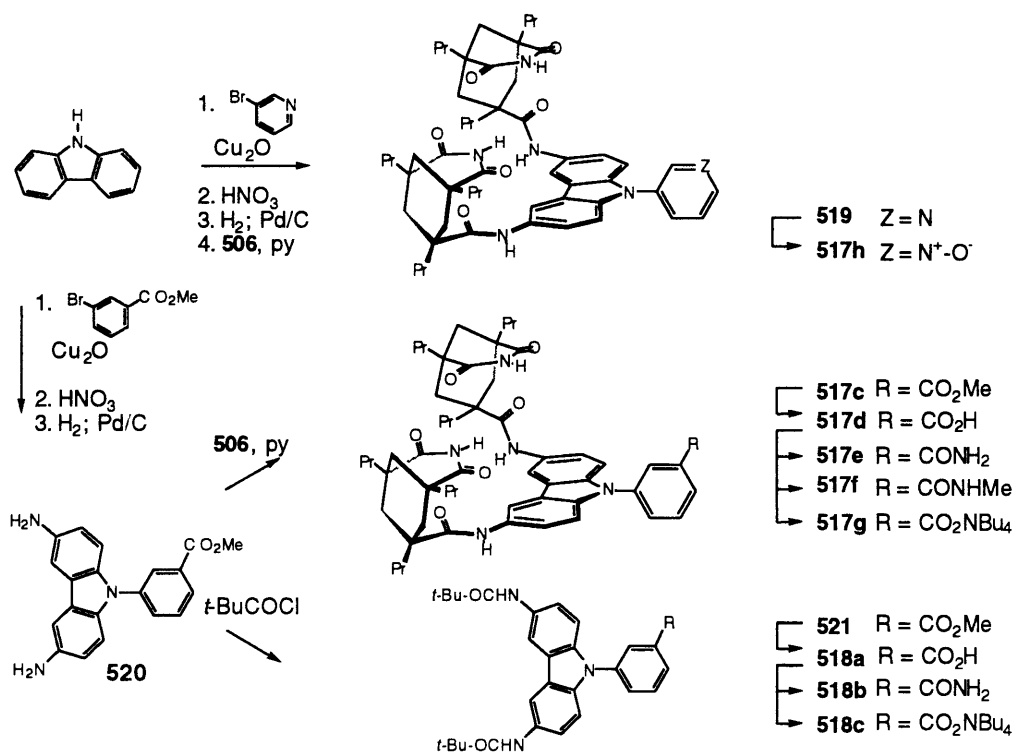


Figure V-7 Structures of the molecules used as catalyst and control compounds in the reaction of BuNH₂ and 502.



Scheme V-4. Synthesis of receptors and control compounds.

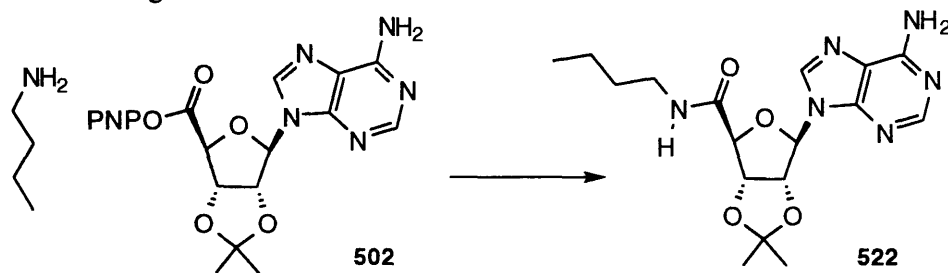
The receptors **517a-i** used in this study and control compounds **518a-c** (Figure V-7) were synthesized according to scheme V-4. The specific reaction studied was the formation of amide **522** from p-nitrophenyl (PNP) adenosine ester **502** and n-butylamine in CHCl_3 (Scheme V-5). Reactions were run under pseudo first order conditions with excess amine and also NEt_3 present. It was established that k_{obs} only contains a first order term in amine, i.e. no second order term in amine or first order term in NEt_3 was observed. A plot of $[\text{amine}]$ vs. k_{obs} gave a straight line and no rate dependency was seen on $[\text{NEt}_3]$. The system can be described by:

$$\text{rate} = k_{\text{obs}} [\text{Ester}]$$

$$k_{\text{obs}} = k_2 [\text{amine}]$$

In presence of the receptors (1 equiv), accelerations of up to a hundred-fold were observed (see Table V-4). Functional groups were placed on attached phenyl groups with orientation both meta and para to the carbazole. Only the meta substituents effected significant increases in rates. In entry 3-9 the functional groups are all in the meta position and since all the molecular complexes are expected to have practically the same geometry,

the different activities of the carbonyl derivatives **517c-g** reflect their intrinsic catalytic ability, i.e. assisting in the breakdown of the tetrahedral intermediate.



Scheme V-5 Covalent coupling which was used for the studies with the catalytic receptors.

Entry	Catalyst:	Rate Acceleration:
1	517a	1.2
2	517b	2
3	517c	3
4	517d	8
5	517e	5
6	517f	5
7	517g	95
7	517h	12
9	517i	4

Table V-4 Observed rate accelerations in the butylaminolysis of **502** (0.05 mM) by 1 equiv of various catalysts and NEt₃ (4 mM), in CHCl₃, at 25 °C.

Ester carbonyls have weak hydrogen bonding ability in chlorinated solvents,¹⁵ and their effect on the rate was, accordingly, negligible. The more basic amides¹⁶ show slightly higher activities. The *primary* amide **517e** is not measurably more active than the

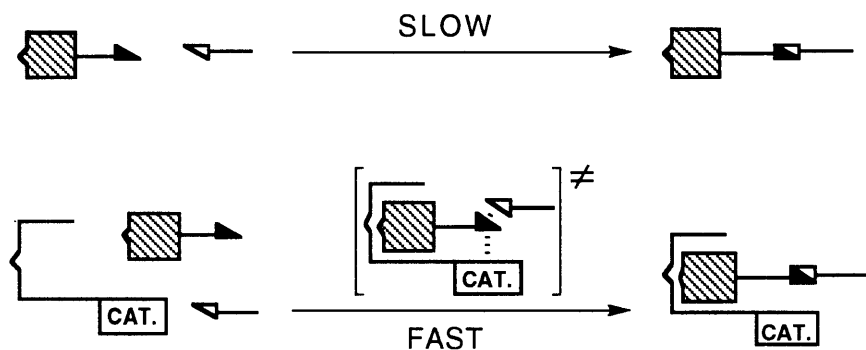
(15) Besseau, F.; Laurence, C.; Berthelot, M. *J. Chem. Soc., Perkin Trans. 2* **1994**, 485.

(16) Le Questel, J. Y.; Laurence, C.; Lachkar, M.; Helbert, M.; Berthelot, M. *J. Chem. Soc., Perkin Trans. 2* **1992**, 2091.

trans secondary amide **517f**, therefore concerted or tautomeric catalysis by **517e** is unlikely, that is, either the carbonyl or the *anti* NH is involved, but not both.

The high activity of the carboxylate **517g** likely arises from its enhanced basicity. (The catalytic activity observed for the corresponding acid **517d** may be due to its partial deprotonation by the large amount of base present). The well known acylation catalyst DMAP (4-dimethylaminopyridine) had no effect on the reaction rate as an external additive under our conditions.

The following results support the associative nature of the mechanism: (1) Control derivatives **518a-c** (1 equiv), which lack the recognition elements, had no effect on the reaction rate. (2) The presence of 100 equiv of benzamide did not result in a rate enhancement, showing that the effective concentration of the amide group of **517e** in the complex is considerably higher than a 100 times its actual concentration. This in contrast to generalized claims of acylation catalysis by amides.¹⁷ (3) Lower reaction rates were observed in the presence of 9-ethyladenine **510**, as expected for a competitive inhibitor. For example in the case of **517g**, the presence of 0.5 mM **510** reduced the acceleration by an order of magnitude.



V-8. Schematic representation of the aminolysis catalysis by **517**.

V.8 Polar Transition State Stabilization

The mode of catalysis by the receptors **517** can be schematically depicted as in Figure V-8. The observed rate accelerations in this series can be traced to a single functional group. The most effective catalyst **517g** contains a carboxylate group. In order to predict

(17) Menger, F. M.; Eliseev, A. V.; Khanjin, N. A. *J. Am. Chem. Soc.* **1994**, *116*, 3613.

the most stable structure for the complex between **517g** and the reaction intermediate, molecular modeling was carried out. A 1000-step MacroModel/SUMM¹⁸ conformational search using AMBER*¹⁹ force field and GB/SA²⁰ CHCl₃ solvation was undertaken. The most stable structure found allows for the simultaneous accommodation of two hydrogen bonds to the ammonium group; an intramolecular one from the N3 of the purine and an intracomplex one to the carboxylate (see Figure V-9).

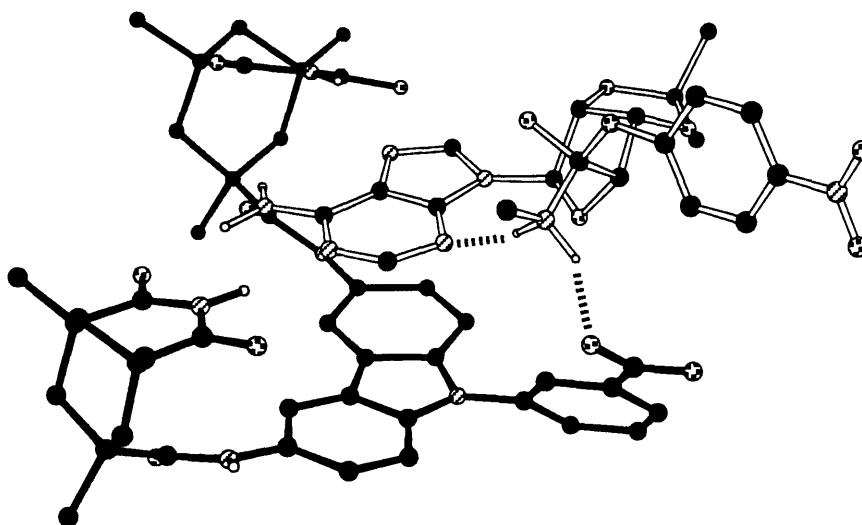


Figure V-9. Predicted structure of the complex between **517g** and the reaction intermediate. Carbon-bound hydrogens are not represented. The Monte-Carlo conformational search was carried out with methyl groups instead of propyl and butyl groups. The stereoconfiguration at the C5' carbon of the adenosine was arbitrarily chosen. No counter-ion was used for the carboxylate.

As stated earlier the k_{obs} term contains a first order term in amine. This is in contrast to earlier studies of the butylaminolysis of p-nitrophenylacetate in chlorobenzene^{12a}, which claimed the following rate expression:

$$k_{\text{obs}} = k_2 [\text{amine}] + k_3 [\text{amine}]^2 + k_3' [\text{amine}][\text{cat}]$$

Where [cat] is a term for concentration of added bases or hydrogen bond acceptors. In that study the k_2 term was only observable at high temperatures or with secondary amines. The ester **2** is about 1000 times more reactive than p-nitrophenylacetate. This precludes a direct kinetic comparison under the same dilute conditions in CHCl₃. The high reactivity can be attributed to a stabilizing intramolecular contact of one of the ammonium hydrogens

(18) Goodman, J. M.; Still, W. C. *J. Comput. Chem.* **1991**, *12*, 1110.

(19) McDonald, D. Q.; Still, W. C. *Tetrahedron Lett.* **1992**, *33*, 7743.

(20) Still, W. C.; Tempczyk, A.; Hawley, R. C.; Hendrickson, T. *J. Am. Chem. Soc.* **1990**, *112*, 6127.

of the tetrahedral intermediate with N₃ of the adenine. Simply stated, the purine N₃ provides an intramolecular pathway for (partial) removal of the ammonium hydrogen thus avoiding the high energy protonated amide product. This role is normally played by either a molecule of amine or by a catalyst; hence the higher order terms in the kinetics. The molecular modeling studies support a role for the purine N₃. On the other hand, acylation reactions of the adenosine amine **501**, show no special enhancement relative to butylamine, even though the N₃ could act in the same role, albeit in different conformational costumes.

The system follows simple second order kinetics in both the catalyzed and the uncatalyzed reactions. In the uncatalyzed reaction butylamine couples directly to the ester and in the catalyzed reaction butylamine reacts with the ester/receptor complex. This allows a more direct analysis of the polar transition state stabilization in the catalysis whereas in most model systems entropy effects dominate.²¹

The binding energy of the substrate can be measured independently. Titration of adenosine derivative **514** with receptor **517d** can be regarded as a model for all of meta carboxylic acid derivatives **517**. The binding energy was measured to be 5.9 kcal mol⁻¹ which means that under the reaction conditions 38% of the receptor sites are occupied by active ester. With this information a "corrected" intracomplex acceleration of 250-fold for **517g**, corresponding to an energy advantage of 3.3 kcal mol⁻¹ is estimated. This can be attributed entirely to the carboxylate-tetrahedral intermediate interaction²² or, more precisely, the carboxylate-ammonium interaction, since only one functional group was varied. Similar calculations give 1.2 kcal mol⁻¹ for the ester-ammonium interaction (using **517c**), 1.5 kcal mol⁻¹ for the amide-ammonium interaction (using **517e** and **517f**) and 2.0 kcal mol⁻¹ for the pyridine-N-oxide-ammonium interaction (using **517h**). Rate accelerations, however, do not reflect the interactions of the functional groups with the tetrahedral intermediate but with the transition state of its decomposition. The structure of this transition state is not known but believed to be similar to the tetrahedral intermediate.^{12a} If the rate determining step would be formation (rather than breakdown)

(21) For a conceptually similar system see ref 5a.

(22) Since the pK_a's of a carboxylic acid and an ammonium are much closer to equality in aprotic non polar media than in water (Kokesh, F. C.; Westheimer, F. H. *J. Am. Chem. Soc.* **1971**, *93*, 7270), the formation of a low barrier hydrogen bond may be responsible for the observed acceleration, although the 10-20 kcal/mol quoted for them inside enzyme active sites is far from the 3.3 kcal/mol as estimated here. See: Cleland, W. W.; Kreevoy, M. M. *Science* **1994**, *264*, 1887 and Frey, P. A.; Whitt, S. A.; Tobin, J. B. *ibid.* 1927). We note that only the less basic syn lone pair of the oxygen can reach the ammonium group. (Gandour, R. D. *Biorg. Chem.* **1981**, *10*, 169.)

of the tetrahedral intermediate due to the efficient intramolecular catalysis by purine N3, a different role of the functional groups would have to be considered. A basic functional group could weakly interact with the amine hydrogens of the attacking butylamine, while the interaction becomes stronger when moving towards the tetrahedral intermediate on the reaction coordinate. The functional groups than stabilize the building ammonium ion of the zwitterionic intermediate rather than the collapsing one.

V.9 Conclusions

The aminolysis chemistry presented here shows two aspects of catalysis which are both used by enzymes. The first involves overcoming entropic barriers and the second is based on polar transition state stabilization. The synthetic templates described here promote a bimolecular reaction to an unimolecular (intracomplex) one. An increase in effective molarity of 700-fold has been achieved in the best case. Binding studies confirm the ability of both receptor sites to be involved in binding, and product binding is roughly paralleled by catalytic activity. Other bimolecular aminolysis reactions were accelerated by receptors containing several functional groups. The most effective group was a carboxylate which is believed to interact with the ammonium group of the collapsing tetrahedral intermediate. A 3.3 kcal/mol stabilization energy due to this interaction as reflected in rate acceleration was estimated.

With the present systems rate accelerations in aminolysis reactions of 700 and 250-fold have been achieved by template catalysis and transition stabilization, respectively. If these two features could be merged into one system, enzymatic reactivity, in a model system could be within reach. In the meantime one can perceive that if accelerations of the magnitude as described here can be achieved using enantioselective receptors²³ and racemic reactants, selective coupling reactions can be anticipated.

V.10 Experimental Section

General Infrared spectra were obtained from a Perkin Elmer 1600 FT-IR spectrophotometer. ¹H NMR spectra were measured with Bruker WM-250 (250-MHz), AC-250 (250 MHz) and Varian XL-300 (300 MHz), Unity 300 (300MHz). UV measurements were taken on a Perkin Elmer Lambda 2 spectrophotometer. High-

(23) For such receptors see e.g. ref. 6f and 6i.

resolution mass spectra were obtained with a Finnegan Mat 8200 instrument. In the FAB mode (3-nitrobenzyl alcohol matrix) the molecular ion ($[M + H]^+$ or M^+) almost invariably formed the most intense peak. Melting points were taken on a Electrothermal 9100 melting point apparatus. Several of the receptor molecules do not have sharp melting points. Commercial-grade solvents were used without further purification with the exception of THF which was distilled from Na/benzophenone ketyl. The following compounds have been made as previously published: **501**, **502** and **504**,²⁰ **509**^{9a} (Me ester instead of Et ester), **517a,b**,²⁴ **517i**,²⁵ and **513**.²⁶

Ethyl Bis-receptor (505a). To a suspension of 3,6-dinitrocarbazole (200 mg, 0.78 mmol) and 18-crown-6 (206 mg, 0.78 mmol) in anhydrous THF (10 mL) was added a solution of *t*-BuOK in THF (1 M, 777 μ L). The suspension turned to a deep red solution and 1,2-dibromoethane (27 μ L, 59 mg, 0.31 mmol) was added. The mixture was heated at reflux under Ar for 24 h. A precipitate formed which was filtered, washed thoroughly with THF and dried. It was identified by ¹H NMR as N,N'-(ethylene)-3,6,3',6'-tetranitro-dicarbazole. ¹H NMR (250 MHz, DMSO-*d*₆): δ 9.28 (s, 4H), 8.11 (d, *J* = 9.3 Hz, 4H), 7.31 (d, *J* = 9.1 Hz, 4H), 5.10 (s, 4H). This material (21 mg) and Pd/C (10%, 20 mg) were suspended in DMF (4 mL) and the mixture was stirred under balloon pressure of H₂ at 100 °C for 4 h at room temperature for 10 h. The catalyst was then filtered off and the filtrate was evaporated to dryness. The imide acid chloride **506** (60 mg, 4.5 equiv) was added, followed by pyridine (3 mL). The mixture was heated at reflux for 3 h, evaporated to dryness, and the residue was purified using column chromatography on silica gel eluting with MeOH/CH₂Cl₂. yielding 39 mg (8%) of a white solid: IR (KBr) 3379, 3227, 2958, 2872, 1698, 1467, 1381, 1308, 1196, 802 cm⁻¹; ¹H NMR (300 MHz, DMSO-*d*₆): δ 10.42 (s, 4H), 9.12 (s, 4H), 7.97 (s, 4H), 7.25 (AB system, 8H), 4.80 (s, 4H), 2.69 (d, *J* = 13.4 Hz, 8H), 2.03 (d, *J* = 13.5 Hz, 4H), 1.79 (m, 8H), 1.60-1.00 (m, 52H), 0.88 (t, *J* = 6.7 Hz, 24H), 0.81 (t, *J* = 7.2 Hz, 12H); HRMS (FAB), *m/e* calcd for C₉₈H₁₃₃N₁₀O₁₂ (M + H): 1642.0104; found: 1642.0151.

***o*-Xylene Bis-receptor (505b).** In DMF (8 mL) were mixed 3,6-dinitrocarbazole (300 mg, 1.17 mmol), α,α' -dibromo-*o*-xylene (103 mg, 0.388 mmol) and K₂CO₃ (1.612 g, 11.67 mmol). The mixture was heated at 110 °C for 2 h. After

(24) Kato, Y.; Conn, M. M.; Rebek, J., Jr. *J. Am. Chem. Soc.* **1994**, *116*, 3275.

(25) Shimizu, K. D., upcoming Dissertation, Massachusetts Institute of Technology, **1995**.

(26) Schmidt, R. S.; Schloz, U.; Scwille, D. *Chem. Ber.* **1968**, *101*, 590.

cooling, the precipitate was filtered off, washed with cold DMF, H₂O, EtOH and hexanes. Obtained was 198 mg (83%) of the yellow tetranitro-dicarbazole: ¹H NMR (250 MHz, DMSO-*d*₆) δ 9.64 (s, 4H), 8.49 (d, *J* = 8.9 Hz, 4H) 7.98 (d, *J* = 9.1 Hz, 4H), 6.93 (br s, 2H), 6.25 (s, 4H), 6.03 (br s, 2H). Of this material 100 mg (0.16 mmol) was hydrogenated in DMF (60 mL) with Pd/C catalyst (10%, 175 mg) at room temperature for 14 h with a balloon of H₂. After removal of the catalyst and the solvent, the tetra-amine was suspended in hexanes and filtered off (57 mg). All of this material was dissolved in pyridine (10 mL) after which imide acid chloride **506** (196 mg, 0.574 mmol, 5 equiv) and a catalytic amount of DMAP were added. The mixture was heated at reflux for 3 h after which the solvent was removed and the residue was subjected to chromatography over silica gel using up to 4% MeOH in CH₂Cl₂. Obtained was 84 mg (25% overall) of an off-white solid: mp 253 °C (dec); IR (KBr) 3379, 3217, 2958, 1698, 1467, 1383, 1308, 1200 cm⁻¹; ¹H NMR (300 MHz, DMSO-*d*₆) δ 10.42 (s, 4H), 9.18 (s, 4H), 8.25 (s, 4H), 7.48 (s, 8H), 6.87-6.84 (m, 2H), 6.02 (br s, 2H), 5.92 (s, 4H), 2.67 (d, *J* = 13.9 Hz, 8H), 2.02 (*J* = 13.5 Hz, 4H), 1.83-1.75 (m, 8H), 1.60-1.00 (m, 52 H), 0.95-0.85 (m, 36 H); HRMS (FAB) *m/e* calcd for C₁₀₄H₁₃₇N₁₀O₁₂ (M + H): 1718.0418; found: 1718.0380.

***m*-Xylene Bis-receptor (505c).** This compound was prepared using the same procedure as for **505b** now starting with α,α'-dibromo-*m*-xylene. The corresponding tetranitro-dicarbazole: ¹H NMR (300 MHz, DMSO-*d*₆) δ 9.32 (d, *J* = 2.0 Hz, 4H), 8.12 (dd, *J* = 9.1, 2.3 Hz, 4H), 7.54 (d, *J* = 9.1 Hz, 4H), 7.38 (t, *J* = 6.3 Hz, 1H), 7.29 (d, *J* = 6.7 Hz, 2H), 5.89 (s, 1H), 5.69 (s, 4H). Bis receptor **505c** was obtained in 40% overall yield as an off-white solid: mp 231 °C (dec); IR (KBr) 3379, 3219, 2958, 1698, 1467, 1198, 801 cm⁻¹; ¹H NMR (300 MHz, DMSO-*d*₆) δ 10.40 (s, 4H), 9.15 (s, 4H), 8.15 (s, 4H), 7.44 (s, 8H), 7.35 (s, 1H), 7.01 (t, *J* = 7.7 Hz, 1H), 6.71 (d, *J* = 7.7 Hz, 2H), 5.55 (s, 4H), 2.67 (d, *J* = 13.7 Hz, 8H), 2.02 (d, *J* = 12.2 Hz, 4H), 1.87-1.70 (m, 8H), 1.55-1.00 (m, 52H), 0.95-0.75 (m, 36H); HRMS (FAB) *m/e* calcd for C₁₀₄H₁₃₇N₁₀O₁₂ (M + H): 1718.0418; found: 1718.0380.

***p*-Xylene Bis-receptor (505d).** This compound was prepared using the same procedure as for **505b** now starting with α,α'-dibromo-*p*-xylene except that due to the low solubility of the tetranitro-dicarbazole the first 2 h of the hydrogenation were run at 120 °C. Bis-receptor **505d** was obtained in 10 % overall yield as an off-white solid: mp 235 °C (dec); IR (KBr) 3379, 2958, 1698, 1467, 1308, 1197, 802 cm⁻¹; ¹H NMR (300 MHz, DMSO-*d*₆) δ 10.35 (s, 4H), 9.11 (s, 4H), 8.10 (s, 4H), 7.41 (s, 8H), 6.99 (s, 4H), 5.50 (s, 4H), 2.64 (d, *J* = 13.7 Hz, 8H), 2.01 (d, *J* = 13 Hz, 4H), 1.85-1.70 (m,

8H), 1.55-1.00 (m, 52H), 0.95-0.75 (m, 36H); HRMS (FAB) *m/e* calcd for C₁₀₄H₁₃₇N₁₀O₁₂ (M + H): 1718.0418; found: 1718.0363.

1,10-Phenanthroline Bis-receptor (505e). In DMF (80mL) were mixed 3,6-dinitrocarbazole (1.061 g, 5.150 mmol) and K₂CO₃ (5.70 g, 41.2 mmol) and the mixture was stirred at 120 °C for 20 min. A DMF (5 mL) solution of 2,9-Bis(chloromethyl)-1,10-phenanthroline (381 mg, 1.376 mmol) was added all at once and the resulting mixture was maintained at 120 °C for 14 h. After cooling the precipitate was filtered off, washed with H₂O, EtOH and hexanes. Obtained was 930 mg (94%) of the yellowish tetranitro compound; mp > 300 °C; IR (KBr): 3420, 1628, 1602, 1588, 1509, 1474, 1336, 1199, 1101, 860, 822, 751, 720, 666 cm⁻¹; ¹H NMR (300 MHz, DMSO-*d*₆) δ: 9.56 (d, *J* = 1.9 Hz, 4H), 8.40 - 8.30 (m, 2H), 8.37 (dd, *J* = 9.1 and 2.2 Hz, 4H), 8.05 (d, *J* = 9.1 Hz, 4H), 7.88 (s, 2H), 7.40 (d, *J* = 8.3 Hz, 2H), 6.23 (s, 4H); HRMS (EI) *m/e* calcd. for C₃₈H₂₂N₈O₈: 718.1561; found: 718.1565. The tetranitro-dicarbazole was hydrogenated and coupled as before and gave **505e** as a cream-colored solid (25% overall yield); mp 270 °C (dec.); IR (KBr) 3379, 2958, 1698, 1466, 1197, 806 cm⁻¹; ¹H NMR (300 MHz, DMSO-*d*₆) δ 10.38 (s, 4H), 9.18 (s, 4H), 8.26 (d, *J* = 8.6 Hz, 2H), 8.23 (d, *J* = 1.7 Hz, 4H), 7.84 (s, 2H), 7.58 (d, *J* = 9.0 Hz, 4H), 7.47 (dd, *J* = 8.8, 1.6 Hz, 4H), 6.75 (d, *J* = 8.3 Hz, 2H), 6.14 (s, 4H), 2.67 (d, *J* = 13.7 Hz, 8H), 2.02 (d, *J* = 12.7 Hz, 4H), 1.92-1.70 (m, 8H), 1.55-1.00 (m, 52 H), 0.95-0.85 (m, 36 H); HRMS (FAB) *m/e* calcd for C₁₁₀H₁₃₉N₁₂O₁₂ (M + H): 1820.0635; found: 1820.0619.

N,N'-(2,6-pyridinylene)-dicarbazole (508) A mixture of 2,6-dibromo-pyridine (1.0 g, 4.2 mmol), carbazole (2.8 g, 16.7 mmol), Cu₂O (2.7 g, 18.9 mmol.) and xylenes (3 mL) were heated at reflux for 72 h. The mixture was cooled and toluene (40 mL) was added. The suspension was filtered and the filtrate was concentrated after which the residue was dissolved in boiling CCl₄ (minimal amount). Upon cooling a precipitate of carbazole formed, which was filtered off. The filtrate was concentrated and chromatographed on silica gel eluting with CCl₄ yielding 0.60 g (35%) of **508**: mp 220 °C; ¹H NMR (250 MHz, CDCl₃): δ 8.15 (d, *J* = 7.4 Hz, 4H), 8.14 (t, *J* = 7.8 Hz, 1H), 8.03 (d, *J* = 8.1 Hz, 4H), 7.65 (d, *J* = 7.9 Hz, 2H), 7.43 (t, *J* = 7.8 Hz, 4H), 7.34 (t, *J* = 7.3 Hz, 4H); IR (KBr) 1599, 1570, 1452, 1331, 1223, 1188, 1151, 800, 742, 720 cm⁻¹; HRMS (EI) *m/e* calcd for C₂₉H₁₉N₃: 409.1579; found: 409.1569.

Pyridinyl-bis-receptor (505f). A suspension of **508** (100 mg, 0.244 mmol) in AcOH/Ac₂O (1:2, 9 mL) was heated to 35 °C and Cu(NO₃)₂·2.5 H₂O (0.70 g, 3.0 mmol) was added portionwise. After stirring at 35 °C for 24 h the mixture was poured

onto ice water. The resulting solid was filtered off, washed with concentrated aqueous ammonia, followed by water, and dried over P₂O₅. The tetranitro-dicarbazole was hydrogenated and coupled as before and gave **505f** as an off-white solid (6% overall yield): mp 257-259 °C; ¹H NMR (250 MHz, DMSO-*d*₆): δ 10.40 (s, 4H), 9.28 (s, 4H), 8.36 (t, *J* = 8.0 Hz, 1H), 8.32 (s, 4H), 7.87 (d, *J* = 8.8 Hz, 4H), 7.78 (d, *J* = 7.9 Hz, 2H), 7.47 (d, *J* = 9.1 Hz, 4H), 2.69 (d, *J* = 13.4 Hz, 8H), 2.03 (d, *J* = 13.5 Hz, 4H), 1.79 (m, 8H), 1.60-1.00 (m, 52H), 0.88 (t, *J* = 6.7 Hz, 24H), 0.81 (t, *J* = 7.2 Hz, 12H); IR (KBr) 3379, 2958, 1701, 1447, 1310, 1189, 803 cm⁻¹; HRMS (FAB), *m/e* calcd for C₁₀₁H₁₃₁N₁₁O₁₂ (M + H): 1691.0057; found: 1691.0149.

N,N'-(4,4'-biphenylene)-dicarbazole (507). A mixture of 4,4'-dibromobiphenyl (3.0 g, 9.6 mmol), carbazole (4.1 g, 24.5 mmol), ground K₂CO₃ (3.3 g, 23.9 mmol), copper bronze (0.2 g, 3.1 mmol), and 1-methyl-2-pyrrolidinone (3 mL) was heated at 240 °C for 72 h. After cooling, toluene (40 mL) was added and the suspension was refluxed for 1 h, then cooled and filtered through celite. The filtrate was washed with water (3 x 100 mL), dried (Na₂SO₄) and evaporated. The residue was dissolved in boiling CCl₄ (minimal amount). Upon cooling, a precipitate of carbazole formed, which was filtered off. The filtrate was concentrated and chromatographed on silica gel, eluting with CCl₄. The product is a white solid (2.5 g, 55 %): mp 281 °C; ¹H NMR (250 MHz, DMSO-*d*₆): δ 8.27 (d, *J* = 7.8 Hz, 4H), 8.10 (d, *J* = 8.4 Hz, 4H), 7.79 (d, *J* = 8.3 Hz, 4H), 7.48 (m, 8H), 7.29 (m, 4H); IR (KBr) 1601, 1508, 1448, 1334, 1226, 828, 750, 718 cm⁻¹; HRMS (EI) *m/e* calcd for C₃₆H₂₄N₂: 484.1940; found: 484.1937.

Biphenyl Bis-receptor (505h). A suspension of **505** (137 mg, 0.283 mmol) in AcOH/Ac₂O (1:2, 15 mL) was heated to 35 °C and Cu(NO₃)₂·2.5 H₂O (1.5 g, 6.4 mmol) was added portionwise. Stirring at 35 °C was continued for 96 h and the suspension was poured onto ice. The solid was filtered off, washed with concentrated aqueous ammonia followed by water and dried over P₂O₅. The tetranitro-dicarbazole was hydrogenated and coupled as before and gave **505h** as an off-white solid (7% overall yield): mp 310-315 °C (dec.); ¹H NMR (300 MHz, DMSO-*d*₆): δ 10.39 (s, 4H), 9.25 (s, 4H), 8.33 (s, 4H), 8.10 (d, *J* = 8.1 Hz, 4H), 7.76 (d, *J* = 8.1 Hz, 4H), 7.51 (d, *J* = 9.3 Hz, 4H), 7.41 (d, *J* = 8.8 Hz, 4H), 2.69 (d, *J* = 13.4 Hz, 8H), 2.03 (d, *J* = 13.5 Hz, 4H), 1.79 (m, 8H), 1.60-1.00 (m, 52H), 0.88 (t, *J* = 6.7 Hz, 24H), 0.81 (t, *J* = 7.2 Hz, 12H); IR (KBr) 3380, 3220, 2958, 1699, 1499, 1466, 1201, 805 cm⁻¹; HRMS (FAB), *m/e* calcd for C₁₀₈H₁₃₇N₁₀O₁₂ (M + H): 1766.0417; found: 1766.0402.

N-(3-(methoxycarbonyl)phenyl)-3,6-diaminocarbazole (520). Methyl 3-bromo-benzoate (2.67 g, 12.4 mmol), carbazole (2.08 g, 12.4 mmol), and Cu₂O (4.44 g, 31.03 mmol) were suspended in xylenes (4 mL). The mixture was heated at reflux under Ar for 26 h. After cooling to room temperature, CH₂Cl₂ (20 mL) was added. The suspension was filtered and the filtrate concentrated and chromatographed on silica gel with toluene/hexanes (4:6) yielding 3.02 g (81%) of N-(3-(methoxycarbonyl)phenyl)-carbazole: mp 109 °C; ¹H NMR (300 MHz, CDCl₃): δ 8.27 (m, 1H), 8.15 (m, 3H), 7.79 (m, 1H), 7.70 (dd, *J* = 7.7, 7.7 Hz, 1H), 7.40 (m, 4H), 7.31 (m, 2H), 3.95 (s, 3H); IR (KBr) 3052, 1722, 1587, 1495, 1448, 1290, 1264, 1223, 1081, 756 cm⁻¹; HRMS (EI) *m/e* calcd for C₂₀H₁₅NO₂: 301.1103; found: 301.1095. Some of this material (400 mg, 1.33 mmol) was suspended in AcOH (7 mL). The mixture was heated to 70 °C and nitric acid (70%, 3.5 mL) was added dropwise. After stirring for 3 h at 70 °C, the suspension was cooled with an ice bath, and water was added. The yellow precipitate was filtered and dried. After dissolving it in DMF (10 mL), Pd/C (10%, 40 mg) was added. The suspension was shaken at room temperature under a H₂ atmosphere for 24 h. The catalyst filtered off using celite, and the filtrate was concentrated and chromatographed on silica gel with 2% MeOH in CH₂Cl₂ yielding 260 mg (59%) of **520**: mp 210-212 °C; ¹H NMR (250 MHz, DMSO-*d*₆): δ 8.01 (t, *J* = 1.7 Hz, 1H), 7.94 (dt, *J* = 7.6, 1.4 Hz, 1H), 7.83 (m, 1H), 7.73 (dd, *J* = 7.8, 7.8 Hz, 1H), 7.11 (m, 4H), 6.70 (dd, *J* = 8.5, 2.1 Hz, 2H), 4.82 (br s, 4H), 3.88 (s, 3H); IR (KBr) 3397, 3333, 3212, 1716, 1630, 1578, 1493, 1465, 1291, 1215, 1081, 808, 755 cm⁻¹.

Diimide Ester (517c). A solution of diamine **520** (120 mg, 0.36 mmol) and imide acid chloride **506** (248 mg, 0.73 mmol) in pyridine (2 mL) was heated at reflux for 4 h. The pyridine was removed and the residue was chromatographed on silica gel using 1.5% MeOH in CH₂Cl₂ yielding 305 mg (90%) of **517c**: IR (KBr) 3223, 2957, 2871, 1693, 1491, 1466, 1292, 1200, 798 cm⁻¹; ¹H NMR (250 MHz, DMSO-*d*₆): δ 10.37 (s, 2H), 9.24 (s, 2H), 8.29 (d, *J* = 1.3 Hz, 2H), 8.07 (m, 2H), 7.93 (m, 1H), 7.83 (dd, *J* = 8.0, 8.0 Hz, 1H), 7.48 (dd, *J* = 8.9, 1.4 Hz, 2H), 7.30 (d, *J* = 8.8 Hz, 2H), 3.89 (s, 3H), 2.67 (d, *J* = 13.5 Hz, 4H), 2.03 (d, *J* = 11.9 Hz, 2H), 1.79 (m, 4H), 1.60-1.00 (m, 26H), 1.36 (t, *J* = 7.1 Hz, 3H), 0.88 (t, *J* = 6.7 Hz, 12H), 0.81 (t, *J* = 7.3 Hz, 6H); HRMS (FAB), *m/e* calcd for C₅₆H₇₁N₅O₈ (M + H): 942.5318 found: 942.5381.

Diimide Acid (517d). The methyl ester **517c** (300 mg, 0.32 mmol) was dissolved in EtOH/THF (1:1, 40 mL). A 1 N solution of NaOH (1.9 mL, 1.9 mmol)

was added, and the mixture was stirred at room temperature for 24 h. The reaction was quenched with aqueous HCl (10 %) and most of the EtOH and THF were removed *in vacuo*. Water (10 mL) was added, and the product was extracted with CH₂Cl₂ (30 mL). The organic phase was concentrated and the residue was chromatographed on silica gel (15% MeOH/CH₂Cl₂) to give 271 mg (92 %) of **517d**: ¹H NMR (300 MHz, DMSO-*d*₆): δ 10.34 (s, 2H), 9.23 (s, 2H), 8.27 (d, *J* = 1.5 Hz, 2H), 8.04 (m, 2H), 7.63 (m, 2H), 7.46 (dd, *J* = 8.7, 1.5 Hz, 2H), 7.25 (d, *J* = 8.7 Hz, 2H), 2.67 (d, *J* = 13.5 Hz, 4H), 2.03 (d, *J* = 11.9 Hz, 2H), 1.79 (m, 4H), 1.60-1.00 (m, 26H), 0.88 (t, *J* = 6.7 Hz, 12H), 0.81 (t, *J* = 7.3 Hz, 6H); IR (KBr) 3378, 2959, 2872, 1700, 1466, 1400, 1295, 1198, 807 cm⁻¹; HRMS (FAB) *m/e* calcd for C₅₅H₇₀N₅O₈ (M + H): 928.5224; found: 928.5228.

Diimide Tetrabutylammonium Carboxylate (517g). Acid **517d** (50 mg, 0.054 mmol), was dissolved in CH₂Cl₂ (2 mL), and a 1 M solution of Bu₄NOH in THF (54 μL, 0.054 mmol) was added. The mixture was concentrated and the solid residue was dried under high vacuum over P₂O₅: IR (KBr) 3383, 2959, 2872, 1700, 1570, 1466, 1364, 1293, 1182, 880, 806, 769 cm⁻¹; ¹H NMR (250 MHz, DMSO-*d*₆): δ 10.40 (s, 2H), 9.23 (s, 2H), 8.29 (s, 2H), 7.92 (m, 2H), 7.50 (m, 2H), 7.44 (d, *J* = 8.8 Hz, 2H), 7.25 (d, *J* = 8.6 Hz, 2H), 3.14 (m, 8H), 2.67 (d, *J* = 13.5 Hz, 4H), 2.03 (d, *J* = 11.9 Hz, 2H), 1.79 (m, 4H), 1.60-1.00 (m, 42H), 1.00-0.70 (m, 30H).

Diimide Carboxamide (517e). The acid **517d** (100 mg, 0.11 mmol), pentafluorophenol (60 mg, 0.33 mmol) and DMAP (21 mg, 0.17 mmol) were dissolved in anhydrous THF (3 mL) and EDC (62 mg, 0.32 mmol) was added. The mixture was stirred at room temperature for 20 h. After cooling in an ice bath, anhydrous NH₃ was gently bubbled through for 10 min. It was then stirred at room temperature for 1 h, and concentrated. The residue was dissolved in CH₂Cl₂ (50 mL) and washed with 1.2 N HCl (30 mL) followed by saturated NaHCO₃ solution (30 mL). The organic phase was concentrated and the residue was chromatographed on silicagel (15% MeOH/CH₂Cl₂) to give 58 mg (58%) of **517e**: IR (KBr) 3377, 2958, 2871, 1699, 1522, 1466, 1387, 1293, 1198, 807 cm⁻¹; ¹H NMR (300 MHz, DMSO-*d*₆): δ 10.36 (s, 2H), 9.23 (s, 2H), 8.30 (s, 2H), 8.14 (br s, 1H), 8.07 (m, 1H), 7.99 (m, 1H), 7.76 (m, 2H), 7.53 (br s, 1H), 7.48 (dd, *J* = 8.7, 1.2 Hz, 2H), 7.29 (d, *J* = 8.7 Hz, 2H), 2.67 (d, *J* = 13.5 Hz, 4H), 2.03 (d, *J* = 11.9 Hz, 2H), 1.79 (m, 4H), 1.60-1.00 (m, 26H), 0.88 (t, *J* = 6.7 Hz, 12H), 0.81 (t, *J* = 7.3 Hz, 6H); HRMS (FAB) *m/e* calcd for C₅₅H₇₀N₆O₇ (M + H): 927.5438; found: 927.5438.

Diimide Methylamide (517f). Acid **517d** (100 mg, 0.11 mmol) was treated similarly as in the preparation of primary amide **517e**. Anhydrous methylamine was used instead of NH₃. Yield 86 mg (85%); IR (KBr) 3378, 2959, 2872, 1700, 1654, 1534, 1488, 1293, 1198, 807 cm⁻¹; ¹H NMR (300 MHz, DMSO-*d*₆): δ 10.35 (s, 2H), 9.23 (s, 2H), 8.60 (m, 1H), 8.30 (s, *J* = 1.8 Hz, 2H), 8.02 (s, 1H), 7.94 (m, 1H), 7.75 (m, 2H), 7.48 (dd, *J* = 8.7, 1.2 Hz, 2H), 7.29 (d, *J* = 8.7 Hz, 2H), 2.80 (d, *J* = 3.3 Hz, 3H), 2.67 (d, *J* = 13.5 Hz, 4H), 2.03 (d, *J* = 11.9 Hz, 2H), 1.79 (m, 4H), 1.60-1.00 (m, 26H), 0.88 (t, *J* = 6.7 Hz, 12H), 0.81 (t, *J* = 7.3 Hz, 6H); HRMS (FAB) *m/e* calcd for C₅₆H₇₂N₆O₇ (M + H): 941.5541; found: 941.5518.

N-(3-(methoxycarbonyl)phenyl)-3,6-bis(tert-butylcarbonylamino)carbazole (521). To a solution of **520** (120 mg, 0.363 mmol) in THF (5 mL) at 0 °C were added NEt₃ (0.14 mL, 1.0 mmol) and trimethylacetyl chloride (0.13 mL, 1.1 mmol). The mixture was stirred at room temperature for 4 h and concentrated. The residue was chromatographed on silicagel (15% MeOH/CH₂Cl₂) yielding 175 mg (97%) of **521**: mp 255-257 °C; IR (KBr) 3315, 2957, 1731, 1651, 1587, 1514, 1368, 1292, 1268, 1214, 870, 803, 754, 691 cm⁻¹; ¹H NMR (250 MHz, DMSO-*d*₆): δ 9.31 (s, 2H), 8.48 (d, *J* = 1.5 Hz, 2H), 8.06 (m, 2H), 7.94 (m, 1H), 7.83 (dd, *J* = 8.1, 8.1 Hz, 1H), 7.57 (dd, *J* = 8.8, 1.8 Hz, 2H), 7.34 (d, *J* = 8.8 Hz, 2H), 3.89 (s, 3H), 1.27 (s, 18H); HRMS (EI) *m/e* calcd for C₃₀H₃₃N₃O₄: 499.2471; found: 499.2467.

N-(3-carboxyphenyl)-3,6-bis(tert-butylcarbonylamino)carbazole (518a). Ester **521** was saponified following the same procedure as for ester **517c**. Yield 55%: mp 252 °C; IR (KBr) 2964, 1654, 1534, 1489, 1384, 1303, 1211, 807 cm⁻¹; ¹H NMR (250 MHz, DMSO-*d*₆): δ 9.31 (s, 2H), 8.48 (s, 2H), 8.04 (m, 2H), 7.75 (m, 2H), 7.57 (d, *J* = 8.8 Hz, 2H), 7.32 (d, *J* = 8.8 Hz, 2H), 1.27 (s, 18H); HRMS (EI) *m/e* calcd for C₂₉H₃₁N₃O₄: 485.2315; found: 485.2311.

N-(3-(aminocarbonyl)phenyl)-3,6-bis(tert-butylcarbonylamino)carbazole (518b). The same procedure was used as for the preparation of primary amide **517e**. Acid **518a** (50 mg, 0.10 mmol) was used and the product was chromatographed on silica gel (2.5% MeOH/CH₂Cl₂) to give 38 mg (78%) of **518b**: mp 184-186 °C; IR (KBr) 3332, 2960, 1654, 1528, 1489, 1397, 1209, 921, 808, 696 cm⁻¹; ¹H NMR (300 MHz, DMSO-*d*₆): δ 9.29 (s, 2H), 8.49 (s, 2H), 8.14 (br s, 1H), 8.07 (s, 1H), 7.99 (m, 1H), 7.75 (m, 2H), 7.57 (d, *J* = 8.7 Hz, 2H), 7.54 (br s, 1H), 7.33 (d, *J* = 8.7 Hz, 2H), 1.28 (s, 18H); HRMS (EI) *m/e* calcd for C₂₉H₃₂N₄O₃: 484.2474; found: 484.2469.

Tetrabutyl ammoniumsalt (518c). The same procedure was used as for the preparation of **517g** starting from **518a**. ^1H NMR (300 MHz, CDCl_3) δ 8.29 (s, 2H), 8.24-8.15 (m, 2H), 7.78 (s, 2H), 7.49 (t, $J = 7.5$ Hz, 1H), 7.43-7.37 (m, 3H), 7.32-7.25 (m, 2H), 3.24-3.15 (m, 8H), 1.60-1.20 (m, 34H) including 1.36 (s, 18H), 0.83 (t, $J = 7.4$ Hz, 12H).

Diimide Pyridine (519). A mixture of 3-bromopyridine (2.46 g, 15.6 mmol), carbazole (2.62 g, 15.6 mmol), ground K_2CO_3 (2.38 g, 17.2 mmol), Cu powder (147 mg, 2.31 mmol) and 1-methyl-2-pyrrolidinone (5 mL) was heated at reflux for 24 h. After cooling, CH_2Cl_2 (200 mL) was added, and the suspension was filtered. The filtrate was washed with water (3 x 100 mL), dried (MgSO_4), and concentrated to give 2.2 g (58%) of N-(3-pyridinyl)carbazole: mp 111-113 $^\circ\text{C}$; IR (KBr) 1578, 1452, 1425, 1334, 1228, 1179, 1024, 804, 752, 711 cm^{-1} ; ^1H NMR (300 MHz, CDCl_3): δ 8.91 (s, 1H), 8.73 (d, $J = 4.2$ Hz, 1H), 8.16 (d, $J = 7.8$ Hz, 2H), 7.94 (d, $J = 8.1$ Hz, 1H), 7.58 (dd, $J = 8.1, 5.1$ Hz, 1H), 7.44 (dd, $J = 7.7, 7.7$ Hz, 2H), 7.38 (d, $J = 7.8$ Hz, 2H), 7.33 (dd, $J = 7.2, 7.2$ Hz, 2H); HRMS (EI) m/e calcd for $\text{C}_{17}\text{H}_{12}\text{N}_2$: 244.1001; found: 244.0999. A suspension of N-(3-pyridinyl)carbazole (400 mg, 1.64 mmol) in AcOH/Ac₂O (1:2, 12 mL) was heated at 35-40 $^\circ\text{C}$, and $\text{Cu}(\text{NO}_3)_2 \cdot 2.5(\text{H}_2\text{O})$ (0.8 g, 3.4 mmol) was added over 30 min. The mixture was stirred at 35-40 $^\circ\text{C}$ for 24 h. Water (50 mL) was added and stirring was continued for 30 min. The precipitated dinitrocarbazole was filtered, washed with concentrated aqueous ammonia followed by water, and dried. It was hydrogenated as in the preparation of **520** and the resulting diamine was coupled with imide acid chloride **506** as in the preparation of **517c**. Pyridine **519** was obtained as like a beige solid: IR (KBr) 3377, 3221, 2958, 2871, 1695, 1488, 1466, 1202, 805 cm^{-1} ; ^1H NMR (300 MHz, $\text{DMSO}-d_6$): δ 10.37 (s, 2H), 9.24 (s, 2H), 8.85 (d, $J = 2.4$ Hz, 1H), 8.71 (dd, $J = 4.9, 1.3$ Hz, 1H), 8.32 (d, $J = 1.8$ Hz, 2H), 8.08 (ddd, $J = 8.3, 1.9, 1.9$ Hz, 1H), 7.71 (dd, $J = 8.1, 5.1$ Hz, 1H), 7.48 (dd, $J = 8.8, 1.8$ Hz, 2H), 7.28 (d, $J = 8.8$ Hz, 2H), 2.67 (d, $J = 13.5$ Hz, 4H), 2.03 (d, $J = 11.9$ Hz, 2H), 1.79 (m, 4H), 1.60-1.00 (m, 26H), 0.88 (t, $J = 6.7$ Hz, 12H), 0.81 (t, $J = 7.3$ Hz, 6H); HRMS (FAB) m/e calcd for $\text{C}_{53}\text{H}_{68}\text{N}_6\text{O}_6$ (M + H): 885.5279; found: 885.5233.

Diimide Pyridine N-Oxide (517h). A solution of the pyridine **519** (75 mg, 0.085 mmol) and *m*-CPBA (70 %, 21 mg, 0.085 mmol) in CHCl_3 (2 mL) was stirred at room temperature for 48 h. After addition of CHCl_3 (20 mL), the organic layer was washed with saturated NaHCO_3 solution (20 mL), dried (MgSO_4) and concentrated. The residue was chromatographed on basic alumina with $\text{CH}_2\text{Cl}_2/\text{MeOH}$ yielding in addition to recovered **519** (12 mg) the N-oxide **517h** (32 mg, 42%): IR (KBr) 3378, 2958,

2871, 1697, 1527, 1490, 1465, 1377, 1202, 1002, 805, 683 cm^{-1} ; ^1H NMR (300 MHz, $\text{DMSO-}d_6$): δ 10.38 (s, 2H), 9.25 (s, 2H), 8.59 (s, 1H), 8.35 (d, $J = 6.0$ Hz, 1H), 8.32 (d, $J = 1.6$ Hz, 2H), 7.65 (m, 2H), 7.50 (dd, $J = 8.9, 1.8$ Hz, 2H), 7.38 (d, $J = 8.8$ Hz, 2H), 2.67 (d, $J = 13.5$ Hz, 4H), 2.03 (d, $J = 11.9$ Hz, 2H), 1.79 (m, 4H), 1.60-1.00 (m, 26H), 0.87 (t, $J = 6.7$ Hz, 12H), 0.80 (t, $J = 7.3$ Hz, 6H); HRMS (FAB) m/e calcd for $\text{C}_{53}\text{H}_{68}\text{N}_6\text{O}_7$ (M + H): 901.5228 found: 901.5215.

Adenosine Amide 515 This amide was obtained by treating active ester **502** with anhydrous NH_3 . mp 221-223 $^\circ\text{C}$; IR (KBr) 3411, 3304, 3180, 1687, 1654, 1424, 1381, 1208, 1094, 1061, 866 cm^{-1} ; ^1H NMR (250 MHz, $\text{acetone-}d_6$): δ 8.17 (s, 1H), 8.13 (s, 1H), 7.05 (br s, 2H), 6.67 (br. s, 1H), 6.38 (br s, 1H), 6.29 (d, $J = 2.0$ Hz, 1H), 5.48-5.40 (m, 2 H), 4.55 (d, $J = 1.8$ Hz, 1H), 1.57 (s, 3H), 1.37 (s, 3H). HRMS (EI) m/e calcd for $\text{C}_{13}\text{H}_{16}\text{N}_6\text{O}_4$: 320.1233; found: 320.1224.

Aminolysis Kinetics Typically, CHCl_3 solutions of the amine (125 μL , 0.4 mM adenosineamine or 40 mM BuNH_2), NEt_3 (125 μL , 32 mM) and other additives (template, catalyst, inhibitors), were mixed together in a quartz cuvette (1 cm pathlength). The volume was adjusted to 875 μL with CHCl_3 , and a solution of active ester was added (125 μL , 0.4 mM). The cuvette was closed with a teflon cap, shaken and quickly transferred to the temperature controlled ($25\text{ }^\circ\text{C} \pm 0.1\text{ }^\circ\text{C}$) compartment of the spectrometer. The reaction was periodically monitored at 330 nm. The data were collected using the PECSS software package v. 4.2 (Perkin-Elmer). The reactions were generally followed to at least 80% completion. Initial rates were determined from the first 10% of reaction. Reactions were run in duplicate or triplicate and numbers were averaged. Reactions were run with and without amine nucleophile to ensure the p-nitrophenol release was due to aminolysis rather than hydrolysis from residual water or undetected impurity.

Hydrolysis kinetics The hydrolysis kinetics with **505e** were measured in the same way as the aminolysis kinetics except no amine was added. The solvent consisted for 50 % of "wet" CHCl_3 .¹³

Analysis of Product in Butylamine Reaction. The U.V. data were confirmed by quenching a reaction with a large amount of MeOH and after standing for 20 min. analyzing the ratio of **522** vs. quenching product **514** by ^1H NMR in $\text{DMSO-}d_6$. After 40 sec., the aminolysis of **501** (0.05 mM) by BuNH_2 (5 mM) was over 95 % completed in the presence of 1 eq. of **509** and only 5 % in its absence. Ester **514**: mp

240-241 °C. IR (KBr) 3306, 3319, 1726, 1672, 1600, 1582, 1088, 836, 664 cm^{-1} ; ^1H NMR (300 MHz, CDCl_3) δ 8.25, (s, 1H), 7.93, (s, 1H), 6.19 (s, 1H), 5.70 (dd, $J = 6.0, 1.4$ Hz, 1H), 5.52 (s, 2H), 5.50 (d, $J = 6.0$ Hz, 1 H), 4.83 (s, 1H), 3.40 (s, 3H), 1.61 (s, 3H), 1.43 (s, 3H); HRMS (EI) m/e calcd for $\text{C}_{14}\text{H}_{17}\text{N}_5\text{O}_5$: 335.1230; found: 335.1220. Amide **22**: mp 154-155 °C; IR (KBr) 3298, 3158, 2960, 1727, 1677, 1604, 1531, 1478, 1380, 1331, 1248, 1208, 1158, 1093, 1060, 870, 790 cm^{-1} ; ^1H NMR (250 MHz, $\text{DMSO-}d_6$): δ 8.25 (s, 1H), 8.08 (s, 1H), 7.52 (t, $J = 5.4$ Hz, 1H), 7.31 (s, 2H), 6.31 (s, 1H), 5.37 (m, 2H), 4.52 (s, 1H), 2.77 (m, 2H), 1.52 (s, 3H), 1.32, (s, 3H), 0.97 (m, 4H), 0.74 (t, $J = 6.1$ Hz, 3H); HRMS (EI) calcd for $\text{C}_{17}\text{H}_{24}\text{N}_6\text{O}_4$: 376.1859; found: 376.1857.

UV-titrations A host solution of 0.01 mM in CHCl_3 was prepared. Guest solutions of equal concentration were prepared in both CHCl_3 and the host solution. In the double beam spectrophotometer were placed two cuvettes: one with the host solution and in a reference cuvette an equal amount of CHCl_3 . A spectrum was taken and incremental guest additions were made to both the host solution cuvette (with the host containing guest solution) and the reference cuvette (with the CHCl_3 guest solution) until no further spectral changes occurred. From the collected data the absorbance changes at 312 nm were fitted to a 1:1 binding isotherm using a nonlinear least squares regression. Standard deviations were ± 0.2 kcal mol^{-1} (95% confidence level) and somewhat higher for the **504-505b** titration (± 0.4 kcal mol^{-1}).

Chapter VI. Synthesis of Adenine Receptors Linked to a Peptide Backbone.

VI.1 Introduction

Peptide Nucleic Acids (PNA) are DNA analogues in which the ribose-phosphodiester backbone is replaced by one consisting of (2-aminoethyl)glycine units (Figure VI-1). They were shown to bind to natural DNA sequences with higher affinity than DNA itself,¹ following Watson-Crick base pairing² and in a double helical conformation.³ The higher affinity may result from the neutral backbone, which does not create charge-charge repulsions as in the pairing of two natural DNA's with negatively charged phosphodiester linkages.

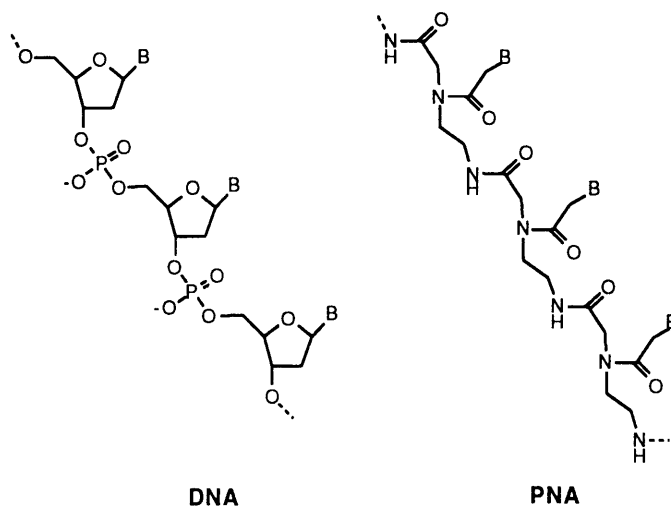


Figure VI-1. The structure of DNA and PNA.

The higher binding affinity along with their higher in vivo stability make them attractive candidates for anti-sense drugs. These potential drugs block the action of unwanted genes.

(1) (a) Nielsen, P. E.; Egholm, M.; Berg, R. H.; Buchardt, O. *Science*, **1991**, *254*, 1497. (b) Egholm, M.; Buchardt, O.; Nielsen, P. E.; Berg, R. H. *J. Am. Chem. Soc.* **1992**, *114*, 1895. (c) Egholm, M.; Nielsen, P. E.; Buchardt, O.; Berg, R. H. *J. Am. Chem. Soc.* **1992**, *114*, 9677. (d) Egholm, M.; Behrens, C.; Christensen, L.; Berg, R. H.; Nielsen, P. E.; Buchardt, O. *J. Chem. Soc., Chem. Commun.* **1993**, 800. (e) Cherny, D. Y.; Belotserkovskii, B. P.; Frank-Kamenetskii, M. D.; Egholm, M.; Buchardt, O.; Berg, R. H.; Nielsen, P. E. *Proc. Natl. Acad. Sci. U.S.A.* **1993**, *90*, 1667.

(2) Egholm, M.; Buchardt, O.; Christensen, L.; Behrens, C.; Freier, S. M.; Driver, D. A.; Berg, R. H.; Kim, S. K.; Norden, B.; Nielsen, P. E. *Nature*, **1993**, *365*, 566.

(3) Wittung, P.; Nielsen, P. E.; Buchardt, O.; Egholm, M.; Nordén, B. *Nature*, **1994**, *368*, 561.

These genes could be mutated genes or viral genes and blocking is usually envisioned at the mRNA stage. The current major problem with the PNAs as anti-sense drugs is that they are not able to pass through cell membranes, i.e. they will have to be injected into individual cells in order to work. Another potential field of applications for PNAs is as a diagnostic tool. The higher binding affinity should be advantageous in identifying specific sequences in dilute medical samples. The synthesis of PNA monomers is relatively straightforward and for oligomerization conventional well established and optimized procedures of peptide chemistry can be used.⁴

As stated above, a major problem with the PNAs for therapeutic application is their inability to pass through cell membranes. We thought that our carbazole based adenine receptors could possibly address this problem. They could possibly act as carriers for adenine-rich sections of PNAs. Some guanidinium containing receptors have already shown to be able to transport di- tri- and higher oligonucleotides across a liquid membrane.⁵ Another approach would be to incorporate an adenine receptor instead of a thymine base, at the beginning or end of the PNA strand. This should increase the binding since our adenine receptors provide both Watson-Crick and Hoogsteen hydrogen bonding. It should also make the molecule more lipophilic and increase its transport potential through cell membranes. The solubility properties can be tuned at will by selecting either the propyl or hydroxymethyl versions of the Kemp's imide modules. Despite the geometrical differences between thymine and our adenine receptors, model building suggests that incorporation still allows base pairing of all units of a strand. Even the incorporation of two consecutive receptor units at the terminus of a strand seems to allow duplex formation. It requires that two adenines are separated further to allow the intercalation of the carbazole unit. Figure VI-2 shows a minimized structure of the complex between **606** (see Figure VI-3) and ApA. which represents the terminus of such a duplex.

In this chapter the synthesis of the previously used adenine receptors linked to the PNA backbone is described.

(4) Dueholm, K. L.; Egholm, M.; Behrens, C.; Christensen, L.; Hansen, H. F.; Vulpius, T.; Petersen, K. H.; Berg, R. H.; Nielsen, P. E.; Buchardt, O. *J. Org. Chem.* **1994**, *59*, 5767.

(5) Andreu, C.; Galán, A.; Kobiro, K.; de Mendoza, J.; Park, T.-K.; Rebek, J., Jr.; Salmerón, A.; Usman, N. *J. Am. Chem. Soc.* **1994**, *116*, 5501.

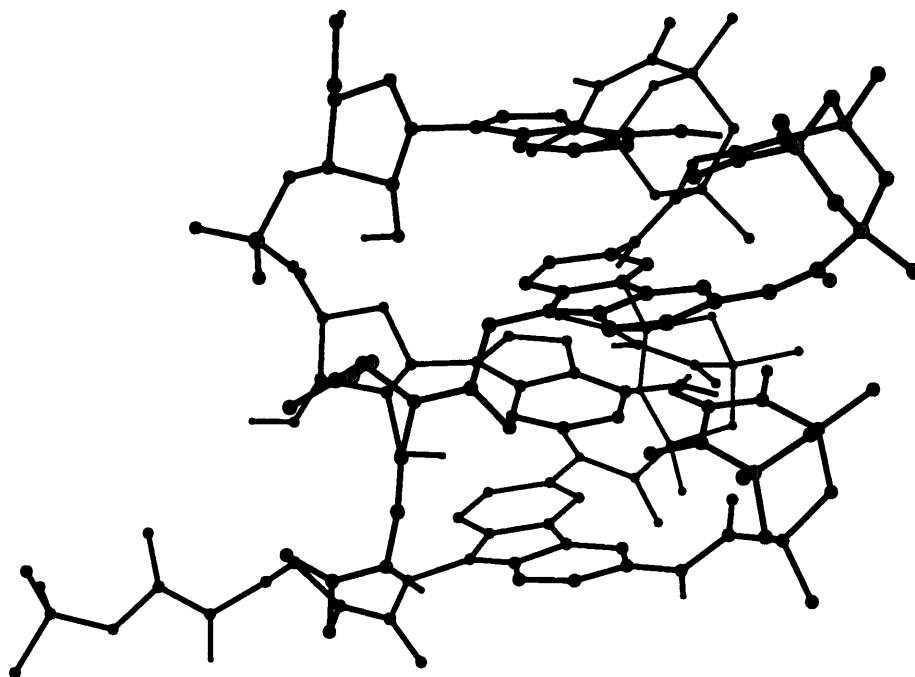
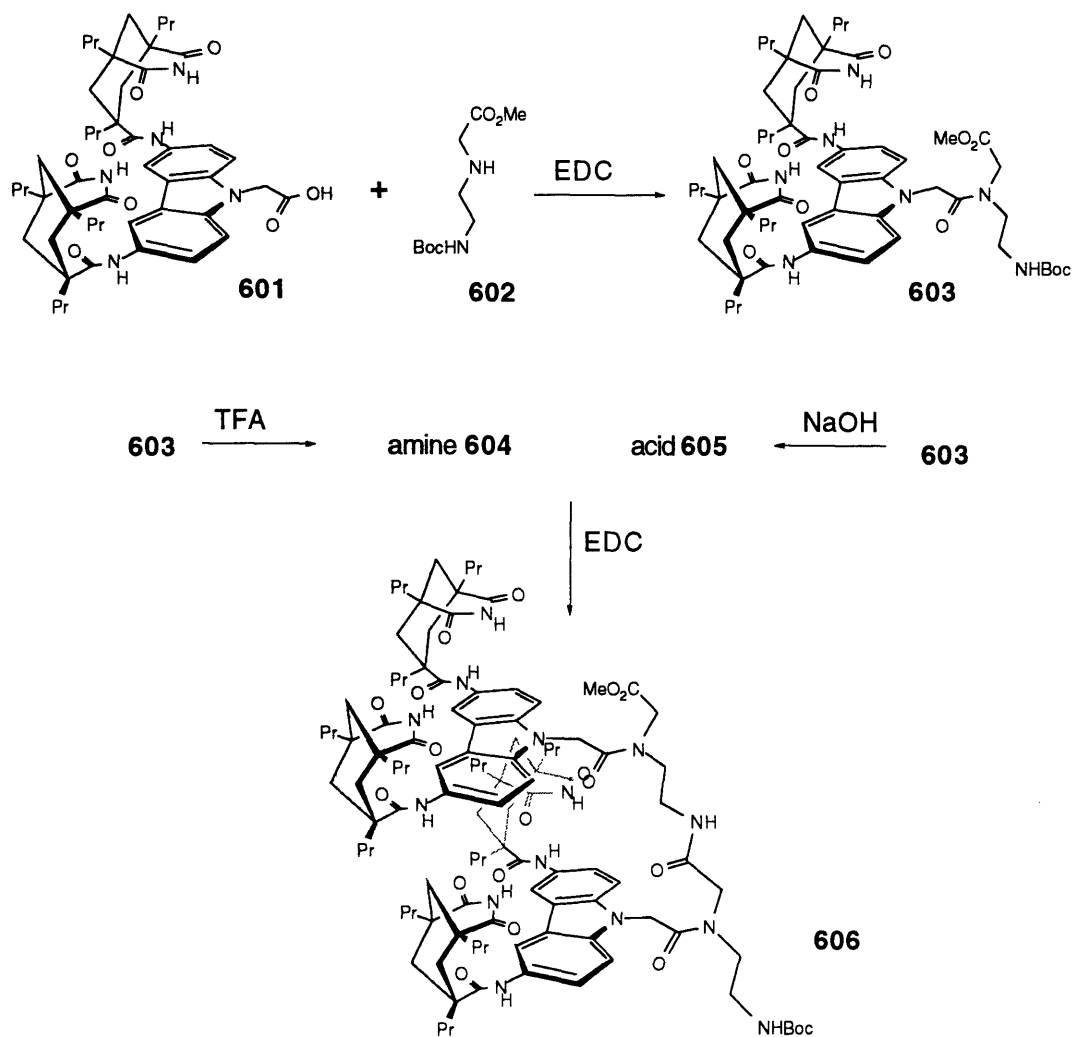


Figure VI-2. Minimized structure of the complex between **606** and ApA. Methyl groups were used on the Kemp's imide modules instead of propyl groups

VI.2 Synthesis

In order to make a receptor-containing monomer, acid **601** and amine **602** were coupled with EDC in THF to give the fully protected monomer **603** (Scheme VI-1). The Boc group was easily removed with trifluoroacetic acid (TFA) and the methyl ester was selectively hydrolyzed with NaOH. The resulting amine **604** and acid **605** were coupled with EDC to form the dimer **606**, which was purified by chromatography. A plasma desorption mass spectrum confirmed the success of the coupling. The ^1H NMR spectra (in $\text{DMSO-}d_6$) of the monomer units show separate signals for the cis and trans conformers about the tertiary amide bond. The spectrum of the dimer is due to this restricted amide rotation very complex, but sharpens up at higher temperature. These observations are similar to those of Chen et al.⁶ using the regular PNAs in aqueous solution. Their NMR data suggested a 70:30 rotamer distribution in monomer and dimer, but surprisingly, a single conformer at the octamer stage.

(6) Chen, S.-M.; Mohan, V.; Kiely, J. S.; Griffith, M. C.; Griffey, R. H. *Tetrahedron. Lett.* **1994**, *35*, 5108.



Scheme IV-1. The synthesis of the dimer

VI.3 Conclusions

The carbazole based adenine receptors are easily attached to the PNA backbone. The fully protected monomer could be prepared in a single step. This monomer should be compatible with conventional solid phase peptide synthesis. A dimer synthesis using solution based chemistry was demonstrated.

VI.4 Experimental Section

General. See chapter 5. The amine **602** was prepared from N-(2-aminoethyl)glycine methyl ester-2HCl⁷ and di-*t*-butyl dicarbonate in CH₂Cl₂ in the presence of NEt₃. For a recent procedure for large scale preparations see ref 8.

Protected Monomer (603). In THF (15 mL) were mixed together acid **605** (455 mg, 0.525 mmol), amine **604** (575 mg, 2.48 mmol), EDC (330 mg, 1.72 mmol) and NEt₃ (144 μL, 1.03 mmol). After stirring for 14 h the solvent was removed and the mixture was purified by column chromatography over silica gel (5% MeOH/CH₂Cl₂) to give 446 mg (80%) **603** as a white powder. ¹H NMR (300 MHz, DMSO-*d*₆) in some cases separate signals are seen due to restricted tert. amide rotation (3:1 ratio). δ 10.37 (s, 2H), 9.14 (s, 2H), 8.12 (s, 1.5H), 8.08 (s, 0.5H), 7.48-7.37(m, 2H), 7.33-15 (m, 2.25H), 6.80-6.65 (br d, 0.75H), 5.34 (s, 1.5H), 5.16 (s, 0.5H), 4.45 (s, 0.5H), 4.02 (s, 1.5H), 3.80 (0.75H), 3.65-3.53 (m, 4.25H), 3.05-2.90 (m, 2H), 2.67 (d, J = 13.7 Hz, 4H), 2.02 (d, J = 11.9 Hz, 2H), 1.85-1.70 (m, 4H), 1.55-1.00 (m, 35H), 0.90-0.70 (m, 18H). HRMS (FAB in 3-nitrobenzyl alcohol) m/e calcd for C₆₀H₈₆N₇O₁₁ (M + H): 1080.6385; found: 1080.6363.

Amine (604). The protected monomer **603** (22 mg, 0.020 mmol) was dissolved in CH₂Cl₂ (1 mL) after which trifluoroacetic acid (1 mL) was added. The mixture was stirred for 15 min and the solvents were removed and the residue dried at high vacuum to yield **605** (quantitative) which was used in the next step without further purification.

Acid (605). The protected monomer **603** (32 mg, 0.0296 mmol) was dissolved in 1 mL of a 1:1:1 mixture of EtOH, THF and 1N NaOH. After stirring for 30 min. the mixture was acidified and the organic solvents were evaporated. After addition of CH₂Cl₂ (25 mL) the mixture was washed with brine (10 mL), dried (MgSO₄) and concentrated to give **605** (23 mg, 73%) as a white solid. ¹H NMR (300 MHz, acetone-*d*₆) δ in most cases separate signals are seen due to restricted tert. amide rotation (3:2 ratio). 9.50 (br s, 0.8H), 9.38 (s, 1.2H), 8.68 (s, 0.8H), 8.55 (s, 1.2H), 8.06 (s, 1.2H), 8.02 (s, 0.8H), 7.52 (d, J = 8.8 Hz, 1.2H), 7.40 (d, J = 8 Hz, 0.8H), 7.25 (d, J = 8.8 Hz, 1.2H), 6.98 (br d, 0.8H), 6.50 (br s, 0.6H), 5.95 (br s, 0.4H), 5.31 (s, 1.2H), 4.55 (br s, 0.8H), 4.40 (s, 0.8H), 4.13

(7) Heimer, E. P.; Gallo-Torres, H. E.; Felix, A. M.; Ahmad, M.; Lambros, T. J.; Scheidl, F.; Meienhofer, J. *Int. J. Peptide Protein Res.* **1984**, *23*, 203.

(8) Dueholm, K. L.; Egholm, M.; Buchardt, O. *Org. Prep. Proc. Int.* **1993**, *25*, 457.

(s, 1.2H), 3.80-3.70 (m, 1.2H), 3.55-3.38 (m, 1H), 3.24-3.14 (m, 0.8H), 2.84 (d, J = 11.8 Hz, 4H), 2.30-2.18 m, 2H), 2.00-1.85 (m, 4H), 1.70-1.20 (m, 35H), 1.00-0.80 (m, 18H).

Dimer (606). In THF (1 mL) were mixed together: acid **605** (23 mg, 0.022 mmol), amine **604** (25 mg, 0.026 mmol), EDC (40 mg, 0.21 mmol) and NEt₃ (50 μL, 0.36 mmol). After 14 h the solvent was removed and the residue was purified by chromatography over silica gel (10% MeOH/CH₂Cl₂) to give 10 mg (22%) as a white powder. MS (plasma desorbition on nitro cellulose targets): M⁺ m/e calcd.: 2027; found: 2024 (100% peak), . M+Na⁺ calcd.: 2050; found: 2048.

Chapter VII Synthetic Catalysts for RNA Hydrolysis

VII.1 Introduction

The development of a sequence-specific artificial RNase is an important goal in science.¹ A successful nuclease has potential application in molecular genetics and in medicine. Therapeutic uses can be envisioned as antiviral and antifungal agents through interception of e.g. viral RNA. Hydrolytic cleavage has several advantages over oxidative cleavage. There is no need for oxidation reagents and no unselectively destructive (highly reactive) species are generated. In addition, RNA strands that have been cleaved hydrolytically can be religated if this is desired. Several approaches to RNA hydrolysis have been used. At high concentrations, polyamines,² imidazole³ and polypeptides⁴ were able to effect RNA hydrolysis. In addition, progress has been made with the use of catalysts that are effective at lower concentration. Anslyn et al.⁵ have prepared a staphylococcal nuclease active site mimic which was shown to accelerate cleavage of RNA up to 20-fold in the presence of imidazole. The proposed mechanism of action is shown in Figure VII-1.

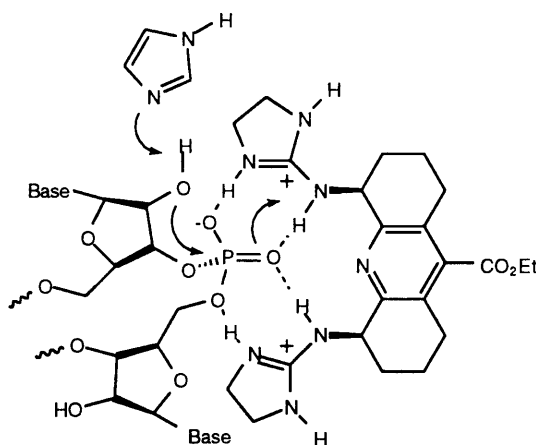


Figure VII-1. RNA hydrolysis by a bis-alkylguanidinium receptor.

(1) (a) Bashkin, J. K. *Bioinorganic Chemistry of Copper*; Karlin, K. D., Tyeklár, Z., Eds.; Chapman & Hall, New York 1993, pp 132-139. (b) Sigman, D. S.; Mazumder, A.; Perrin, D. M. *Chem. Rev.* **1993**, *93*, 2295.

(2) Yoshinari, K.; Yamazaki, K.; Komiyama, M. *J. Am. Chem. Soc.* **1991**, *113*, 5899.

(3) Breslow, R. *Proc. Natl. Acad. Sci. U.S.A.* **1993**, *90*, 1208, and references cited therein.

(4) Barbier, B.; Brack, A. *J. Am. Chem. Soc.* **1992**, *114*, 3511.

(5) Smith, J.; Ariga, K.; Anslyn, E. V. *J. Am. Chem. Soc.* **1993**, *115*, 362.

Of the many metal complexes that have been screened for catalytic RNA hydrolysis, lanthanide complexes were the most effective.⁶ An example is shown in Figure VII-2. This complex (200 μM) was able to cleave 70% of 190 μM A₁₂-A₁₈ (adenosine concentration) at pH 7 in just 4 h.

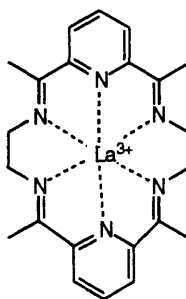


Figure VII-2. A lanthanide complex effective in RNA hydrolysis.

A sequence selective artificial ribonuclease has been prepared by linking a lanthanide complex to the 5'-end of a 15-mer DNA.⁷ At pH 8 and 37 °C, this molecule (Figure VII-3) selectively hydrolyzes a 39-mer RNA exactly at the target site.

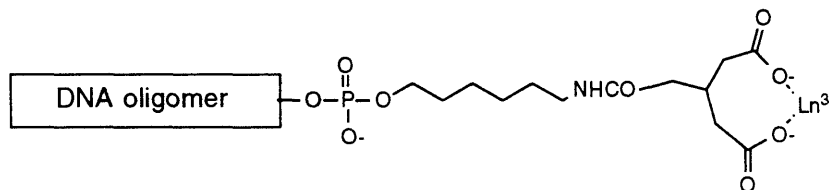


Figure VII-3. Structure of the sequence-selective artificial hydrolytic ribonuclease.

Recently also more non-metal catalysts have appeared in the literature. Three different groups used a similar strategy.⁸ Their designs were inspired by the structurally well characterized RNase A, or rather its proposed mechanism of action.⁹ In RNase A, a protonated imidazole and a neutral one act as general acid and base catalysts. The

(6) Morrow, J. R.; Buttrey, L. A.; Shelton, V. M.; Berback, K. A. *J. Am. Chem. Soc.* **1992**, *114*, 1903.

(7) Matsumura, K.; Endo, M.; Komiyama, M. *J. Chem. Soc., Chem. Commun.* **1994**, 2019

(8) (a) Tung, C.-H.; Wei, Z.; Leibowitz, M. J.; Stein, S. *Proc. Natl. Acad. Sci. U.S.A.* **1992**, *89*, 7114. (b) Podyminogin, M. A.; Vlassov, V. V.; Giegé, R. *Nucleic Acids Res.* **1993**, *21*, 5950. (c) Shinozuka, K.; Shimizu, K.; Nakashima, Y., Sawai, H. in *Nucleic Acids Symposium Series no. 31*; Oxford University Press, Oxford, 1994, pp 167-168.

(9) Breslow, R.; Huang, R. *Proc. Natl. Acad. Sci. U.S.A.* **1989**, *86*, 1746.

synthetic catalysts all contain an intercalating aromatic unit which provides the RNA affinity. The intercalators are conjugated with one or two imidazoles, which are believed to be the catalytic groups. Their most successful molecules are shown in Figure VII-4. Catalytic activity was highly dependent on the nature of the functional groups used and on their three dimensional orientation.

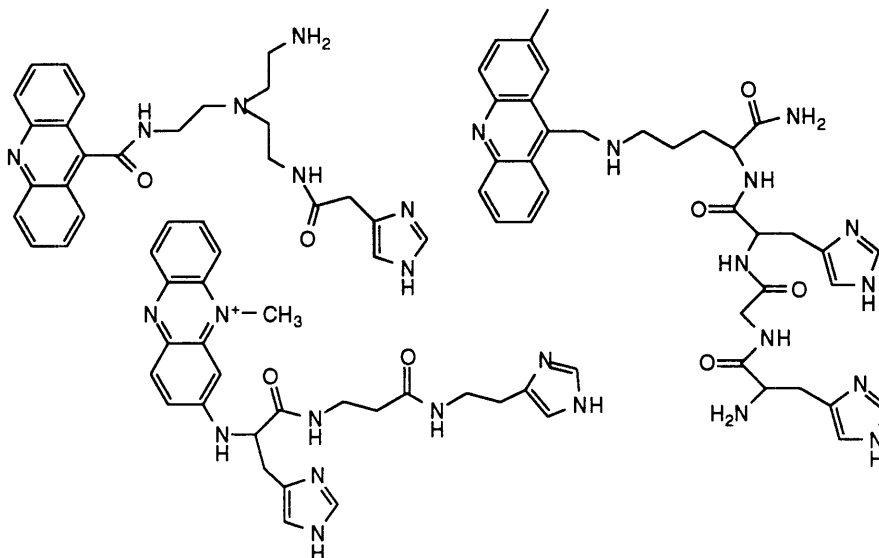


Figure VII-4. Successful non-metal RNA-cleaving molecules.

A report that $\text{Cu}(\text{bpy})^{2+}$ (bpy = 2, 2'-bipyridine) complexes have RNase activity¹⁰ incited the investigation described in this chapter, of bpy molecules covalently linked to our synthetic adenine receptors as catalysts in RNA hydrolysis reactions. Having both a receptor and a catalytic group in the same molecule can potentially lead to higher reactivity and selectivity.

VII.2 RNA hydrolysis with Adenine Receptors

In chapter II the synthesis of **701** (Figure VII-5) and its ability to bind both adenine derivatives and Cu(II) ions in water is described. Using a similar synthetic strategy, **702** was prepared containing a pyridine instead of a 2,2'-bipyridine unit.

(10) Modak, A. S.; Gard, J. K.; Merriman, M. C.; Winkeler, K. A.; Bashkin, J. K.; Stern, M. K. *J. Am. Chem. Soc.* **1991**, *113*, 283.

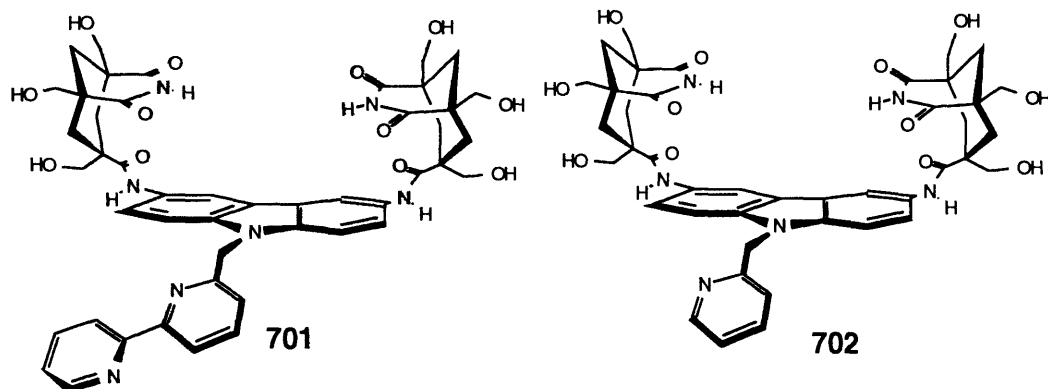


Figure VII-5. Structure of the receptors screened for RNase activity.

These molecules were tested in the hydrolysis of two oligonucleotides: **RNA-1** and **RNA-2**. Both RNAs contain a stretch of adenosines, the anticipated target, and a stretch of pyrimidines. **RNA-1** is not expected to have a significant degree of secondary structure. **RNA-2** however, is somewhat self-complementary and is likely to form a bulge of three cytosines.

RNA-1: 5' AAA AAA AAC CCC CCC C 3'

RNA-2: 5' CCC UUU CCC UUU AAA AAA 3'

Both RNAs were radiolabelled at the 5' end and incubated at 25 °C and pH 7, with **701**, **702** and bpy and in all cases with and without Cu(II).¹¹ Reactions were analyzed by gel electrophoresis (Figure VII-6). Several features became apparent. Surprisingly, cleavage activity was observed for **701** in the absence of Cu(II) and the activity was completely suppressed when Cu(II) was added. In **RNA-1** cleavage occurred only in the cytosine region. Similarly, in **RNA-2** cleavage was observed in the center CCC region. This region is found in a bulge when A/U base-pairs are formed. **RNA-2** also shows a spot of self-cleavage at the purine-pyrimidine interface. In molecules where internal A/U base-pairs are formed this interface is at the point where the RNA folds back onto itself. In certain cases bpy showed some activity with similar selectivity as **701** but much weaker. Compound **702** however, was completely inactive as a catalyst. Experiments with other RNA oligonucleotides gave similar results and consistently showed **701** as a cleavage catalyst. No degradation was observed with a DNA oligonucleotide, supporting the notion that **701** catalyzes hydrolytic cleavage.

(11) All the RNA hydrolysis experiments were conducted by Dr. Stefan Wölfl, MIT, Dept. of Biology.

These results indicate that matters are more complicated than anticipated. The reaction is actually inhibited by Cu(II) rather than catalyzed by it. Selectivity for cytosine was observed instead of adenine. The first observation had prompted us to prepare **702** in order to see if the bpy unit is simply functioning as a general base in assisting the 2' OH for attack of the phosphodiester bond. The fact that **702** showed no activity indicates that the remaining pyridine ring is not capable by itself in effecting cleavage. Perhaps the deleted ring was better positioned to act as a general base. The fact that cytosine selectivity was obtained questions the role of the Kemp's binding modules complementary to adenine. It is conceivable that the carbazole simply acts as an intercalator.

VII.3 Conclusions

Adenine receptors conjugated with a 2,2'-bipyridine were shown to effect RNA hydrolysis. The hydrolysis was inhibited by Cu(II)-ions, which binds to the bpy unit. Deletion of one of the bpy rings suppressed the activity. Selectivity was observed for cytosine rather than adenine. In order to fully understand the system more experiments are necessary. By making successive deletions of all functionality of **701** the activity can be traced to its origin and perhaps optimizations can start from there.

RNA-1: 1 2 3 4 5 6 7 8

RNA-2: 1 2 3 4 5 6 7

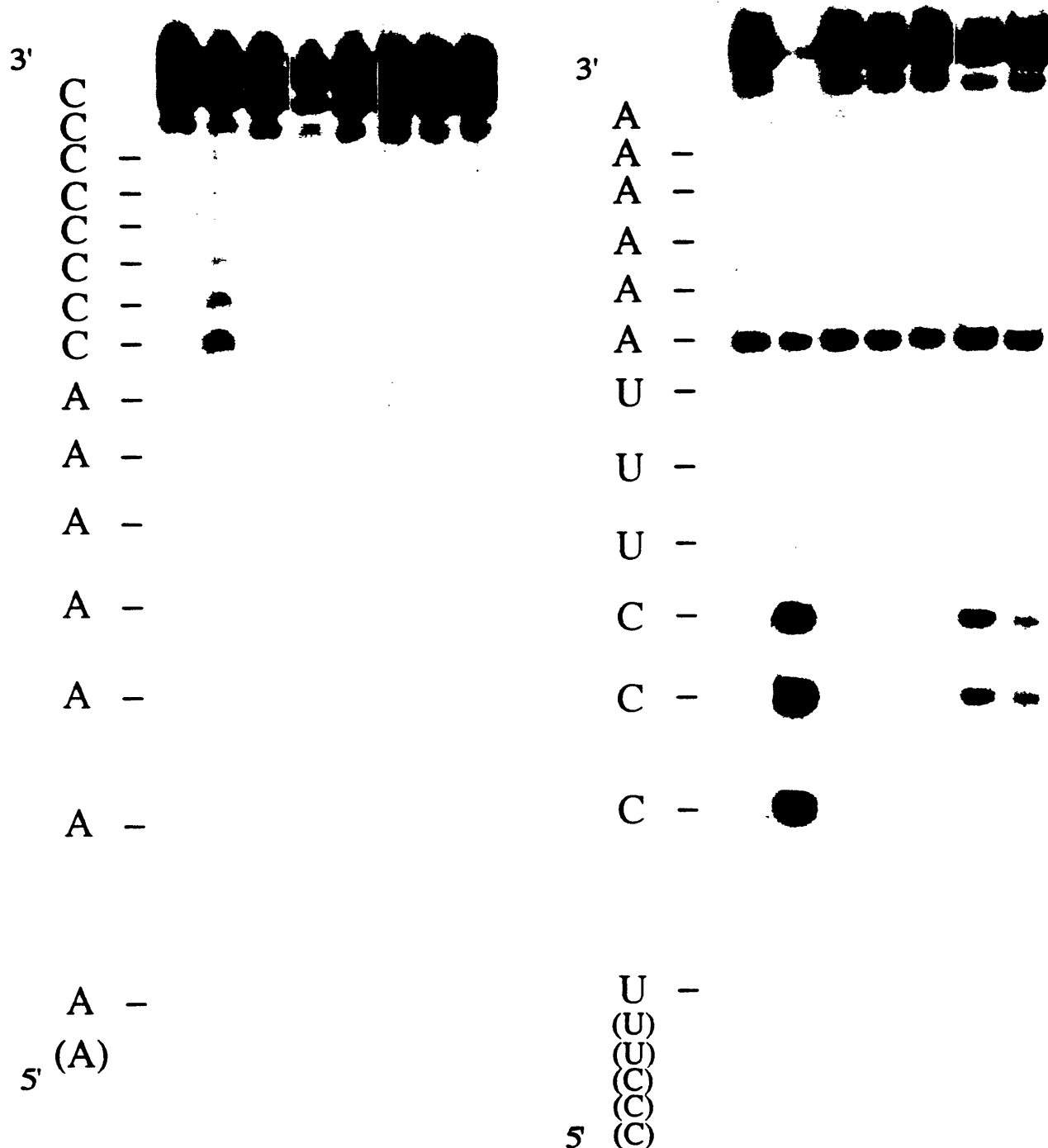


Figure VII-6. Autoradiographs of 20% denaturing polyacrylamide gels showing the partial cleavage of RNA-1 and RNA-2 (^{32}P labelled at the 5'-end) at pH 7 and 25 °C. Concentration of RNA about 1 μM . lane 1, control; lane 2, 1 (150 μM); lane 3, 1 + Cu^{2+} (both 150 μM); lane 4, 2 (150 μM); lane 5, 2 + Cu^{2+} (both 150 μM); RNA-1: lane 6, Cu^{2+} (150 μM); lane 7, Cu^{2+} (150 μM)+bpy (150 μM); lane 8, bpy (150 μM); RNA-2: lane 6, bpy (300 μM); lane 7, bpy (300 μM)+ Cu^{2+} (150 μM).

VII.4 Experimental Section

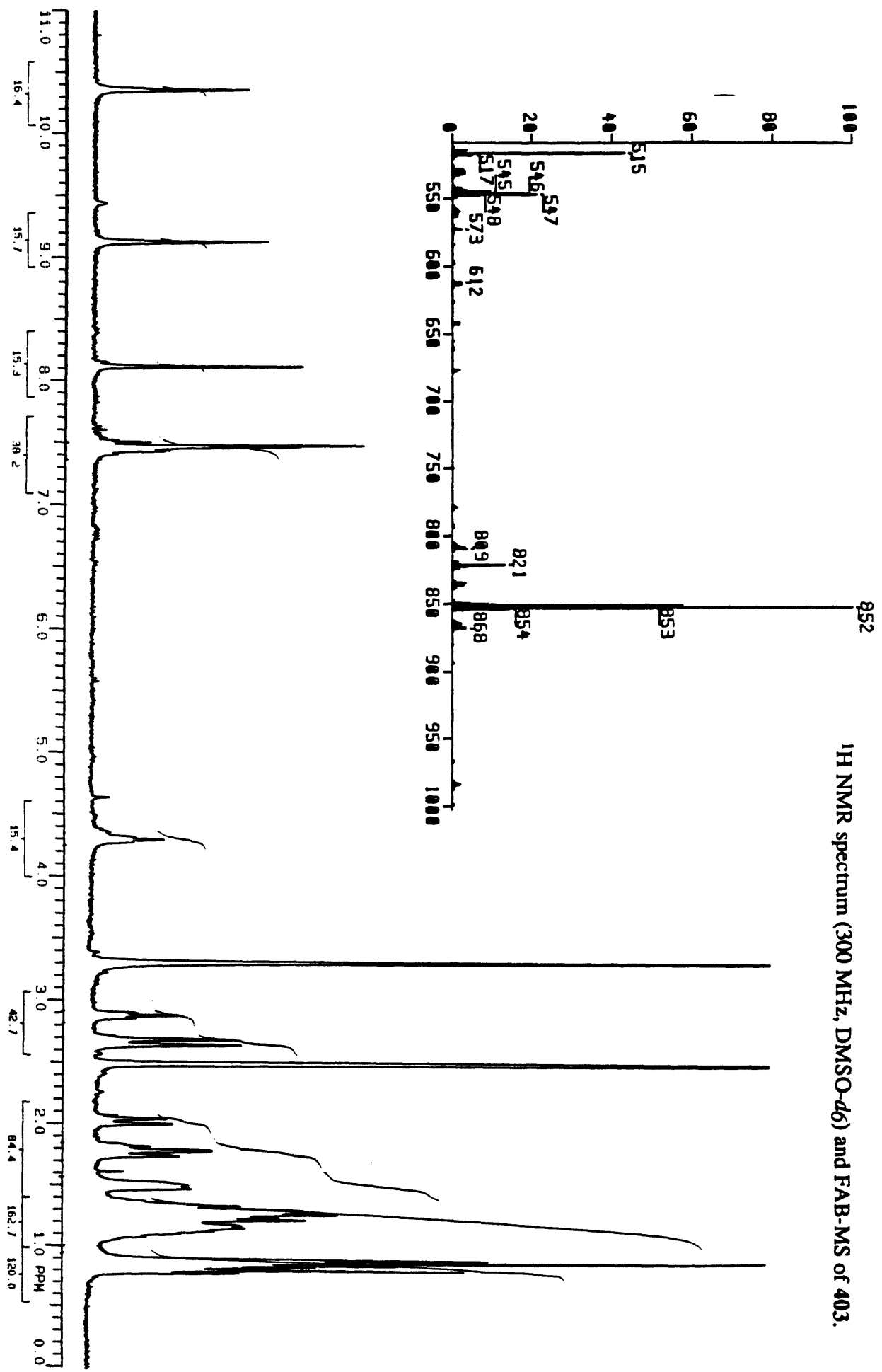
Pyridyl Receptor (HBr salt) (702). In DMF (10 mL) were mixed together 3,6-dinitrocarbazole (500 mg, 1.95 mmol), 2-picolychloride hydrochloride (383 mg, 2.33 mmol) and K_2CO_3 (2.69 mmol, 19.5 mmol). The mixture was heated at 110 °C for 14 h after which it was poured into H_2O (100 mL). The resulting precipitate was filtered off washed with H_2O and dried to give 653 mg (94%) of a yellow solid. 1H NMR (300 MHz, $DMSO-d_6$) δ 9.52 (s, 2H), 8.45-8.38 (m, 3H), 7.92 (d, $J = 9.1$ Hz, 2H), 7.77 (t, $J = 7.6$ Hz, 1H), 7.38 (d, $J = 7.8$ Hz, 1H), 7.27 (t, $J = 7.0$ Hz, 1H), 5.96 (s, 2H). The dinitro compound (100 mg, 0.279 mmol) was hydrogenated in THF and the resulting diamine was coupled with benzyloxyimide acid chloride (**209**, chapter II) as in the preparation of **210** to give 35 mg (9%) of the protected cleft, which was deprotected quantitatively by a brief treatment with HBr (30 min in formic acid at 0 °C) followed by removal of the solvent and further drying at high vacuum and was obtained as the HBr salt. mp > 300 °C. 1H NMR (300 MHz, $DMSO-d_6$) δ 10.41 (s, 2H), 9.17 (s, 2H), 8.63 (d, $J = 4.2$ Hz, 1H), 8.24 (d, 2H), 7.84 (t, 1H), 7.48-7.37 (m, 5H), 6.87 (d, $J = 7.8$ Hz, 1H), 5.78 (s, 2H), 3.77 (d, $J = 10.4$ Hz, 4H), 3.38 (s, 4H), 3.31 (d, $J = 10.4$ Hz, 4H), 2.39 (d, $J = 14$ Hz, 4H), 2.19 (d, $J = 12$ Hz, 2H), 1.48 (d, $J = 14$ Hz, 4H), 1.33 (d, $J = 13$ Hz, 2H). HRMS (FAB in 3-nitrobenzyl alcohol) m/e calcd for $C_{42}H_{47}N_6O_{12}$ (MH)⁺ (-Br): 827.3252; found: 827.3270.

RNA-hydrolysis assay. Both RNA oligonucleotides were labeled at the 5' end using polynucleotide kinase and $\gamma^{32}P$ -ATP. To assure uniformity of the labeled RNA, the oligonucleotides were loaded on a polyacrylamide gel and the full length oligonucleotide was eluted from the gel. The eluted RNA 's were than purified on Sep-Pak-C18 cartridges to avoid residual amounts of urea, buffer and gel remnants. The lyophilized RNA molecules were resuspended in water. Cleavage of RNA was analyzed in potassium cacodylate buffer pH 7.0 with **1**, **2**, 2,2'-bipyridine and $CuCl_2$, including combinations and control reactions. After 24 h incubation at room temperature 0.75 volumes 8 M urea loading dye was added to each sample. Prior to loading on the gel samples were briefly heated to 90 °C.

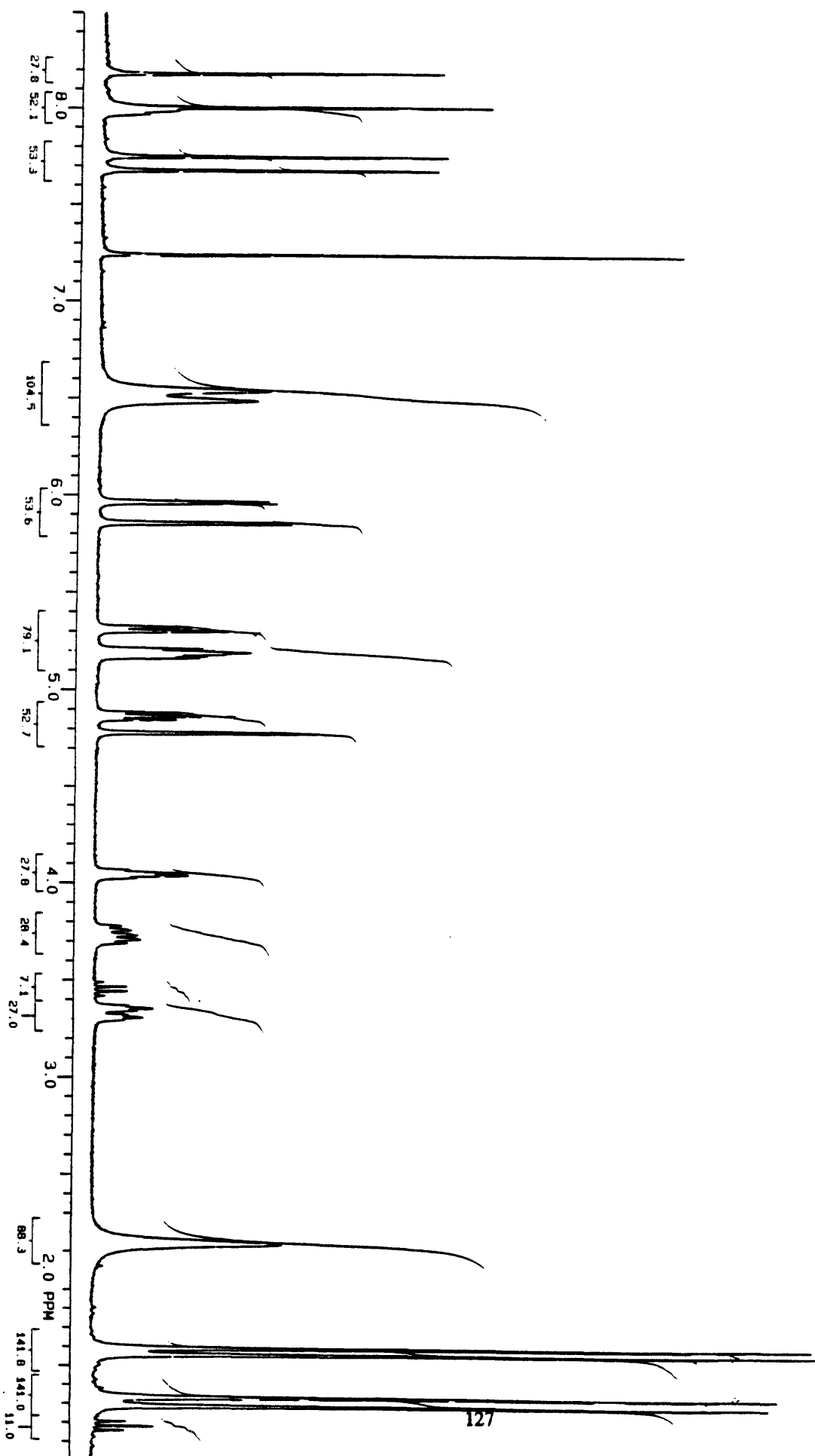
Appendix

Selected ^1H NMR and mass spectra.

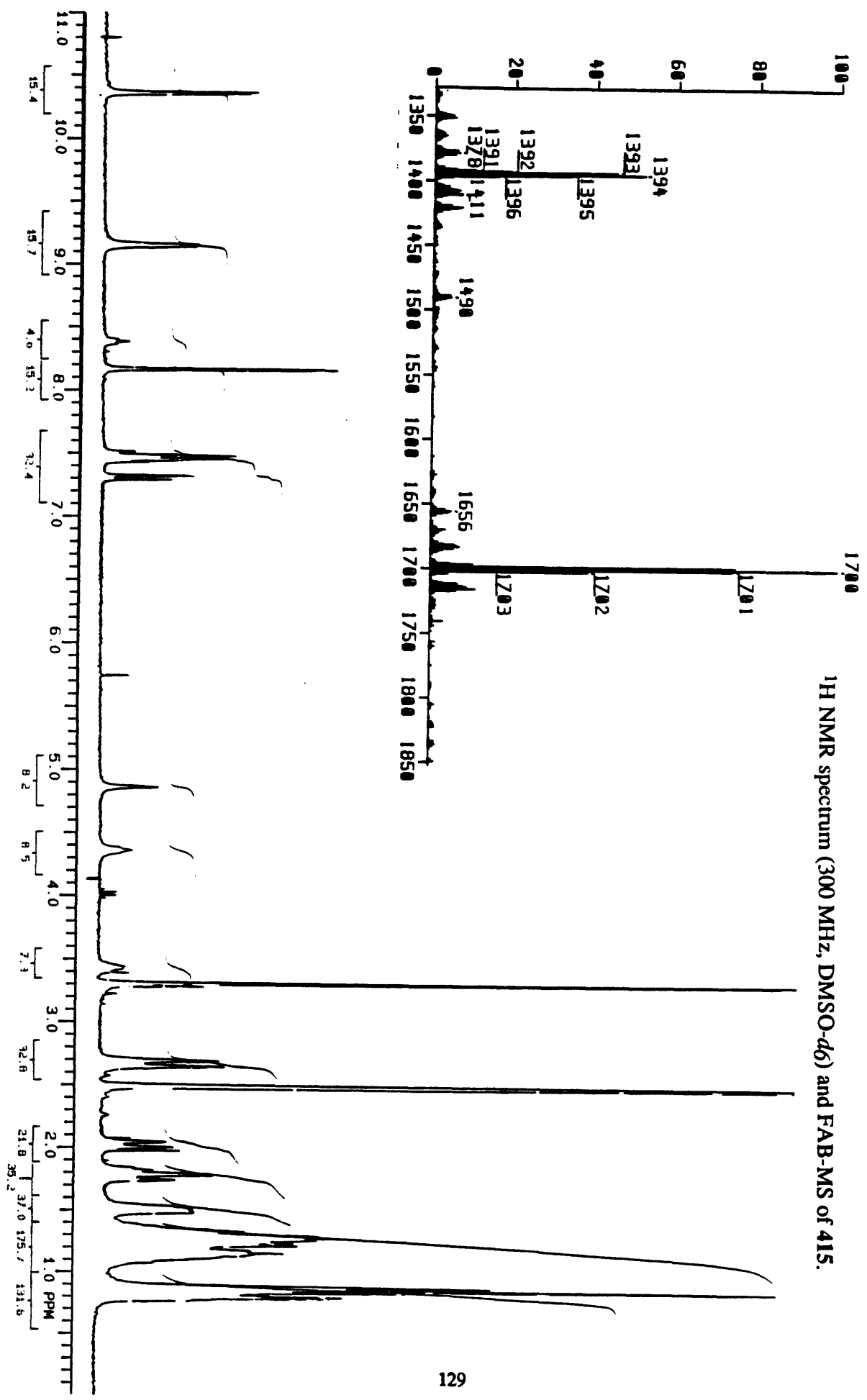
¹H NMR spectrum (300 MHz, DMSO-d₆) and FAB-MS of 403.



¹H NMR spectrum (300 MHz, CDCl₃) of 414.

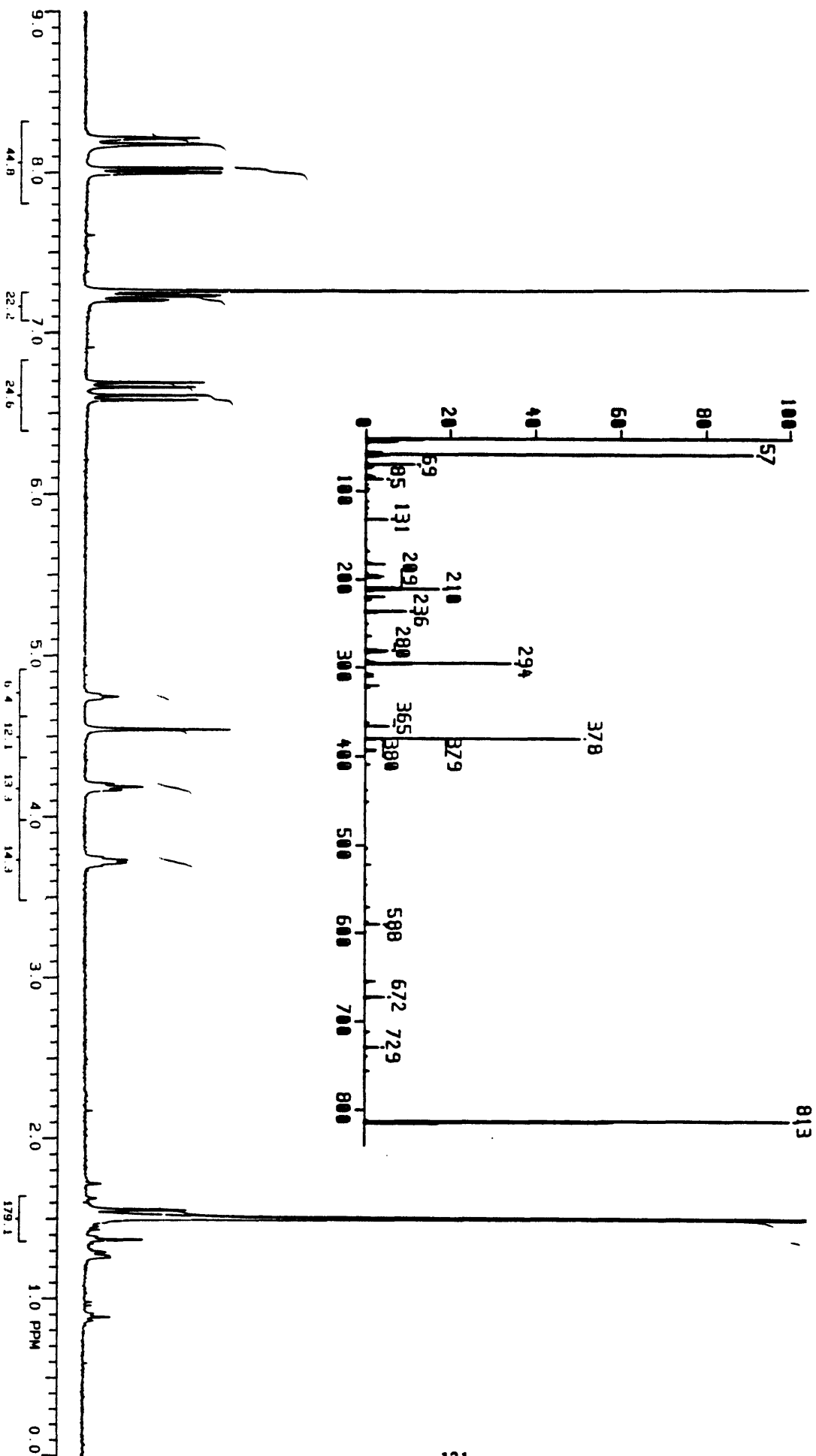


¹H NMR spectrum (300 MHz, DMSO-d₆) and FAB-MS of 415.

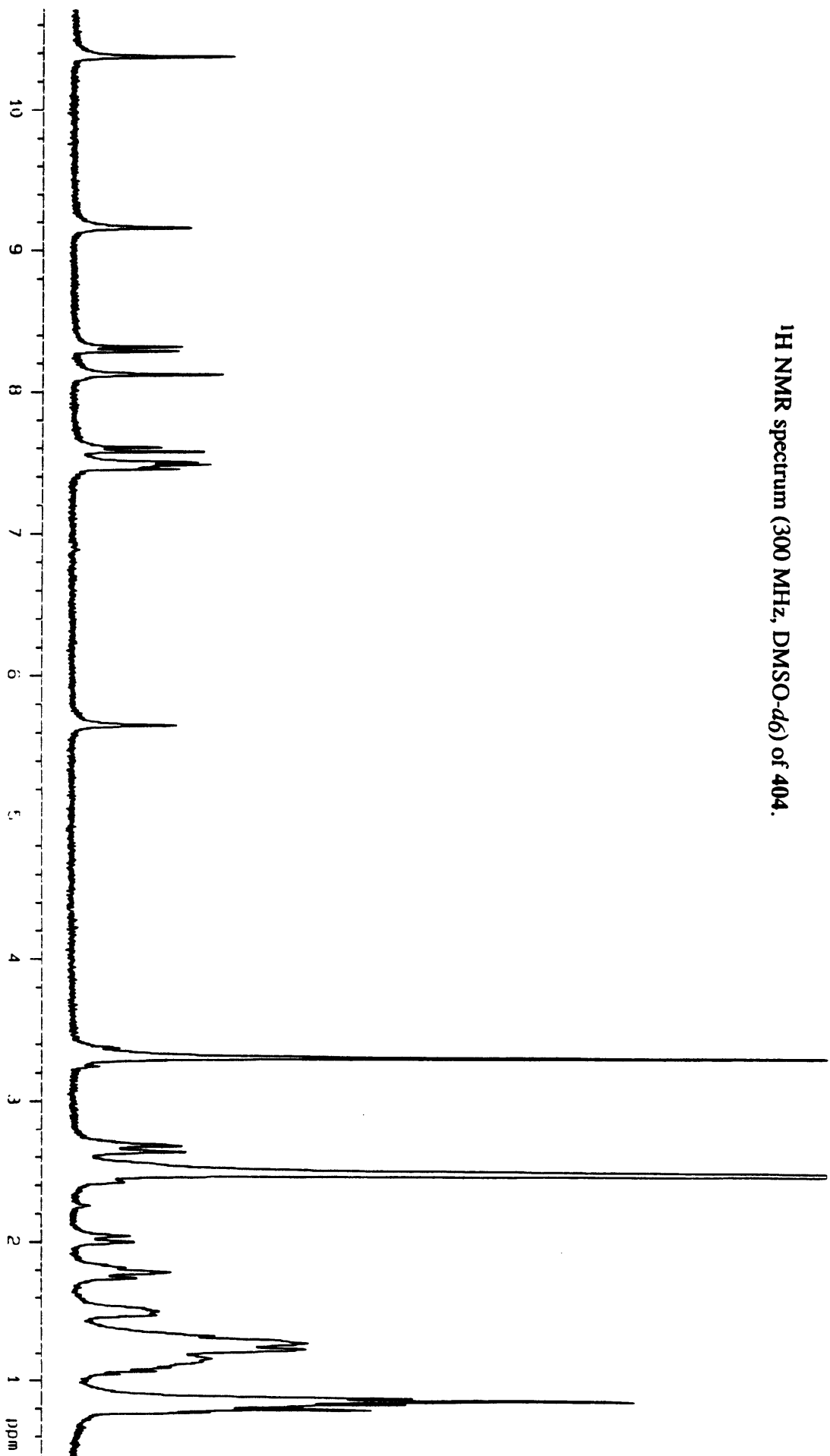


•

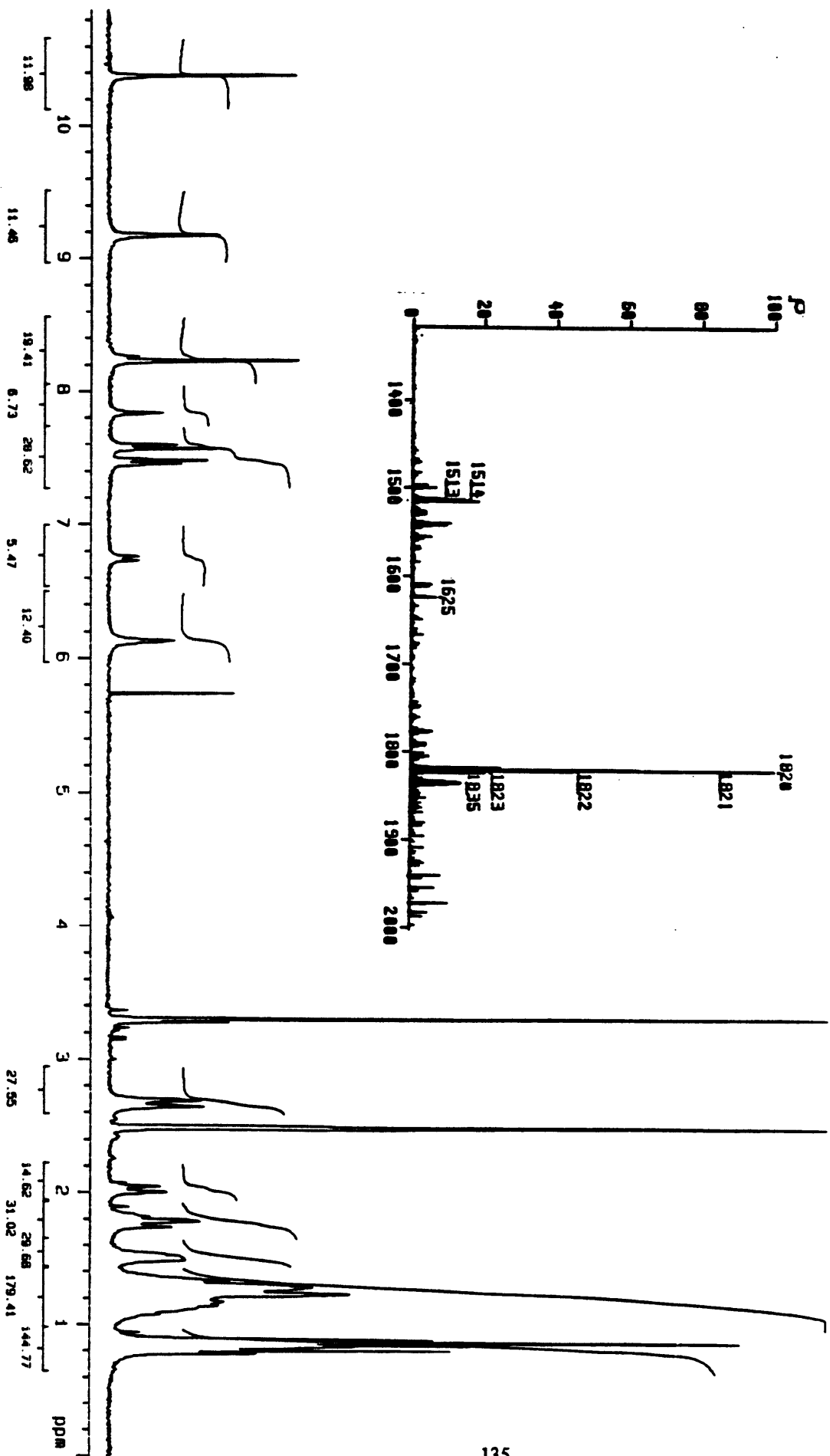
¹H NMR spectrum (300 MHz, CDCl₃) and EI-MS of 409.



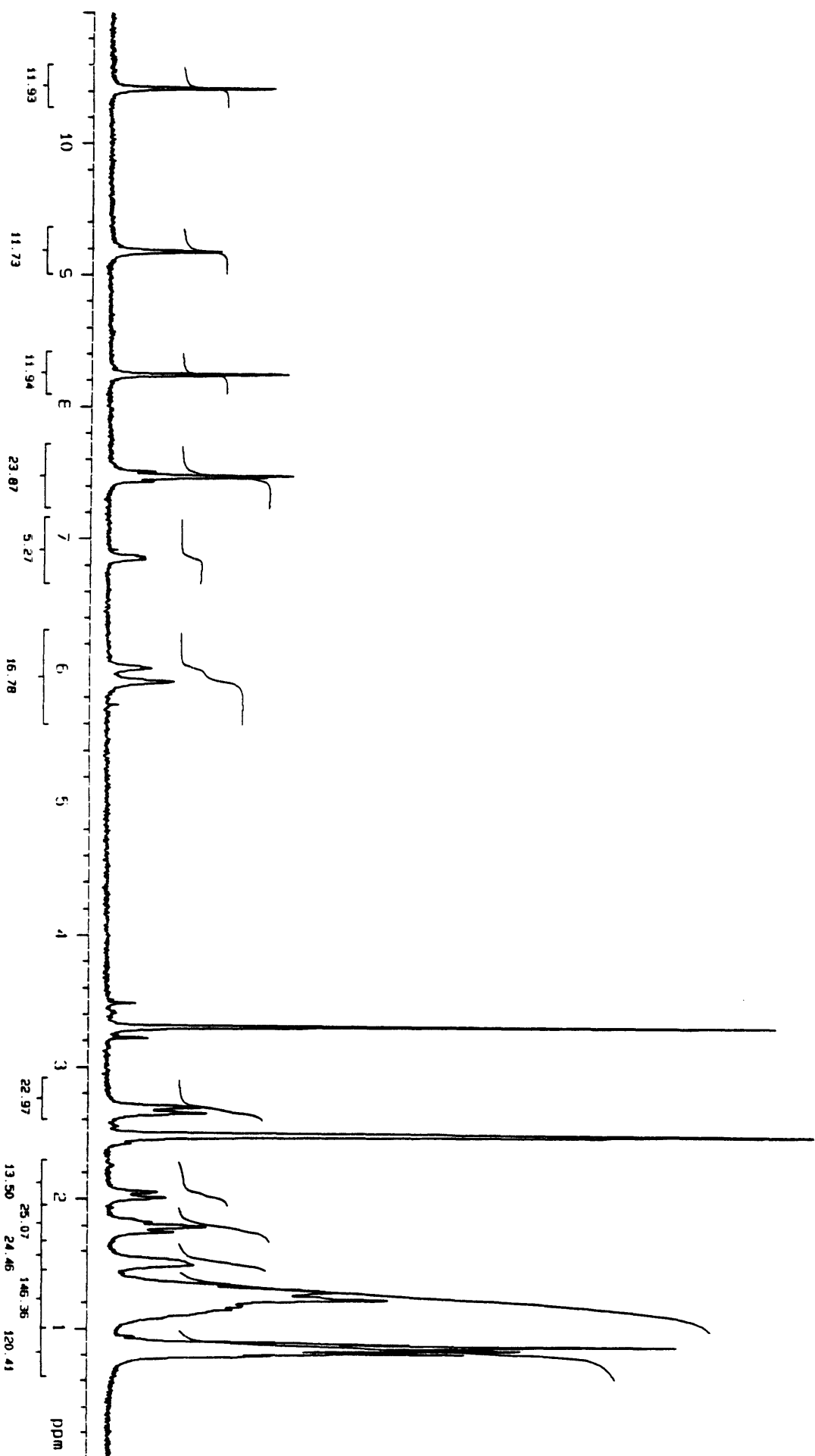
¹H NMR spectrum (300 MHz, DMSO-*d*₆) of 404.



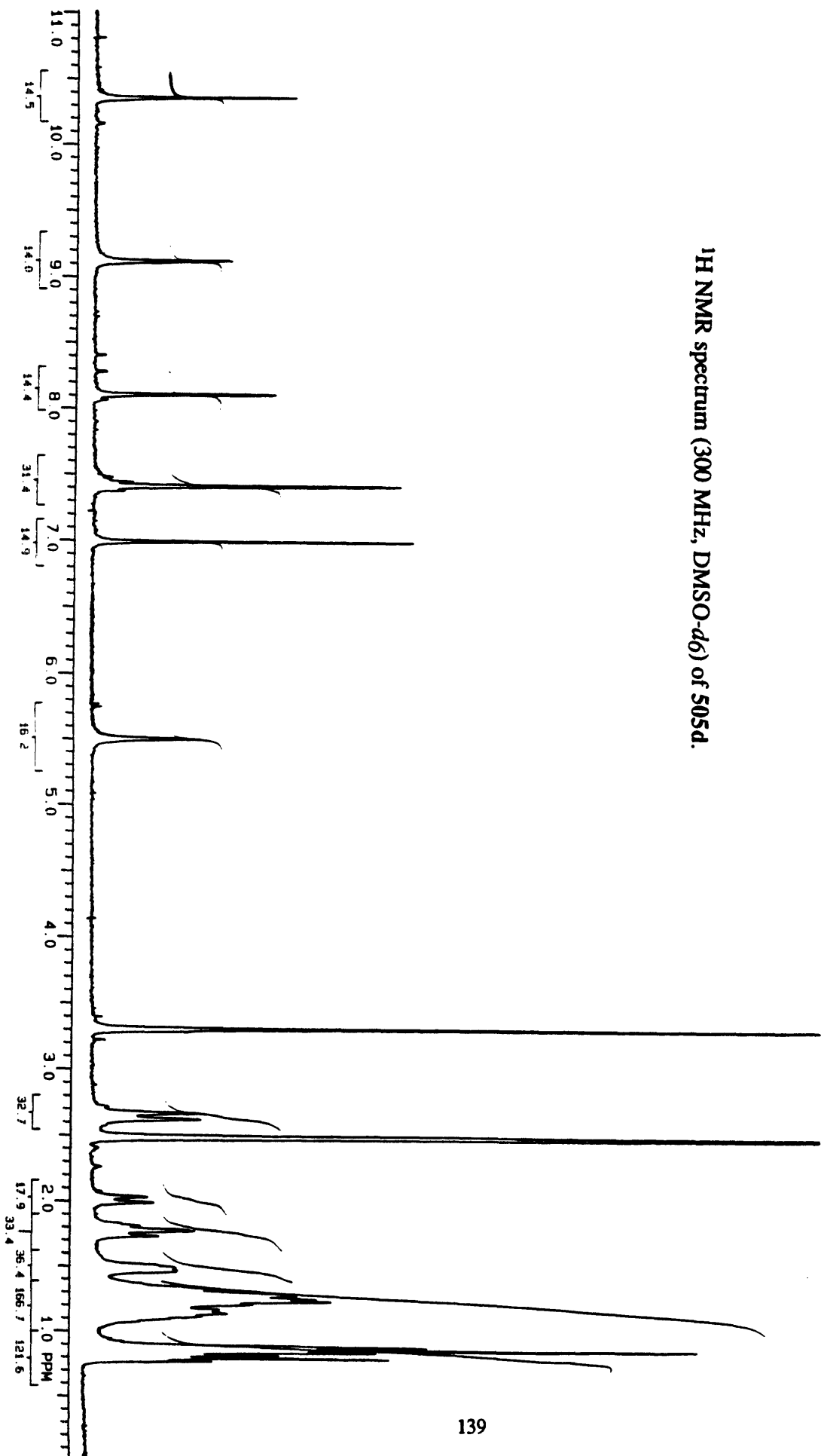
¹H NMR spectrum (300 MHz, DMSO-d₆) and FAB-MS of 505c.



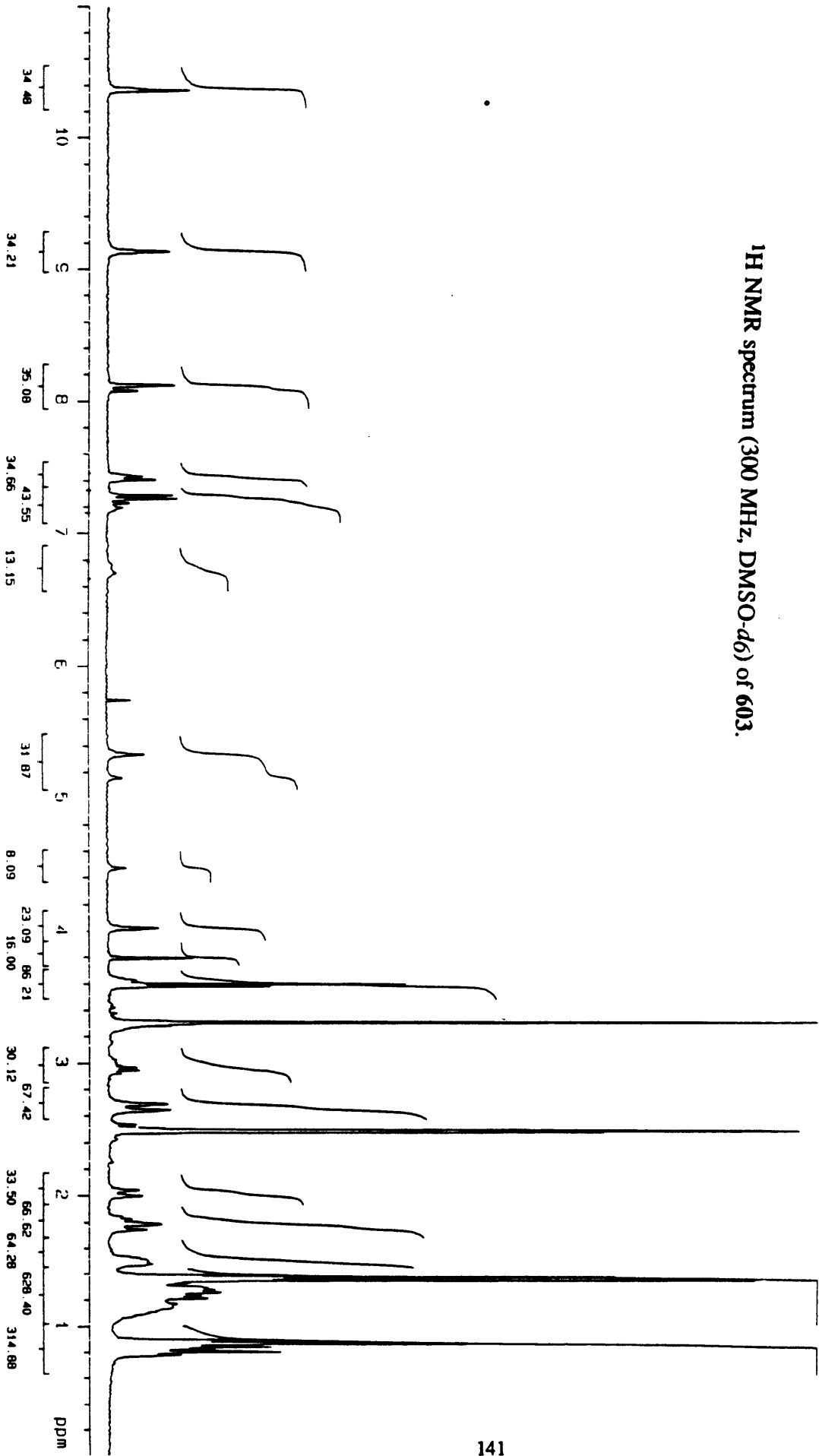
¹H NMR spectrum (300 MHz, DMSO-d₆) of 505b.



¹H NMR spectrum (300 MHz, DMSO-d₆) of 505d.



¹H NMR spectrum (300 MHz, DMSO-d₆) of 603.



^1H NMR spectrum (300 MHz, $\text{DMSO-}d_6$) of 211.

